CHALMERS

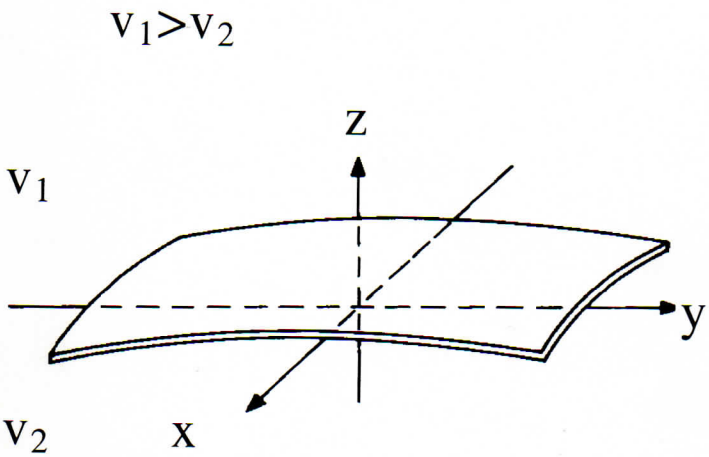

Hygro-Elastic Deformation of High Pressure Laminates

A Macroscopic Analysis
Theoretical Modelling and Measurements

BIJAN ADL ZARRABI

Department of Building Physics
CHALMERS UNIVERSITY OF TECHNOLOGY
Sweden 1998

Doctoral thesis for the degree of Doctor of Philosophy

Hygro-Elastic Deformation of High Pressure Laminates

A Macroscopic Analysis

Theoretical Modelling and Measurements

By

Bijan Adl Zarrabi

Department of Building Physics
Chalmers University of Technology
Göteborg, 1998

Keywords:

Moisture transport
Expansion
Elastic deformation
High Pressure Laminate
Orthotropic
Numerical simulation

ISSN 91-7197-704-X
P-98:4

Chalmers University of Technology
Department of Building Physics
S-412 96 Göteborg

Telephone: +41 31 772 1985
Telefax: +46 31 772 1993
Internet: http://www.buildphys.chalmers.se

ABSTRACT

Deformation due to environmental changes in moisture arises in many engineering problems of practical interest. The purpose of this work is to develop a theoretical model for the determination of moisture induced deformations in thin plates made of High Pressure Laminates. For the determination of moisture induced deformations, a set of material properties is required. Measuring these properties is also a part of this work.

The theoretical models for moisture transfer and elastic deformation are based on Fick's law and the Kirchhoff plate theory, respectively. High Pressure Laminates are classified as a composite material and the behaviour of composites can be analysed in different classes of theoretical problems. Here, the High Pressure Laminate is treated, on the macroscopic scale of observation, as a homogeneous, elastic and orthotropic material.

A basic result of the thesis is a simple procedure to account for the effect of hygro-expansion. The moisture moment integral, which essentially is proportional to moisture content profile and thickness of plate, gives a basic time-dependent function I(t) which determines the effect of any uneven moisture distribution over the cross-section of the plate. The moisture-induced moments are proportional to I(t) and they only appear as an additional term in the boundary conditions of the plate. Solutions for simply supported plates are presented for different rectangular shape and, for different stiffness and hygro-expansion coefficients in the two orthotropic directions.

Two PC-programmes, MHPL and MecHPL, based on the theoretical models are developed. MHPL deals with determining the moisture content of the material and MecHPL deals with calculating the moisture induced deformations in the plate. These programmes have been validated by using existing programmes and experimental tests. The results of the validations indicate that the models and PC-programmes are correctly formulated.

Keywords: Moisture transport, expansion, elastic deformation, High Pressure Laminate, orthotropic, numerical simulation

PREFACE

This work was carried out at the Department of Building Physics, Chalmers University of Technology, under the supervision of Professor Carl-Eric Hagentoft. Perstorp AB and Professor Carl-Eric Hagentoft initiated the work and my research in this field began at the end of 1994.

I wish to express my deepest gratitude to Professor Carl-Eric Hagentoft for his valuable advice, guidance and understanding.

I am grateful to all my colleagues at the department for their help and support.

I am thankful for the support which I have received from Perstorp AB.

Finally, I would like to thank my wife Sima and my sons Kaiwan and Shahin for their patience, care and understanding during this work.

Göteborg, October 1998
Bijan Adl Zarrabi

CONTENTS

Part C Transient Hygro-elasticity

Summary

The High Pressure Laminate (HPL) studied in this work is built up from phenol impregnated paper sheets pressed together at a temperature of about 150°C. These laminates can be produced in many different qualities and surface finishes. By an alteration in the build-up it is fairly easy to change the properties and size. The laminate is used as a surfacing material in such cases where heavy demands are made on the surface of the product.

The non-uniform distribution of moisture over a cross-section of a thin plate made of High Pressure Laminate causes moisture induced strains/stresses which lead to deformations of the plates. These deformations are not desired in the application of High Pressure Laminates in construction, such as flooring and facade. Furthermore, if any displacement of the plate edges is hindered, the coupling joints of the High Pressure Laminate in a construction will be exposed to moisture induced moments and forces.

The scope of this work is to develop a theoretical model for the determination of moisture induced deformations in High Pressure Laminates. The model is validated by experimental tests. For determining moisture induced deformations, a set of material properties is required. Measuring these properties is also a part of this work. It should be mentioned that HPL are classified as a composite material and the behaviour of composites can be analysed in different classes of theoretical problems. Here, the HPL is treated, on the macroscopic scale of observation, as a homogeneous, orthotropic material.

For determining moisture induced deformations, the moisture distribution over a cross-section of HPL should be known. This distribution can be determined by using Fick's law, if the moisture permeability and sorption curve of the High Pressure Laminates are known. When the moisture distribution is determined, the deformations of the plate can be calculated by using the Kirchhoff plate theory.

A basic result of the thesis is a simple procedure to account for the effect of hygro-expansion. Let $\Delta u(z,t)$ be the moisture distribution through a thin plate at time t. The moisture moment integral (essentially of $z \times \Delta u(z,t)$) gives a basic time-dependent function I(t) which determines the effect of any uneven moisture distribution over the cross-section of the plate.

The moisture-induced moments m_x^m and m_y^m are proportional to I(t) for an orthotropic plate. These moments are independent of x and y. Hence, they only appear as an additional term in the boundary conditions of the plate.

Any problem may be solved for I = 1 only, and the results for any moisture distribution is obtained by multiplication by I(t).

Solutions for I=1 are presented for plates of different rectangular shape and for different stiffness and hygro-expansion coefficients in the two orthotropic directions.

The theory is in particular applied for two basic moisture processes. In the first one, the relative humidity at the boundary is changed by a step, and in the second one, a periodic variation is imposed to the boundary.

Two PC-programmes, MHPL and MecHPL, based on the theoretical models have been developed. The MHPL deals with determining the moisture content of the material and moisture induced forces, and the MecHPL deals with calculating moisture induced deformations in a plate which is exposed to moisture induced forces and moments. These programmes have been validated by using existing programs. The results of the validations indicate that the models and PC-programmes are correctly formulated.
A comparison of the measured results and calculated results indicates that the theoretical model is able to predict moisture induced deformations. Deviations up to 30% between the calculated and measured results have been observed when the specimens are from a batch other than the one used to determine the material properties of the laminate. This means that the material properties of the laminates can vary strongly from one batch to another.

In following paragraphs, some of the results obtained during this work are presented.

- ***Measurement of Moisture Permeability of the HPL***

A High Pressure Laminate is a porous and hygroscopic material. The equilibrium moisture content of a hygroscopic material depends on the relative humidity and the temperature of the ambient air. Fick's law and the Cup method are used for determining the moisture permeability of the HPL at different relative humidities. The measured moisture permeability of the HPL is shown in Figure S1.

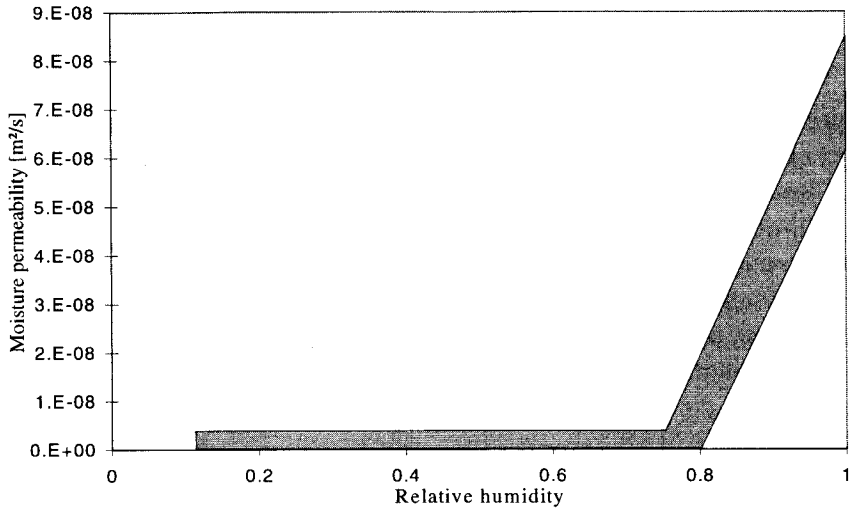

Figure S1 The interval of measured moisture permeability.

- Measurement of Hygro Expansion Coefficients

HPL is an orthotropic material. An orthotropic material has different hygro expansion coefficients in different directions. Thus, the hygro expansion coefficient of the High Pressure Laminate should be determined for both machine and cross directions. Measurement results from the dry chamber for the 6 mm thick specimens are presented in Figure S2. The initial moisture content of the specimens was about 4%.

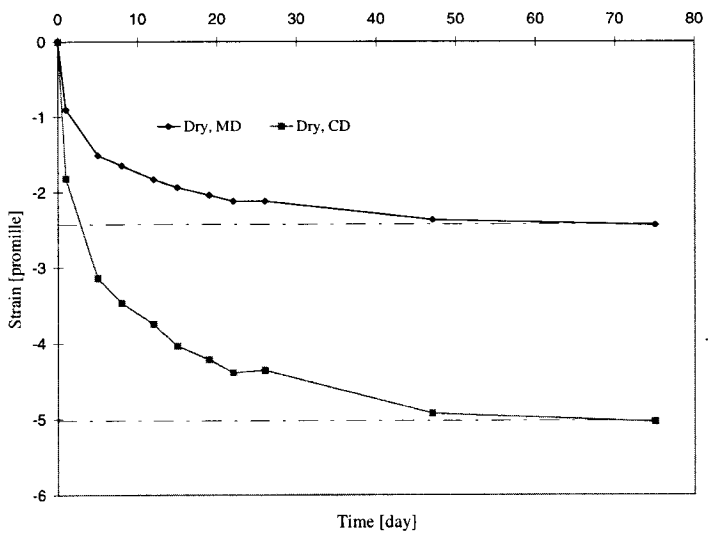

Figure S2 Measurement results from the dry chamber. Changes in strain are shown for machine and cross direction of the specimens.

- ***Measurement of Sorption Isotherm***

The sorption isotherm gives the moisture content of a material from close to 0% relative humidity up to a relative humidity near 100%. For determining the sorption isotherm curve, specimens are conditioned to equilibrium in a climate with a well-defined moisture condition. When the tests start, the specimens are placed in a new well-defined climate. The specimens are weighted regularly until a new equilibrium is reached. By using the measured weight obtained from the equilibrium, moisture content can be determined. The measured absorption and desorption isotherm of the HPL are shown in Figure S3.

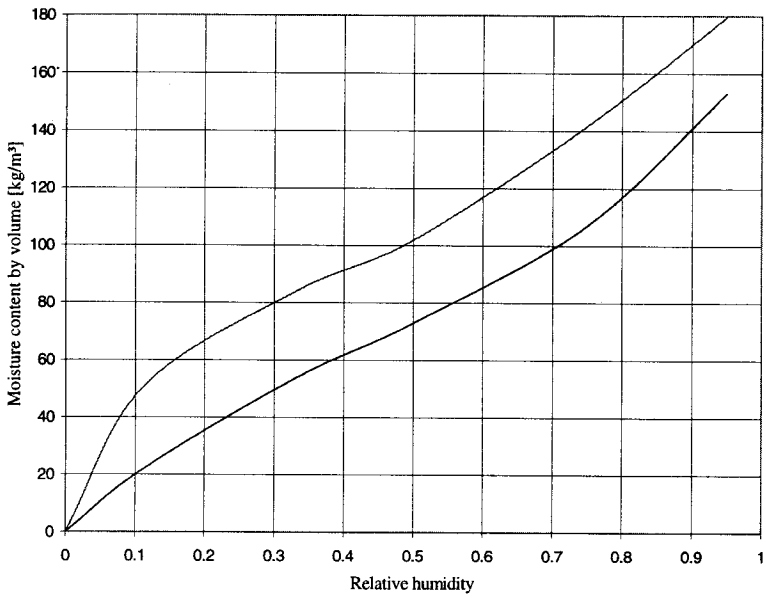

Figure S3 The sorption isotherm of the specimens. Each curve presents the mean value of the eight measurements.

- ***Measurement of Mechanical Properties***

Elastic modulus in both orthotropic directions and corresponding Poisson's ratios have been measured in different relative humidities in order to determine the influence of the moisture content on these properties. According to the results, the Young's modulus is sensitive to different levels of moisture content of the material. However the moisture content of the material has no influence on the Poisson's ratios. The measurement results, the elastic constants E_{MD}, E_{CD}, ν_{MDCD}, ν_{CDMD} and G, are presented in Table S1.

Table S1 The results obtained by static tension tests for determining elastic constants at different relative humidity levels.

RH [%]	E_{MD} [GPa]	E_{CD} [GPa]	ν_{CDMD}	ν_{MDCD}	G [GPa]*
32	17.68	12.37	0.250	0.347	5.712
50	17.45	12.23	0.250	0.346	5.644
95	15.74	10.90	0.243	0.347	5.082

* Estimated value according to Equation (1.6a)

- Comparison of the Calculated and Measured Results

Deformations in a simply supported plate have been measured for an experimental validation of the models. A comparison of the calculated results obtained by PC-programmes and measurement results confirm that the models can predict moisture induced deformation in a HPL plate, see Figures S4, S5. However, there are deviations between measured and calculated values. These deviations are acceptable within the limitations and assumptions of this study.

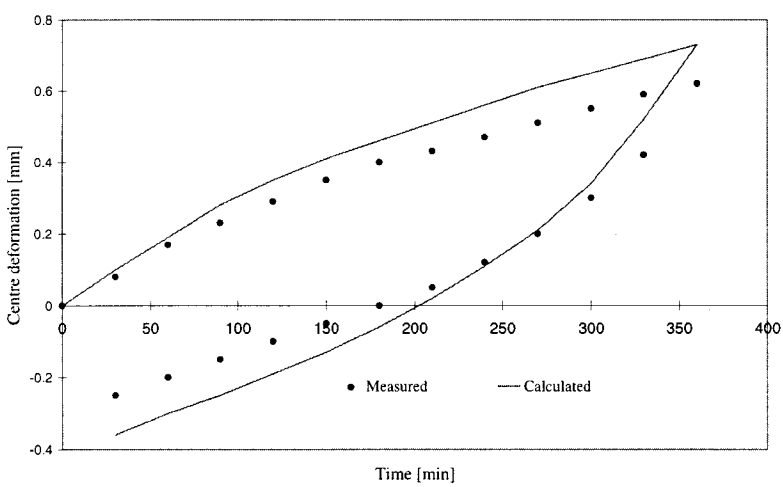

Figure S4 Comparison of the calculated and measured deformation for a simply supported specimen exposed to dynamic moisture loading.

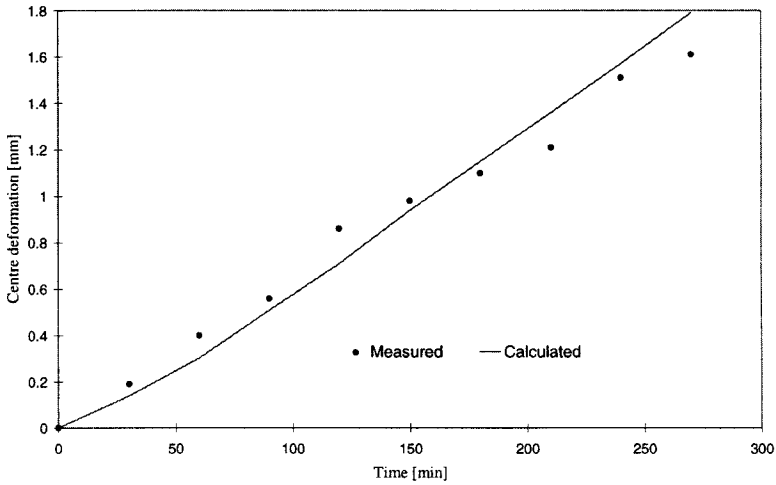

Figure S5 Comparison of the calculated and measured deformation for a simply supported specimen exposed to constant humidity difference.

LIST OF SYMBOLS

The following symbols are used in this work. Occasionally, the same symbols have been used to denote more than one quantity; they are identified when first introduced.

Part A

A	Area	[m^2]
a, b	Constants	[-]
D	Vapour diffusivity	[m^2/s]
d_1, h	Thickness of the material	[m]
d_2	The air gap height between the specimen and water surface	[m]
g	Moisture flow	[kg/m^2s]
m	Weight	[kg]
T	Temperature	[°C]
t	Time	[s]
u	Moisture content mass by mass	[%]
v	Humidity by volume	[kg/m^3]
v_s	Saturated humidity by volume	[kg/m^3]
w	Moisture content mass by volume	[kg/m^3]
w_0	Initial moisture content mass by volume	[kg/m^3]
x,y,z	Cartesian coordinate	[-]
Z	Moisture resistance	[s/m]
Z_{BR}	Surface moisture resistance	[s/m]
Z_{BL}	Surface moisture resistance	[s/m]
β_x, β_{MD}	Expansion coefficient in machine direction	[1/mc %]
β_y, β_{CD}	Expansion coefficient in cross machine direction	[1/mc %]
δ_v	Moisture permeability	[m^2/s]
ε_{MD}	Strain component in machine direction	[%]
ε_{CD}	Strain component in cross machine direction	[%]
ν_{MD}	Poisson's ratio in machine direction	[-]
ν_{CD}	Poisson's ratio in cross machine direction	[-]
ρ	Density	[kg/m^3]
ϕ	Relative humidity	[%]
Ψ	Kirchhoff potential	[kg/ms]

Part B

x, y, z	Cartesian coordinates	[-]
u, v, w	Displacement components in x, y, and z direction	[m]

M	External moment	[Nm]
m	Internal moment	[Nm/m]
m_{xy}	Twisting moment	[Nm/m]
P_z	External load	[N]
p_z	External load	[N/m^2]
p^*	Fictitious load	[N/m^2]
G	Shear modulus	[Pa]
E	Young's modulus	[Pa]
q	Transverse shear forces per unit length	[N/m]
n	In plane axial forces per unit length	[N/m]
γ	Shear strain	[%]
ε_x	Strain component in x-direction	[%]
ε_y	Strain component in y-direction	[%]
ϑ	Rotation angle	[-]
ν_{xy}, ν_{yx}	Poisson's ratio	[-]
σ	Normal stress	[N/m^2]
τ	Shear stress	[N/m^2]

Part C

m^i	Internal moment	[Nm/m]
m^m	Moisture induced moment	[Nm/m]
n^i	Internal axial force	[Nm/m]
n^m	Moisture induced axial force	[Nm/m]
C	Constant	[-]
I	Dimensionless moisture factor	[-]
R	Radius of curvature	[m]
K	Curvature	[1/m]
d_p	Penetration depth	[m]
t_{lag}	Time lag	[s]
δ	Deformation	[m]

1 Background

1.1 Definition

'Decorative High Pressure Laminate' is defined as " A sheet consisting of layers of fibrous sheet material (for example paper) impregnated with thermosetting resins and bonded together by means of heat and a pressure of not less than 7 MPa, a layer or layers on one or both sides having decorative colours or designs", [1].

The decorative High Pressure Laminate (HPL) under consideration is made from phenolic impregnated core layers of paper and a surface layer impregnated with melamine resin. These laminates are made in thicknesses from 0.6 to 30.0 mm. Furthermore, laminates from 2.0 to 30.0 mm are known as 'Compact Laminates'.

1.2 History

The production of laminate based on paper phenolic resin started already in the 1920's. This type of laminate was used as a surfacing material, for instance on cafe tables etc., right up to 1945. However, the major part of the laminate was used for technical purposes, especially in the radio industry (Isolit panels). After 1945, the melamine resin made its entry into laminate industry and from 1950, decorative plastic laminates with a melamine surface have been used to an ever increasing extent. The manufacturing process and the qualities of laminates have been improved since then and, consequently, new fields of application have been found. Today, laminates are widely used in applications such as construction (flooring, facade), furniture, inside ships and other transport vehicles [2]. In the United States and Canada there are some 10 laminate industries and in Europe there are some 50 producers of laminate. One of the best known among them is Perstorp AB in Sweden.

The properties of compact laminates depend on the types of resin and paper used in their manufacture, thickness and surface finish. About 16 properties are specified in the British Standard [3] for compact laminates products, e.g., dimensional stability, resistance to moisture, flatness, flexural strength, flexural modulus and tensile strength. HPLs offer many technical advantages which may be summarised in terms such as 'durability' and 'ease of maintenance' but probably the most important is that they are pre-finished and after fabrication need no protective finish.

1.3 Problem Identification

Almost all types of wood- and cellulose-based sheets are sensitive to environmental differences in temperature and moisture. The non-uniform distribution of moisture over a cross section of a sheet causes differential expansion or contraction. These differentials set up a state of internal stresses/strains even when no mechanical forces are applied to the plate. Under transient conditions, the stresses may vary from tension to compression or vice versa. Moisture induced strain can lead to a departure from a flat form in the form of a cup, twist, crook and bow. The form of the deformation depends on the boundary condition of the sheet, i.e., a sheet with fixed sheet edges does not deform and a free to deform sheet can take any form or a combination of the above mentioned deformations. Even uniform moisture distribution leads to a departure from flat form (due to moisture induced strain), if the cross section of the sheet is non-homogenous. A simple analogy might be the curving of a bi-metalic bar when subjected to varying temperature, see Figure 1.1.

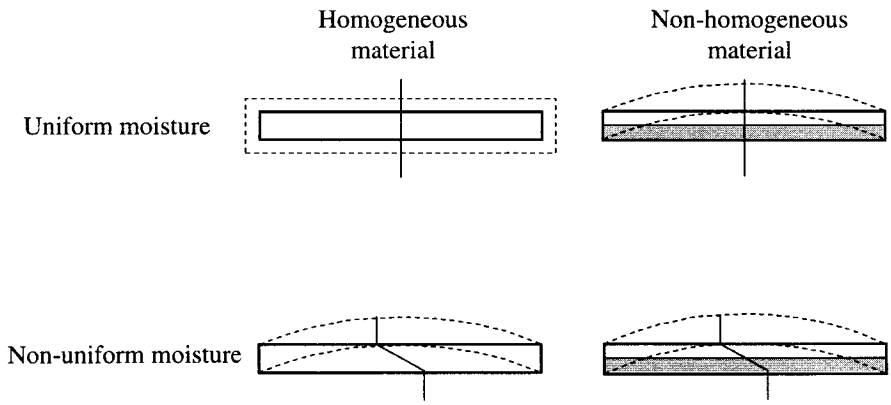

Figure 1.1 Four different cases of deformation for a homogenous and a non-homogenous material due to uniform and non-uniform moisture distribution.

HPL is made from layers of impregnated paper which is a composite and heterogeneous material. This means that even uniform moisture distribution over a cross section of the HPL can cause a departure from flat form. This deformation is not desired in the application of high pressure laminate in flooring and facade. Furthermore, free expansion/contraction of the HPL plates hindered by constructions results in forces acting on the coupling joints of the HPL plates.

The thickness of the HPL under consideration is small compared to its other dimensions. Thus, the determination of moisture induced deformations requires the in-plan mechanical properties of the HPL, the moisture distribution over the cross section and the expansion/contraction coefficients.

HPL plates are classified as a composite material and the mechanical behaviour of composite materials can be analysed in three classes of theoretical problems. They are:
I) interface problems involving the local interaction between fibre and matrix

II) problems concerning the relation of the composite properties and the properties of each individual component

III) the macroscopic behaviour of the composite as a whole

Here, the HPL is treated on the macroscopic scale. Thus, we will not distinguish between the materials which make up the HPL, but will regard it as a single homogeneous material with specified macroscopic properties. However, to be able to understand and assign the macroscopic behaviour of the HPL, it is essential to study its microscopic properties and behaviour. Thus, in Chapter 2, some of the paper properties, as basic elements in HPL which are relevant for this work, will be presented.

2 Properties of Paper

Paper is made from separated fibres from native raw material. Paper-makers reunite fibres into a consolidated structure and give the paper those properties that the user desires. The properties of fibres in paper do not coincide with those of the native wood fibre. The object of this chapter is not to cover all that is known about paper and the paper-making processes. It is rather to identify the properties and behaviours which could be assigned directly or by simplification to high pressure laminates.

2.1 The In-plane Anisotropy of Paper

It has been found in the research and development of paper that it can be considered as an anisotropic material on the macroscopic scale of observation. However, there are certain axes of symmetry, which for machine-made paper are in the machine direction (MD) and the cross machine direction (CD). This means that paper can be treated as an orthotropic material in the plane of the sheet [4].

2.2 Orientation of the Fibres through Thickness

The mode of formation of the paper on a paper machine is such that it will produce non-uniformity of orientation throughout the thickness. The suspension of pulp fibres released from the slice onto the wire cause a high degree of orientation of the fibers of the first layer in the direction of the flow or machine, on the wire side of the paper. Beyond this, further layers of fibers are oriented more randomly which means the pronounced orientation of fibers in the machine direction would be greatly reduced. Thus on the wire side, fibres are oriented in the machine direction and on the side away from the wire side, the topside, fibre orientation is more randomly. This non-uniformity of fibre orientation is called the two sidedness of the paper. For more information about two sidedness refer to [5-6].

2.3 Paper as a Visco-elastic Material

Börje Steenberg [7-9] showed that paper is a visco-elastic material. A visco-elastic material shows time-dependent deformation with constant load. The visco-elastic response of paper to stress can be characterised by immediate elastic deformations (recoverable), delayed elastic deformations (recoverable within periods of time), and delayed non-recoverable deformations.

Figure 2.1 shows the relation between stress and strain for paper when the paper was loaded at a constant rate of loading to a certain load and then unloaded at the same rate. The load was applied again but this time to a higher level. This cycle was repeated until the paper broke.

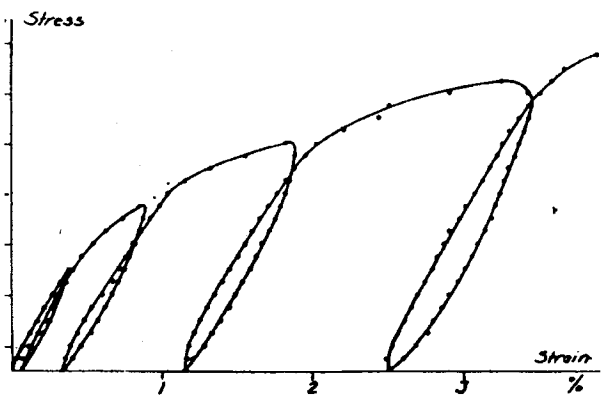

Figure 2.1 Stress-strain diagram for bleached sulphate paper (45° against machine direction). Constant rate of loading and de-loading, [7].

2.4 Influence of Moisture Content on Elastic Modules

As is not unusual, the elastic modules of the paper will be reduced with increased moisture content. This variation should be considered during the calculation of any kind of mechanical analyses. An example of load-extension curves for various relative humidities are shown in Figure, 2.2 [6].

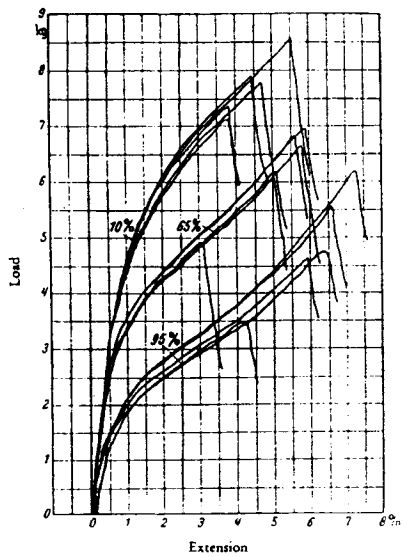

Figure 2.2 Load-extension diagram at different relative humidities obtained by pendulum tester, [6].

How the above mentioned behaviour and properties are going to be used in this thesis is explained in Chapter 4, where the scope and limitations of this work are presented.

3 High Pressure Laminate (HPL)

3.1 Build-up of Plastic Laminate

Plastic laminate is built up from phenol and melamine impregnated paper sheets, pressed together at a pressure of 9-10 MPa, and at a temperature of approx. 150°C. Due to the pressing, which in most cases is made against steel plates, a curing takes place and the plastic laminate gets its hard surface structure. Plastic laminate can be produced in many different qualities and many different surface finishes can be achieved, as well. It is built up according to the outlines in Figure 3.1.

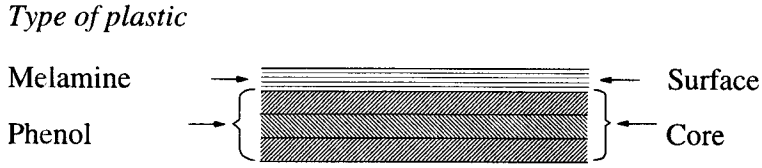

Figure 3.1 A schematic build-up procedure of HPL

By alterations in the build-up it is fairly easy to change the finish, the properties and the size. Here are some examples:

1. By inserting a different number of core sheets the thickness can be changed.
2. With different densities of paper sheets both thickness and properties can be changed.
3. Different paper qualities may influence the dimensional alteration.
4. The degree of impregnation (the quantity of plastic varnish in the core) influences the quality in many respects, for instance, the dimensional stability of laminates.

3.2 Manufacture of High Pressure Laminate

The manufacturing process can be divided into three major parts: impregnation, pressing and after-treatment. A short description of each part follows.

Impregnation: The paper web is run through an impregnation bath and immediately thereafter the web passes a drying oven, where the plastic varnish is partially cured. The web is then cut into various sizes. The impregnated sheets are pre-assembled or 'stacked' which means that core paper, pattern and surface sheets are stacked on each other, depending on the quality to be produced.

Pressing: The impregnated sheets are inserted between press plates in hydraulic presses. The temperature is approx. 150°C and a pressure of approx. 9-10 MPa is applied. The pressing takes place in a closed system. The total time of the press cycle is around 1 1/2 hour. These presses have often 20 - 36 openings and, in each pressing, 1000 - 2000 m^2 of decorative laminate in thickness 1.5 mm can be produced. The feeding in and out can be fully- or semi-automatic.

After-treatment: In the after-treatment the pressed sheets (the plastic laminate) are sawn to standard sizes and the back is often ground to give a substantial

glue attachment, facilitating the application of the laminate to various supporting materials.

3.3 Properties

Laminate is used as a surfacing material in such cases where heavy demands are made on the surface of the product. The following properties are characteristic of this material and contribute to make its field of application manifold and varied:

A high degree of surface hardness; scratch proof
A high resistance to heat and chemicals
High stability to light
Easy to clean
Free from maintenance

A property, very important to know of, is the dimensional change of the decorative laminate. The laminate suffers a dimensional change of around 3.0 mm/m latitudinally (CD) and around 1.5 mm/m longitudinally (MD) when the moisture of the air changes from 20 to 90 % relative humidity. The dimensional changes due to temperature can generally be neglected.

These dimensional changes in length and width depend on the fact that the core of the considered 'Perstorp decorative laminate' consists of impregnated paper in which the fibres are heavily stretched. The fibers are impregnated but, nevertheless, the moisture of the air can partly affect this fibre core. Therefore, the fibres can swell or shrink at changes in moisture, and each specific fibre swelling increases in width - the maximum increase amounting to around 3 mm/m. Longitudinally, the fibres go more into one another as a 'finger-joint' and the movement, in this case, is thus only half the magnitude.

4 Scope and Limitations

The scope of this work is to create a theoretical hygro-elastic model for the determination of moisture induced deformation in High Pressure Laminates. The model is based on the macroscopic behaviour of the HPL plates. Within this scope, numerical models are developed. Both validation of the theoretical and the numerical model are performed.

The HPL contains a core and decorative surfaces. In this work only the core part is considered. The analyses require a set of material properties. Measuring these material data for the core of the HPL is also a part of this work.

To be able to determine moisture induced deformations, one-dimensional transient moisture distribution in the direction perpendicular to the plane of HPL-plate should be known. To determine this distribution, moisture permeability and sorption curve of the HPL must be known. With a given moisture distribution, moisture induced stresses/strains can be calculated for different boundary conditions.

As with any theoretical model, this model is based on some hypotheses. Limitations are introduced, i.e., the total complex behaviour of the material is not covered in this studies.

4.1 Limitations and Hypotheses

4.1.1 Moisture Distribution

In the determination of the moisture permeability and the sorption curve of the HPL it is assumed that Fick's law is valid. The sorption isotherms for absorption and de-sorption are measured. The hysteresis effects are neglected and the sorption curve is simplified to a mean value of the absorption and desorption curve.

The stress/strain gradients are assumed to have a negligible influence on the diffusion process, which means that the moisture distribution can be determined independently from the stress analysis. The influence of the variation of the moisture content on the mechanical properties is, however, considered.

4.1.2 Mechanical Behaviour

On the macro-mechanical scale of observation, High Pressure Laminates can be considered as homogeneous, orthotropic materials. This homogeneity in the HPL is obtained during the production process. In manufacturing HPL, paper layers are stacked in such a way that a top side faces over a wire side.

Only the elastic part of the stress/strain relation will be treated. Moreover, as long as the HPL deforms within the elastic range, the stress field resulting from moisture distribution can be super-imposed upon the ones obtained from the external mechanical load.

Since the thickness of the HPL under consideration is small compared to its other dimensions, the mechanical behaviour will be treated by the use of the Kirchhoff plate theory for small deflections. The Kirchhoff plate theory for

small deflections is limited to deflection approximately less than a fifth of plate thickness.

4.2 The Course of Action

The procedure for determining moisture induced deformations in High Pressure Laminates is set out in Figure 4.1.

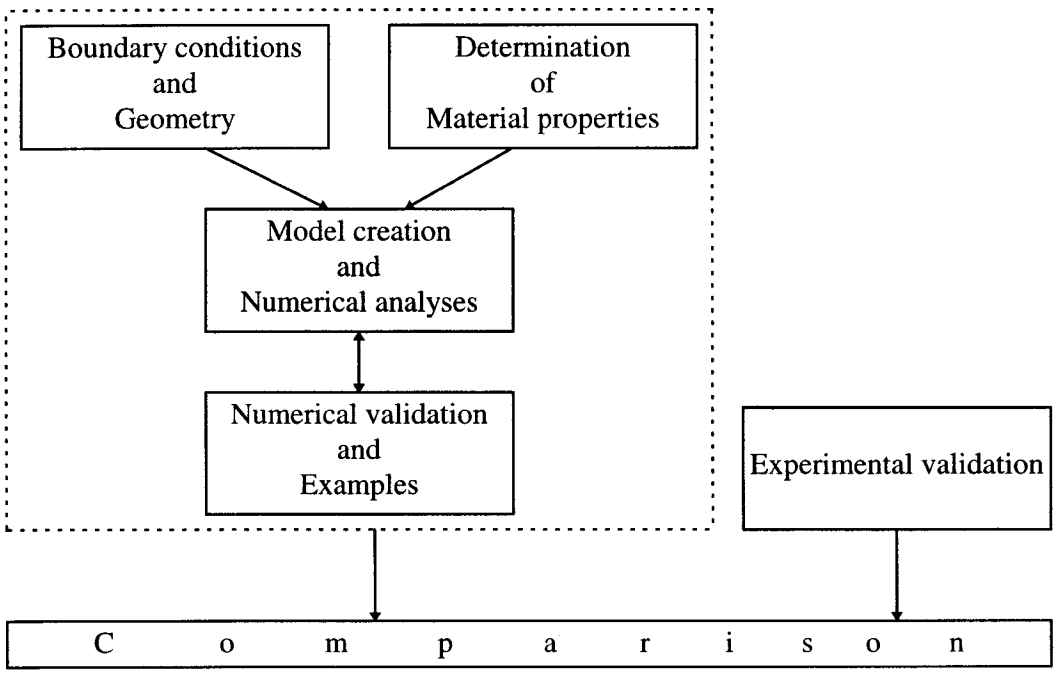

Figure 4.1 Procedure for determination of the model for moisture-induced deformations in High Pressure Laminates.

This thesis is divided into three parts. Part A deals with moisture properties and moisture distribution. In Part B, mechanical properties and mechanical behaviour are treated. Finally in Part C, hygro-elasticity is handled.

Part A, includes the measurements of all material moisture properties which are required, for instance, moisture permeability, the sorption isotherm curves and moisture expansion coefficients. The material properties and boundary conditions will be used in a numerical model for the calculation of moisture distribution. The results of the numerical calculation will be compared with the results of an existing program for numerical validation. The same procedure follows for Part B. The hygro-elastic model is set up in Part C. The numerical results obtained in Part C will be compared with experimental results.

5 References

[1] EN 438-2:1991 Decorative High Pressure Laminates [HPL] - Sheets Based on Thermosetting Resins- Part 2: Determination of Properties

[2] *Thomas C. Hoenigmn, An Introduction to High Pressure Laminates, Plastic Laminates Symposium 1996, Page 5-15, Tappi*

[3] BS 4965: 1991 Decorative Laminated Plastics Sheet Veneered Boards and Panels.

[4] *Alan R. Jones, An Experimental Investigation of the In-plane Elastic Module of Paper, Tappi, May 1968 Vol. 51, No.5, Page 203-209*

[5] *P. Glynn, H. W. H. Jones and W. Gallay, The Fundamentals of Curl in Paper, Pulp and Paper Magazine of Canda, October 1959*

[6] *W. Gallay, Stability of Dimensions and Form of Paper, Tappi, Vol. 56, No. 12, Dec. 1973, page 90-95*

[7] *Börje Steenberg, Paper as a Visco-elastic Body I , Svensk Papperstidning, Årg. 50, Nr 6. 31 mars 1947*

[8] *Börje Steenberg, Paper as a Visco-elastic Body II , Svensk Papperstidning, Årg. 50, Nr 15. 15 aug. 1947*

[9] *Börje Steenberg, Paper as a Visco-elastic Body III , Svensk Papperstidning, Årg. 50, Nr 18. 30 sept. 1947*

Part A Transient Moisture Distribution

Part A Transient Moisture Distribution

Paper is a porous material, thus high pressure laminates are also porous. In High Pressure Laminates, papers are impregnated and because of this the porosity of the HPL is lower than for paper. An electron microscopic picture of a paper before and after impregnation and pressing is shown in Picture 1.

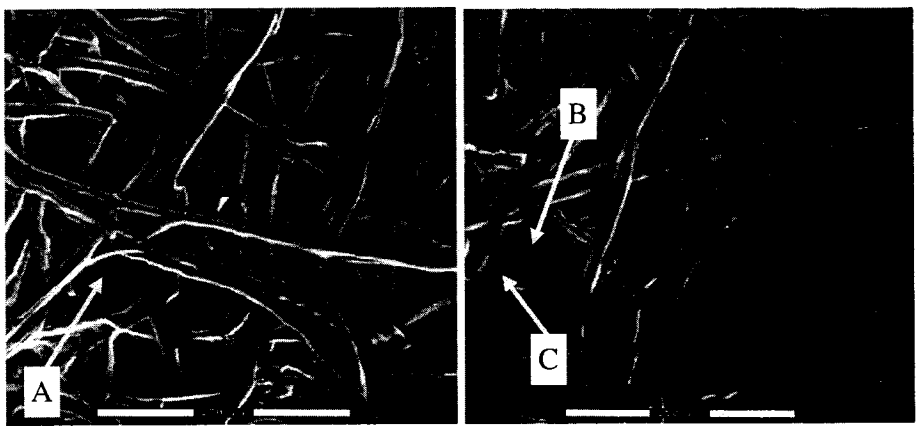

a) b)

Picture 1 An electron microscopic picture, SEM, of a paper before and after impregnation and pressing. The dark bar in the picture represents 250 μm. a) Non-impregnated paper. b) Impregnated paper.

In non-impregnated paper, in addition to pores in the fibres, the fibres create a network of pores, see arrow A in Picture 1a. The pores are covered partly by a polymer film during the impregnation process, see arrow B, but there are still gaps in the film, arrow C in Picture 1b. This means that the network of pores in the HPL is reduced by impregnation but the HPL remains a porous material.

1 Theory of Moisture Transport in Porous Material

A hygroscopic material has the capacity to store water molecules at the inner surfaces of its pore system. The equilibrium moisture content of the material depends on the relative humidity, ϕ (%), and the temperature, T (°C), of the ambient air. The pore system is normally very complicated. There is absorbed moisture on the surfaces, capillary condensed water in pores, water absorption by solid structure (cell walls and edges), and the remaining pore volume is filled with humid air. The moisture is stored in both liquid and vapour phases. Since it is difficult to exactly identify the different states of the moisture, because of continuous changes in the ratio of each phase of moisture in the material, it is useful to take their total sum. The moisture content mass by volume, w (kg/m^3),

of the porous material is a function of relative humidity and temperature. In building physics applications, effects of temperature and differences between absorption and desorption isotherm, hysteresis phenomena, are normally neglected. This means that the water storage capacity is given by a simple function w(ϕ).

1.1 Isothermal Moisture Flow, Fick's Law

Fick's law is applicable for moisture flow in porous material. Consider a slab with thickness *h*. See Figure 1.1. The one-dimensional moisture flow through the slab area is denoted by *g* (kg/m^{2}s). According to Fick's law, for isothermal conditions, the moisture flow in the x-direction becomes:

$$g = -\delta_v \frac{\partial v}{\partial x} \tag{1.1}$$

Here v(x,t) (kg/m^3) is the humidity by volume and δ_v (m^2/s) is the moisture permeability, which may vary strongly with the relative humidity.

1.2 Conservation Equations, Boundary Conditions and Initial Values

The moisture balance equation based on the law of conservation is fundamental for the determination of the moisture distribution in the porous material. This has been treated and discussed by many authors. Therefore, only the basic equations will be presented here.

The moisture distribution for any time and space, w(x,t), can be obtained from solutions of the moisture balance equation, Equation (1.2a). Equation (1.2b) gives the boundary conditions at the left- and right-hand side of the slab (x=-h/2, x=h/2), and Equation (1.2c) describes the initial moisture content.

$$-\frac{\partial}{\partial x}\left(-\delta_v \frac{\partial v}{\partial x}\right) = \frac{\partial w}{\partial t} \tag{1.2a}$$

$$-\delta_v \left.\frac{\partial v}{\partial x}\right|_{x=-h/2} = \frac{v_{BL} - v(-\frac{h}{2}, t)}{Z_{BL}}, \quad -\delta_v \left.\frac{\partial v}{\partial x}\right|_{x=h/2} = \frac{v(\frac{h}{2}, t) - v_{BR}}{Z_{BR}} \tag{1.2b}$$

$$w(x,0) = w(\phi_0) = w_0 \tag{1.2c}$$

The boundary value for the humidity by volume is denoted by v_{BL} for the left-hand side, and v_{BR} for the right-hand side. The corresponding surface moisture

resistances are denoted by Z_{BR} and Z_{BL} [s/m]. The initial constant moisture content of the slab is w_0, which corresponds to a material in equilibrium with ambient air at the relative humidity of ϕ_0.

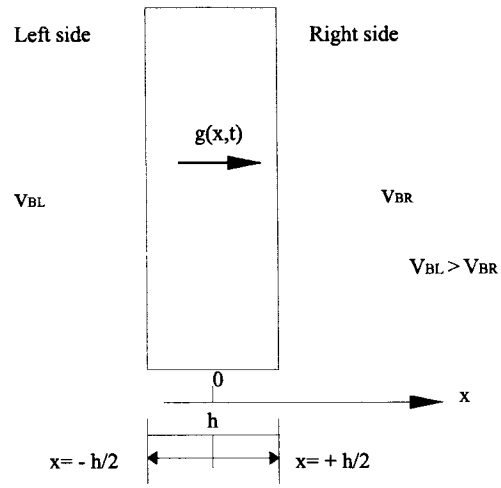

Figure 1.1 The one-dimensional moisture flow g (kg/m^{2}s) in a slab with thickness h.

Equations (1.2a-c) give the foundation for the determination of one-dimensional transient moisture transport. They will be used in the numerical calculations and in the interpretation of the measurements.

2 Measurement

2.1 Measurements of Moisture Permeability

The purpose of these measurements, in addition to determining the moisture permeability at different relative humidity, is to investigate the influence of thickness on moisture permeability.

Here, it should be mentioned that in a homogenous material the thickness of the material has no influence on the moisture permeability, at least as long as Fick's law is valid. A High Pressure Laminate is assumed to behave as a homogenous material. However, due to manufacturing processes (high temperature and pressing) there is a possibility that there is an influence of the thickness on the moisture permeability of the specimens. Because of this, it is important to investigate influence of the thickness on moisture permeability.

The cup method is used for measuring the moisture permeability of the plastic laminates in the study. In the measurements, three relative humidity differences over the specimens are used. For each case, three thicknesses of the plastic laminates are investigated.

2.1.1 Short Description of the Cup Method

In the cup method, a cup is sealed with a specimen (plastic laminate), see Figure 2.1. There is distilled water in the cup which can sustain a relative humidity close to 100 %. The cup is placed in an atmosphere of constant temperature and relative humidity, the latter is lower than 100 %, either in a climate box or directly exposed to the air of the climate chamber. The relative humidity is higher inside the cup than outside, which results in a moisture flow outwards through the specimen, thus, the weight of the cup will decrease. The cup is weighed regularly until steady-state condition is reached, i.e. constant weight loss during a given period of time. The moisture resistance can then be calculated by Equation (2.4). It should be noted that the moisture resistance Z refer for difference in v, i.e. humidity by volume. When the moisture resistance of the specimen is determined, the moisture permeability can be calculated by Equation (2.5). The following relations are valid:

$$g = \frac{\Delta v}{Z_{tot}} \tag{2.1}$$

$$Z_{tot} = Z_{specimen} + Z_{air\ gap} + Z_u \tag{2.2}$$

$$Z_{specimen} = Z_{tot} - Z_{air\ gap} - Z_u \tag{2.3}$$

The first term, $Z_{specimen}$, in Equation (2.2) represents the moisture resistance of the material, and the second term, $Z_{air\ gap}$, the vapour resistance of the air gap between the water surface and specimen. The third term, Z_u, represents the outer surface vapour resistance, i.e. the resistance between the surface of the specimen and the surrounding air. The outer surface moisture resistance has been estimated to 100 s/m, using the Lewis formula with the convective transfer coefficient obtained from the case of forced convection with an air speed of 2 m/s in the climate box [3]. The moisture resistance of the specimen becomes:

$$Z_{specimen} = \frac{A \cdot \Delta t \cdot \Delta v}{\Delta m} - \frac{d_2}{0.025 \cdot 10^{-3}} - Z_u \qquad (2.4)$$

Here Δm [kg] is the weight reduction over a time period of Δt. A is the area of the specimen, d_2 is the air gap height between the specimen and the water surface. The moisture permeability of the specimen becomes:

$$\delta_v = \frac{d_1}{Z_{specimen}} = \frac{d_1}{\frac{A \cdot \Delta t \cdot \Delta v}{\Delta m} - \frac{d_2}{0.025 \cdot 10^{-3}} - Z_u} \qquad (2.5)$$

Here, the thickness of the specimen is denoted by d_1.

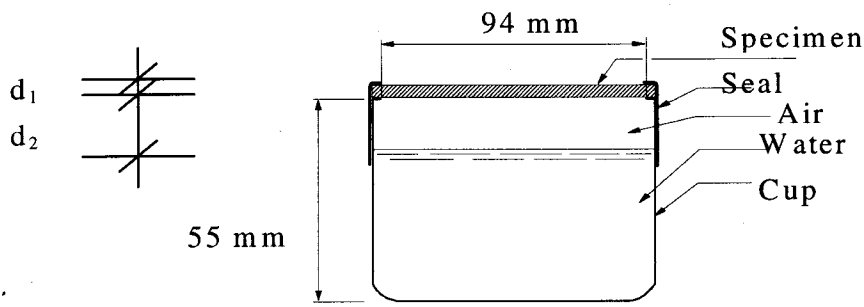

Figure 2.1 Schematic description of the cup.

2.1.2 Relative Humidity

In the measurements, it is important to keep relative humidity and temperature constant over a long period of time. A climate chamber, keeping a constant relative humidity (50 %) and constant temperature (20°C) is therefore used. The accuracy of the temperature and relative humidity is within ± 0.4 °C and ± 3 %. The chamber is used to control the atmosphere outside the cups when 50 % relative humidity is needed. A relative humidity, outside of the cup, of 11% or 75% is sustained by placing open jars with saturated salt solutions in moisture

tight boxes, coded as climate boxes. The climate boxes are also placed in the climate chamber to sustain constant temperature. By choosing these RH-levels the major part of the hygroscopic region was covered.

The salts used in the climate boxes are of high quality (< 1% impurities). The relative humidity in the climate boxes is measured by a moisture sensor (Tiny Tag), for confirmation of the condition of the saturated solution.

Table 2.1 Relative humidity given by saturated salts for maintaining specified relative humidity, [1].

Salt	RH [%] at 20.0 °C
Lithium chloride	11.3±0.3
Natrium chloride	75.5±0.1

The choice of these salts is based on the fact that they remain stable during moderate temperature changes.

2.1.3 Climate Box

The climate boxes, see Figure 2.2, are made of solid PC (Poly Carbonate) which makes them both air- and moisture tight. The volume of the climate box is 380 x 280x 230 mm^3. To reduce the surface vapour resistance between the specimen and the conditioned air, a fan is mounted on one of the short sides of the climate box. The gross effect of the fan is 1.5 W, and the air flux is 0.56 m^3/min. The fan is enclosed in the climate box, which means that the air in the climate boxes is separated from the air in the climate chamber.

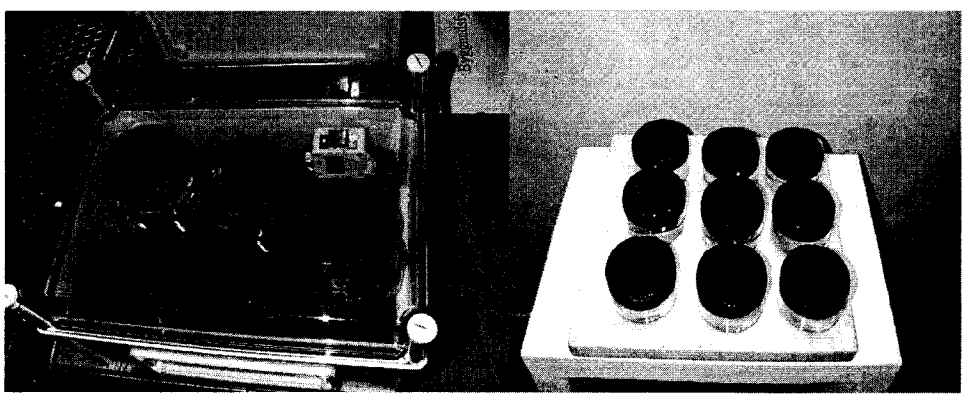

Picture 2 Photos of cups in climatic box and climatic chamber.

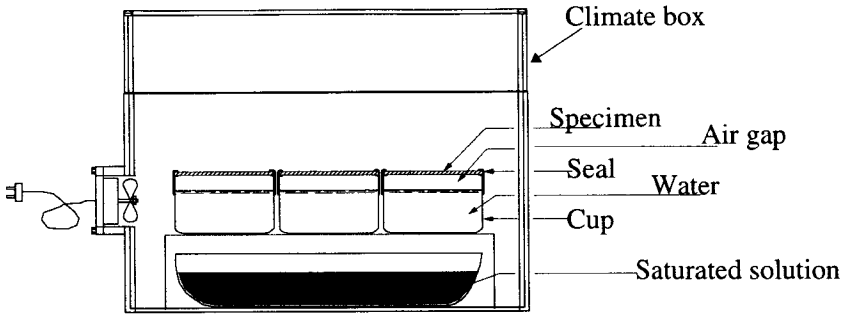

Figure 2.2 Set-up in the climate boxes.

2.1.4 Specimens

The specimens have a circular form with a diameter of about 94 mm and thicknesses of 2, 4 and 6 mm. Different thicknesses are chosen in order to find out if the thickness has any effect on permeability. Maximum and minimum of the thickness are presented in Table 2.2. According to this table, it is obvious that the specimens' thicknesses are not exactly 2, 4 and 6 mm, but these values are used as a classification number (CN) for each thickness.

Table 2.2 Variation in specimen thickness.

CN	Max. Measured value [mm]	Min. Measured Value [mm]
2	1.73	1.68
4	3.95	3.82
6	5.66	5.57

Twenty-seven specimens are prepared, three specimens for each relative humidity level (3 levels), and for each thickness (3 thicknesses). All the specimens, of the same thickness class, are taken from the same laminate plate. The laminate plates had been stored in the same environment,T=20°C and RH= 40%, before testing. The specimens are mounted on to cups in such a way that no effects of masked edges are expected. Specimens are denoted as follows: 'S' for Specimen, followed by number of specimen (Number 1 to 3), thickness classification (2,4 or 6), and the relative humidity in the climate chamber or box. Thus, code S1-2-50 means specimen number 1, with a thickness of 2 mm and 50% relative humidity in the chamber.

2.1.5 Measurements and Weighing

The maximum load of the balance is 1200 g, and the weighing resolution is 1 mg. The weight of the cups is about 400 g, and the decrease in weight was between 100 mg and 1 mg between each weighing.

The cups were weighed regularly until a steady-state condition was reached. It should be mentioned that the samples, which were in the climate boxes (11 % and 75 % relative humidity), were removed to climate chamber (50% relative humidity) for weighing. This means that the specimens could absorb or desorb moisture. The amount of moisture absorption or desorption was checked for a specimen with a weight of about 3.5 g. This control showed that the amount of absorbed or desorbed moisture from the top layer of the specimen on the cup during a measurement period lasting about 5 minutes, was about 1.5 mg which is less than 0.05% of the total weight. This deviation from the true weighing value is neglected because in calculating moisture permeability, the mass difference between two weightings is used.

2.1.6 Evaluation of the Results

The moisture permeability of the plastic laminate is determined by measured weight losses and Equation (2.5). Figure 2.3 presents the typical development of the moisture permeability for 2 mm thick specimens from the start until steady-state condition is reached. The figures for 4 and 6 mm specimens are presented in Appendix A:1.

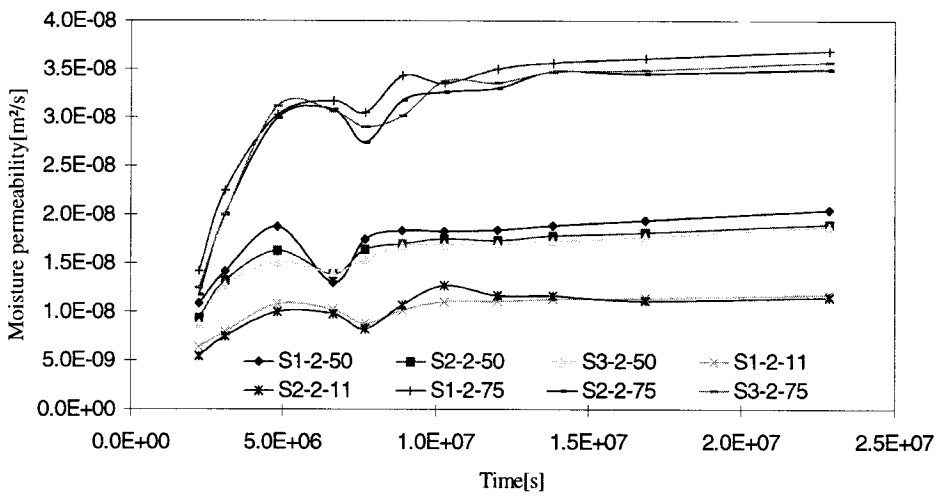

Figure 2.3 Development of the estimated moisture permeability, δ_v, for 2 mm specimens at different relative humidity differences during 290 days. The result of specimen S3-2-11 is excluded due to leakage.

The drop in moisture permeability in Figure 2.3 is caused by a decreased temperature in ambient air. The measurement results for 75% and 50% RH are not quite steady at the end of measurement, 290 days, but they are very close to steady-state condition. It is assumed that this deviation from the steady-state condition has a minor effect on determining the moisture permeability of the specimens.

2.1.6.1 Influence of the Thickness

The mean value of the measured moisture permeability as a function of the mean relative humidity for 2, 4 and 6 mm thick specimens is shown in Figure 2.4 and Table 2.3. The time which is required to reach steady-state conditions depends on the thickness of the specimen and the difference in the relative humidity. For example, it takes at least 8 months for a 6 mm thick specimen to reach steady-state condition with a 25% relative humidity difference.

The measured vapour permeability is associated with the mean value of the relative humidity on the inside and outside of the cups. This is a simplified way of treating the data, since the relative humidity is not linearly distributed within the specimen. In the next chapter, the variation of moisture permeability with relative humidity will be treated more accurately by the use of the Kirchhoff potential.

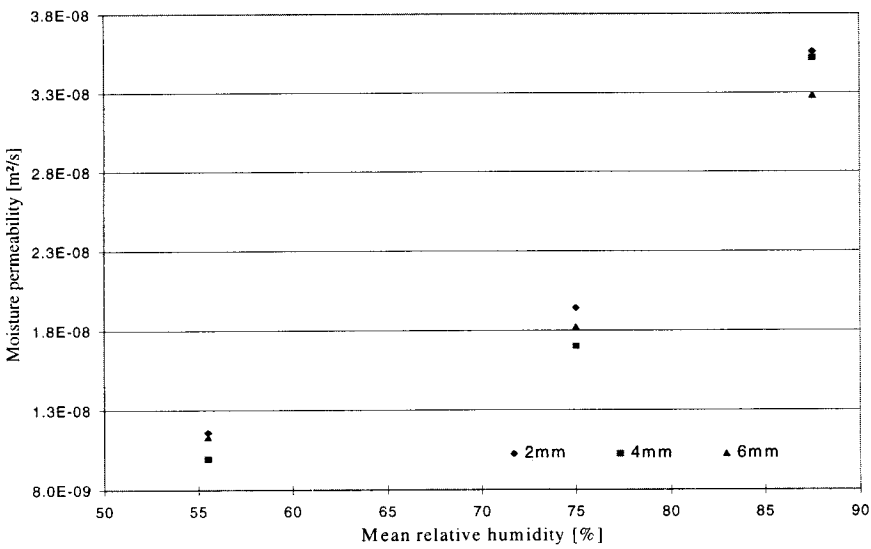

Figure 2.4 Mean moisture permeability, $\overline{\delta}_v$, as a function of the mean relative humidity on the in- and outside of the cup at different thicknesses. Each point represents the mean value of three measurements.

Table 2.3 Moisture permeability, $\bar{\delta}_v$ [10^{-8} m^2/s], as a function of the mean relative humidity for different thicknesses. Each point represents the mean value of three measurements.

Mean relative humidity	Thickness[mm]		
	2	4	6
55.5 %	1.16	0.99	1.13
75.0%	1.94	1.70	1.82
87.5%	3.56	3.52	3.28

According to Figure 2.4 and Table 2.3, the maximum difference in moisture permeability due to different thickness does not exceed 15 % . No specific pattern for any influence of thickness can be identified. The differences may depend on variation in the manufacturing process, as well as the precision and accuracy of the measurements. The conclusion is that there is no influence, or only a negligible one, of thickness on the moisture permeability of the specimens.

2.1.6.2 Precision and Accuracy of the Measurement

The specimens behave as a homogenous material, since there is no influence of thickness on moisture permeability. This means that the results of each relative humidity (measurement results of nine specimens), without considering thickness differences, can be used for the determination of the moisture permeability at each respective relative humidity level. Any uncertainty of the measurement can also be treated by using the measurement values of each relative humidity. It should be mentioned, that in determining the uncertainty of the measurements, the simplified method is considered. In the simplified method, the moisture permeability is associated to the mean relative humidity of the specimens, i.e. the mean values of the in- and outside relative humidity, see Table 2.4.

Table 2.4 The mean value of the inside and outside of the cup

$\phi_{\text{Inside cup}}$ [%]	$\phi_{\text{Outside cup}}$[%]	($\phi_{\text{Inside cup}}$+ $\phi_{\text{Outside cup}}$)/2 [%]
100	11	55.5
100	50	75
100	75	87.5

The uncertainty of the results of a measurement reflects the lack of exact knowledge of the value of the measurand. The result of a measurement after correction for recognised systematic effects, the systematic error, is still only an estimate of the value of the measurand. This is due to the uncertainty arising

from random effects, the random error, and from an imperfect correction of the result for systematic effects.

A: Systematic error

The parameters in Equation (2.5) are used in order to determine the error in moisture permeability. The errors in the different parameters are of different types, for instance, the measured area of the specimens contains an error but this error is the same regardless of the testing event or test material. On the other hand, there are parameters which may vary from measuring event to measuring event. For instance, changes in the relative humidity and temperature of the chamber and climatic boxes may occur. Because of this complexity of errors, a full error analysis is very complicated. A relatively good estimation of a systematic error can be obtained by using a simplified formulation of the maximum systematic error according to Equation (2.6).

$$\Delta\delta_{max} = \left|\frac{\partial \delta}{\partial A}\Delta A\right| + \left|\frac{\partial \delta}{\partial (\Delta m)}\Delta(\Delta m)\right| + \left|\frac{\partial \delta}{\partial (\Delta v)}\Delta(\Delta v)\right| + \left|\frac{\partial \delta}{\partial d_2}\Delta d_2\right| + \left|\frac{\partial \delta}{\partial d_1}\Delta d_1\right| \quad (2.6)$$

The systematic error of the micrometer and the balance are 30 μm and 1 x 10^{-6} kg, respectively. The radius of the circular specimen, r, the specimen thickness, d_1, and the air gap, d_2 are measured by micrometer. Thus, Δr, Δd_1 and Δd_2 are equal to 30μm. The weight of the cups is measured by the balance, thus $\Delta(\Delta m)$ is $1x10^{-6}$. The systematic error of the humidity by volume, Δv, depends on the systematic error of the relative humidity sensor and temperature sensor. After calculating the systematic error of the humidity by volume, Δv, becomes $4x10^{-4}$ kg/m^3. Furthermore, the error in the area depends on the measurement of the radius of the circular specimen. The area of a circle is πr^2. Thus, the systematic error of the specimen area becomes:

$$A + \Delta A = (r + \Delta r)^2 \cdot \pi = \pi \cdot r^2 + 2 \cdot \pi \cdot r \cdot \Delta r + (\Delta r)^2 \cdot \pi$$

The value of $(\Delta r)^2$ is very close to zero. Thus, ΔA is equal to $2 \cdot \pi \cdot r \cdot \Delta r$. Finally, the systematic error of the variables in Equation (2.6) becomes:

$$\Delta r = \Delta d_1 = \Delta d_2 = 30\ \mu m$$
$$\Delta m = 1 \times 10^{-6}\ kg,$$
$$\Delta v = 4 \times 10^{-4}\ kg/m^3$$

The accuracy of the measurements for each thickness at different relative humidity differences is presented in Table 2.5.

Table 2.5 The maximum value of the relative systematic error of the moisture permeability at different relative humidity levels

RH%	Accuracy[%]			Comments
	2mm	4mm	6mm	
55%	± 4.5	± 3.4	± 3.2	Climate box
75%	± 4.2	± 3.3	± 3.0	Climate chamber
87.5%	± 5.3	± 4.3	± 4.1	Climate box

The thickness of the specimen has no influence on the measured moisture permeability, thus in determining the accuracy of the measurements, mean values are used for each relative humidity, see Table 2.6.

Table 2.6 The accuracy of the measurement as a function of the mean of the relative humidity of the in- and outside.

RH[%]	55	75	87.5
Accuracy[%]	± 3.7	± 3.5	± 4.6

As mentioned before in this thesis, it is the 6 mm thick laminates which are under consideration. Maybe it would seem more accurate to account only for the accuracy of the measured moisture permeability for the 6 mm thick specimen. However, due to the assumption that the HPL is a homogenous material, using the mean value of the accuracy of the specimens is reasonable. However, it should be mentioned that the mean accuracy is lower than the accuracy of the 6mm thick specimen, cf. Tables 2.5 and 2.6.

B: Random Error

Random errors presumably arise from the unpredictable and spatial influence of quantities. This error can be reduced by increasing the number of observations. The standard uncertainty of the mean value of the measurement due to random effects is calculated by Equations (2.7) and (2.8).

$$s(\delta_v) = \sqrt{\frac{\sum_1^n (\delta_{v,k} - \bar{\delta}_v)^2}{n - 1}} \qquad (2.7)$$

$$s(\bar{\delta}_v) = \frac{s(\delta_v)}{\sqrt{n}} \qquad (2.8)$$

where

$s(\delta_v)$ = Experimental standard deviation
$\bar{\delta}_v$ = Arithmetic mean
n = Number of measurements
$s(\bar{\delta}_v)$ = Experimental standard deviation of the mean

Table 2.7 shows that there is a spreading of the measured values.

Table 2.7 Mean value, standard deviation, experimental standard deviation of the mean and relative precision of the mean value of the measured moisture permeability.

RH [%]	$\bar{\delta}_v$ [10^{-8}m^2/s]	$s(\delta_v)$ [10^{-8}m^2/s]	$s(\bar{\delta}_v)$ [10^{-8}m^2/s]	$s(\bar{\delta}_v)/\bar{\delta}_v$ [%]
55.5	1.08	0.12	0.041	3.7
75	1.82	0.14	0.045	2.5
87.5	3.44	0.19	0.063	1.8

With 95% probability, the mean values of moisture permeability are in the following ranges:

$$0.99 \cdot 10^{-8} < \bar{\delta}_{v,55\%} < 1.17 \cdot 10^{-8}$$
$$1.72 \cdot 10^{-8} < \bar{\delta}_{v,75\%} < 1.92 \cdot 10^{-8}$$
$$3.30 \cdot 10^{-8} < \bar{\delta}_{v,87\%} < 3.59 \cdot 10^{-8}$$

From the approximation according to the simplified method, the moisture flow for the three cup method tests, with the prescribed relative humidity differences, can be calculated accurately. However, for other differences in relative humidity they must be handled with care. For a more accurate analysis see section 2.1.7.

C: Total Error

The maximum uncertainty, which is the sum of the systematic and random error of the measurements is presented in Table 2.8.

Table 2.8 The maximum uncertainty of the measurements of moisture permeability.

RH[%]	55	75	87.5
Uncertainty [%]	± 7.4	± 6	± 6.5

According to Table 2.8, which gives the sum of the systematic errors of the mean value in Table 2.6 and the random errors Table 2.7, the maximum uncertainty of the measurement is in the range of ±6 % to ± 7.4 % for different relative humidities in the specimen.

2.1.7 Treatment of Measurement Data by the Kirchhoff Potential

There is a flow potential, the Kirchhoff potential, for which the moisture flow coefficient is equal to 1. For a one-dimensional case the moisture flow is obtained by Equation (2.9). For more information about the Kirchhoff Potential refer to [2] and [3].

$$g = -\frac{\partial \psi}{\partial x} \quad D_{\psi} \equiv 1 \tag{2.9}$$

According to Equation (2.9), the dependence of the moisture flow coefficient on the moisture state variable vanishes. Considering a one-dimensional steady-state condition:

$$g_i \cdot d_1 = \psi(\phi_0) - \psi(\phi_i) \tag{2.10}$$

The reference level ψ (ϕ_0) can be chosen arbitrarily. In the following, the reference level ϕ_0 will be chosen to be 100%.

$$\psi(\phi_0) = \psi(100) = 0 \tag{2.11}$$

This gives:

$$\psi(\phi_i) = -g_i \cdot d_1 \tag{2.12}$$

Here g_i refers to the moisture flow rate for the case of the relative humidity equal to ϕ_0 inside the cup and ϕ_i outside the cup. A positive value of g, represents the net outflow from the cup. The thickness of the specimen is d_1. By using Equation (2.12), the relation between ϕ and ψ can be determined. The moisture transport coefficient (δ_v) can be calculated by a derivation of the $\psi(\phi)$ curve. According to Fick's law the moisture flow is:

$$g = -\delta_v \frac{\partial v}{\partial x} \tag{2.13}$$

By using the chain rule in Equation (2.13) we get:

$$g = -\delta_v \frac{\partial v}{\partial x} = -\delta_v \frac{\partial \psi}{\partial x} \frac{\partial \phi}{\partial \psi} \frac{\partial v}{\partial \phi} \tag{2.14}$$

Equations (2.9) and (2.14) give:

$$-\frac{\partial \psi}{\partial x} = -\delta_v \frac{\partial \psi}{\partial x} \frac{\partial \phi}{\partial \psi} \frac{\partial v}{\partial \phi} \Rightarrow \delta_v \frac{\partial \phi}{\partial \psi} \frac{\partial v}{\partial \phi} = 1 \tag{2.15}$$

With $\frac{\partial v}{\partial \phi} = v_s$, Equation (2.15) can be rewritten as:

$$\delta_v = \frac{\partial \psi}{\partial \phi} \frac{1}{v_s} \tag{2.16}$$

A new potential, ψ', is introduced:

$$\psi' = \frac{\psi}{v_s} \tag{2.17}$$

Equation (2.16) can then be written as:

$$\delta_v = \frac{\partial \psi'}{\partial \phi} \tag{2.18}$$

It follows, from Equation (2.11) that $\psi' = 0$ for ϕ_0=100%. From (2.12) we get:

$$\psi'(\phi_i) = -\frac{g_i \cdot d_1}{v_s} \tag{2.19}$$

Equation (2.13) can be rewritten as:

$$g_i = -\bar{\delta}_{v,\bar{\phi}} \frac{(v_i - v_0)}{d_1}$$

Here, $\bar{\phi}$ is the mean value of the relative humidity in- and outside the cup, see Table 2.4. With this moisture flow, Equation (2.19) can be rewritten as:

$$\psi'(\phi_i) = -\bar{\delta}_{v,\bar{\phi}} \cdot (\phi_0 - \phi_i) \tag{2.20}$$

Where ϕ_i is given by the outside relative humidity of the cups, i.e., relative

humidity levels 0.11, 0.5 and 0.75.

By using Equation (2.20) and the measured moisture permeability given in Table 2.7, ψ' can be calculated for the different relative humidity differences.

$$\psi'(0.75) = -\bar{\delta}_{v,87} \cdot 0.25,\ \psi'(0.50) = -\bar{\delta}_{v,75} \cdot 0.50,\ \psi'(0.11) = -\bar{\delta}_{v,55} \cdot 0.89$$

Table 2.9 Value of ψ' calculated by Equation (2.20).

RH [%]	ψ' [10^{-8} m^2/s]
11	- 0.97
50	- 0.91
75	- 0.86
100	0

Figure 2.5 shows the relation between ψ' and the relative humidity.

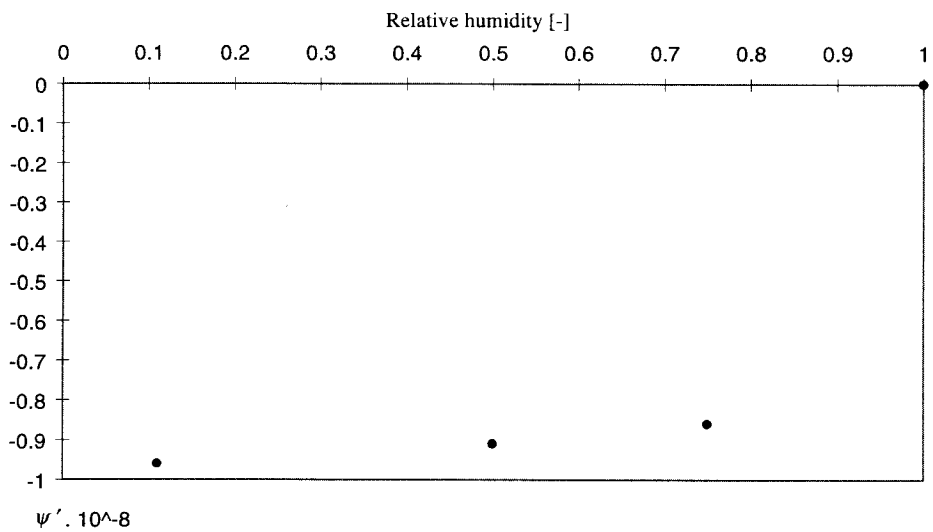

Figure 2.5 The potential ψ' as a function of relative humidity

The next step is to fit a curve to these values, and to use Equation (2.18) to estimate the variation of the moisture permeability as a function of the relative humidity.

2.1.8 Strategy of Curve Fitting

The values of ψ' will be corrected by the total uncertainty for each relative humidity difference, in accordance with Table 2.8. Figure 2.6 shows that it is possible to fit a straight line between the three first points (relative humidity range 11% to 75%). This means that the moisture permeability which can be calculated from the slope of this straight line, is constant at least up to 75% relative humidity. The relation between the last two points (relative humidity range 75% to 100%) is assumed to follow a parabolic curve.

- Determining ψ'

I- The low relative humidity range, $\phi \leq \phi_{bp}$

The minimum and the maximum slopes of the curve are estimated. The minimum slope is zero, this means that it is possible to draw a straight line parallel to the axes of relative humidity (dashed line in the figure).The calculated ψ' value and the range of the correction are shown in Figure 2.6.

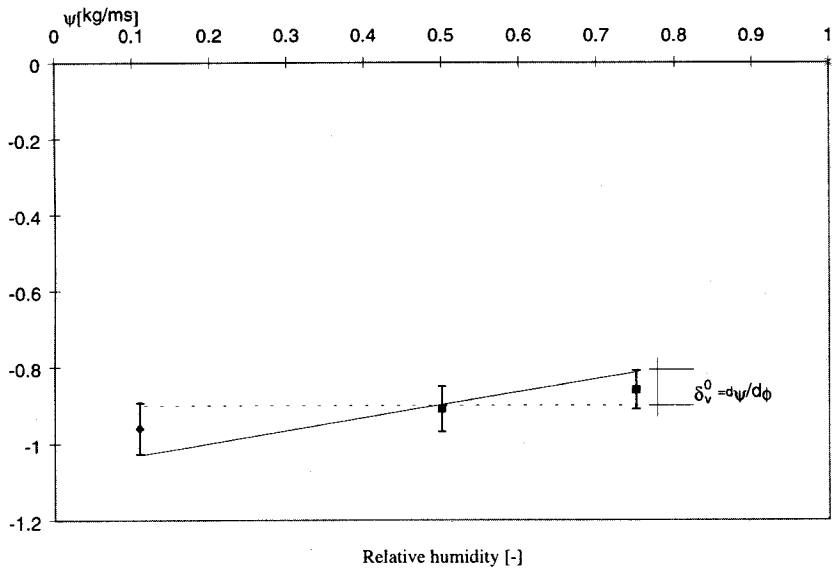

Figure 2.6 The curve fitting in the range of 11%-75% relative humidity. The slope of the curve determines the moisture permeability for low relative humidities.

When the slope of the line is close to zero, it means that the moisture permeability of the specimen is very close to zero. The maximum slope is the slope of the line between the lowest value at 11% relative humidity and the highest value at 75% relative humidity. The maximum and minimum values

indicate that the moisture permeability, δ_v^0 , of the specimen lies between these values.
An approximation of the ψ'-curve in the low range of relative humidity up to a break point ϕ_{bp} becomes:

$$\psi' = \delta_v^0 \cdot \phi + b \qquad \phi \le \phi_{bp} \qquad (2.21)$$

Where b is a constant.

II- The high relative humidity range, $\phi < \phi_{bp} \le 100$

A parabolic curve is fitted to the values of ψ' in the range of ϕ_{bp} and 100% relative humidity. With this type of approximation, the ψ'-curve will be continuous for both the curve and slope. The equation for the curve becomes:

$$\psi'(\phi) = (\phi - \phi_{bp})^2 \frac{a}{2} + \delta_v^0 \phi + b \qquad \phi \ge \phi_{bp} \qquad (2.22)$$

Here, ϕ_{bp} is the same break point as in Equation (2.21) and b is the same constant.

The moisture permeability above the break point is given by a straight line between δ_v^0 and $\delta_v(1.0)$:

$$\delta_v = \delta_v^0 + (\phi - \phi_{bp}) \cdot a \qquad \phi \ge \phi_{bp} \qquad (2.23)$$

From the requirement for the curve in Equation (2.21) to pass the point $\psi'(0.75)$ we can determine the b-value.

$$b = \psi'(0.75) - \delta_v^0 \cdot 0.75 \qquad (2.24)$$

The value of ψ' at ϕ = 1.0 is equal to zero. From Equation (2.22) we get:

$$0 = (1 - \phi_{bp})^2 \frac{a}{2} + \delta_v^0 \cdot 1 + b \qquad (2.25)$$

Combining Equations (2.24) and (2.25) the value of the parameter 'a' can be determined.

$$a = -\frac{(\delta_v^0 + b) \cdot 2}{(1 - \phi_{bp})^2} = -\frac{(\delta_v^0 \cdot 0.25 + \psi'(0.75)) \cdot 2}{(1 - \phi_{bp})^2} \qquad (2.26)$$

Using Equations (2.23) and (2.26), the value of the moisture permeability at 100% relative humidity can be calculated.

$$\delta_v(1.0) = \delta_v^0 + \frac{(-\psi'(0.75) - 0.25 \cdot \delta_v^0) \cdot 2}{1 - \phi_{bp}} \qquad (2.27)$$

The choice of 80 % instead of 75 % as the relative humidity for the break point is examined. It is not reasonable to chose a higher level than 80 % as a break point of the fitting curve, because the diffusion coefficient of almost all wood based panels increases at levels even lower than 75%. The result of these curve fittings are shown in Figure 2.7.

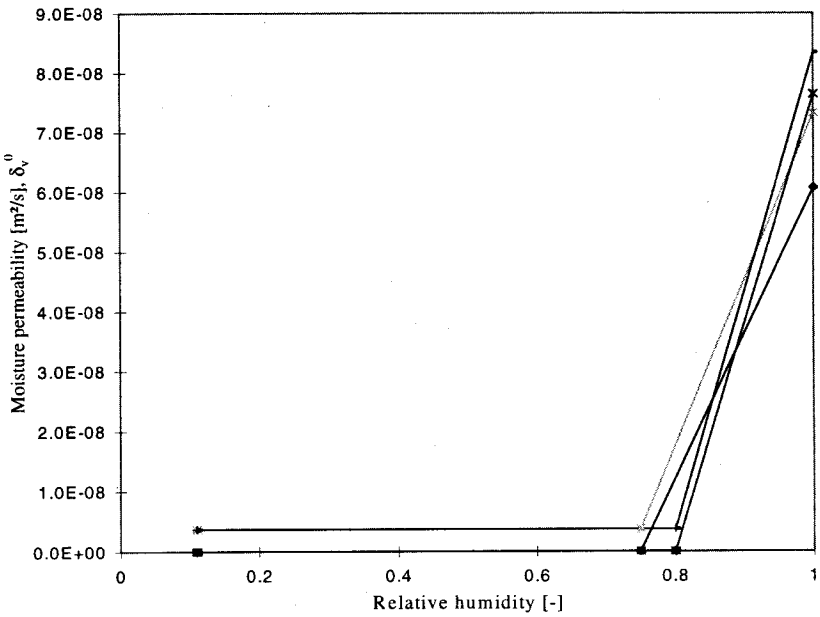

Figure 2.7 Results of the curve fittings using 75% and 80% as break points for the curve.

Finally, the moisture permeability of the specimen could be within the interval shown in Figure 2.8. A curve which is a mean value of the fitted curves, in the marked area of Figure 2.8, will be used for further calculations.

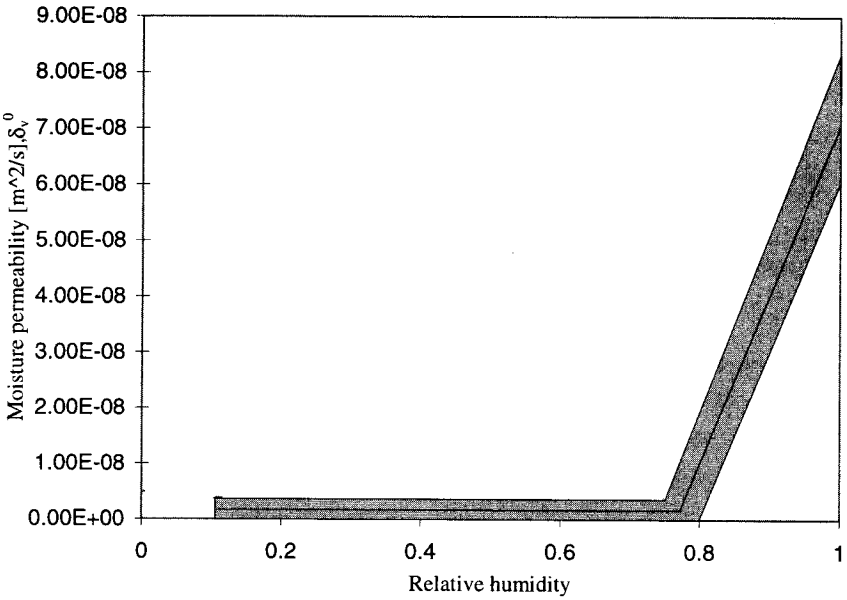

Figure 2.8 The interval of moisture permeability. The mean value of this interval is shown.

2.2 Determination of Sorption Isotherm

The sorption isotherm, or the moisture equilibrium curve, gives the moisture content of a material from close to 0 % relative humidity up to a relative humidity near 100%. Normally, two types of sorption curves are of interest, the absorption and desorption curves. The slopes of these curves are called the moisture differential capacity. The moisture differential capacity indicates the capacity of the observed material for moisture storage.

The measurements of the moisture permeability of High Pressure Laminates with thicknesses of 4-6 mm, indicate that the time scale of the measurement is about 5-12 months, depending on the thickness of the specimens and the accuracy of the measurement. Because of this, the determination of the sorption isotherms is carried out for much thinner specimens than the ones which are used for the determination of moisture permeability. The advantage of using thinner specimens is a shorter measuring time, but on the other hand, it should be proved that the thickness of the specimens has no influence on the sorption curve. However, results obtained from the determination of moisture permeability demonstrate that the thickness of the samples has no influence on moisture transport. This might also be interpreted as a positive sign for determining the sorption curve by using thinner specimens.

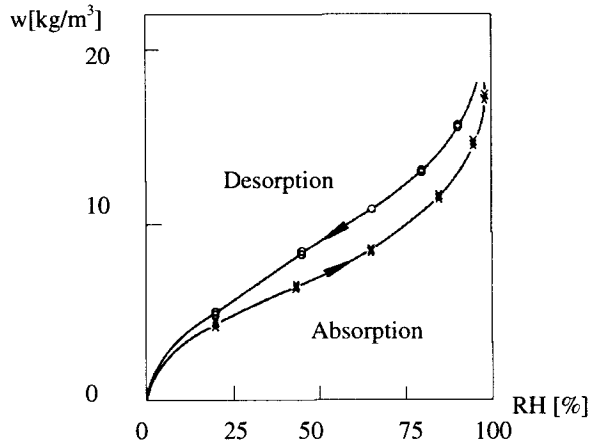

Figure 2.9 A schematic sorption curve. The absorption curve always lies under the desorption curve.

2.2.1 Measurement Method

For the determination of the sorption isotherm curve, specimens were conditioned to equilibrium in a climate with a well-defined moisture condition. When the test starts the specimens were placed in a new, well-defined climate. The specimens were weighed regularly until a new equilibrium was reached. By using the measured weight obtained from the equilibrium and dry weight of the

specimens, the moisture content mass by mass could be determined. When the moisture content mass by mass for each relative humidity level is known, the moisture content mass by volume can be calculated by Equation (2.28).

$$w = u \cdot \rho_{dry} \tag{2.28}$$

w	Moisture content mass by volume	[kg/m^3]
u	Moisture content mass by mass	[kg/kg]
ρ_{dry}	Dry density	[kg/m^3]

According to Equation (2.28), in order to calculate the moisture content mass by volume, the dry density of the material is needed. The dry density of the material is determined at 105 °C to 1384 kg/m^3 and the procedures in prEN ISO 12570 are followed.

2.2.1.1 Relative Humidity

The specimens were conditioned to 95% and 0% as initial relative humidities and the temperature of the climate room was 20°C. The specimens which were conditioned to 95%, were placed in climates of 75%, 50%, 33% , 11% relative humidity and finally dried to 0%. In the same manner, the specimens which were first oven-dried and then, are placed in 11%, 33%, 50% , 75% and finally 95% relative humidity. The relative humidities are sustained by saturated salts according to the same procedures used during moisture permeability measurements. In these measurements, the procedures in prEN ISO 12571 are followed.

Table 2.10 Relative humidities given by saturated salts for maintaining specified relative humidity, [1].

Salt	RH at 20.0 °C
Magnesium chloride	33.1±0.2
Potassium nitrate	94.6±0.7

2.2.1.2 Specimens

Thin specimens, which contain one sheet (about 0.17 mm) and two sheets, were produced. The process of producing these sheets is the same as for the production of the core of the plastic laminates. The specimens have a square form, and the size of the specimens was chosen so that the weight was at least 2 grams, in order to full fill the recommendation of the prEN ISO 12571. Eight specimens of each thickness were prepared for measuring absorption and desorption curves.

2.2.1.3 Weighing

The specimens were weighed with the same balance that was used for determining moisture permeability. The specimens hung under the balance when the specimens were conditioned for 50% relative humidity (see Picture 3). Specimens in climate boxes were temporarily moved to 50 % relative humidity for measurements.

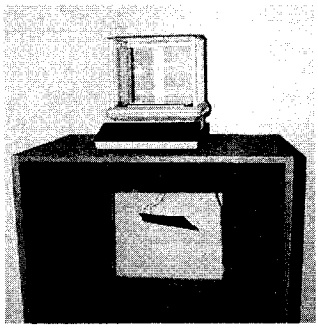

Picture 3 Test arrangement when the specimen were conditioned to 50% relative humidity.

2.2.2 Results and Discussion

Results of the one sheet and two sheet specimens are presented in Figure 2.10. These results are chosen randomly for each thickness for a comparison of the sorption curves of one sheet and two sheet specimens. Figure 2.10 shows that there is almost no deviation between the two curves.

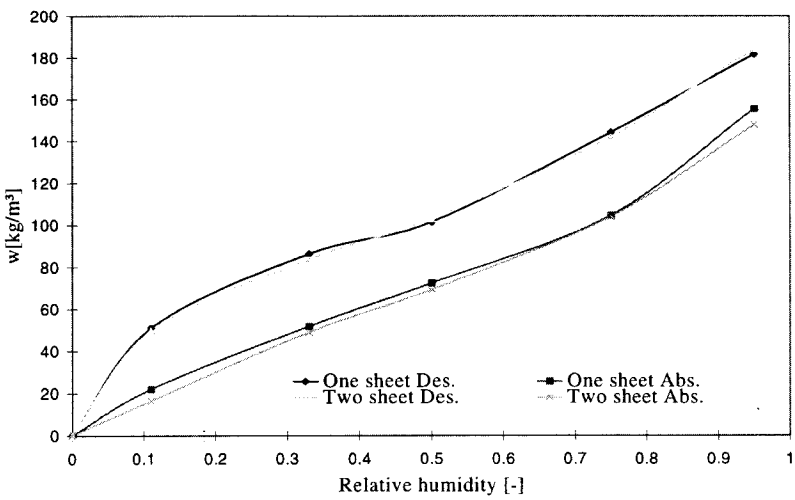

Figure 2.10 Isotherm sorption curve for one sheet and two sheet specimen.

This means that the thickness of the specimen has no effect on the isotherm sorption curve and it is possible to use the thinner ones in order to speed up the

measurements.

Since the thickness has no influence on the sorption isotherm, the results from all the specimens, four specimens for each thickness, can be analysed together. The mean value of the measured sorption curves for these eight specimens is presented in Figure 2.11. The sorption isotherm presented in Figure 2.11 will be used in coming calculations.

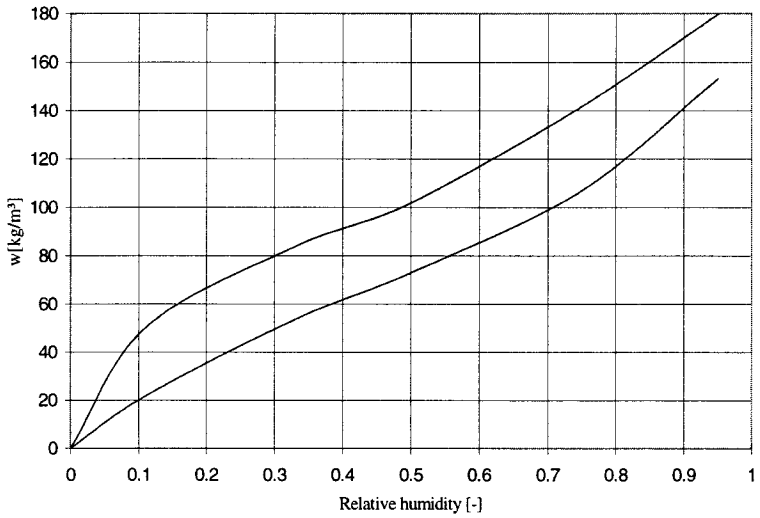

Figure 2.11 The sorption isotherm of the specimens. Each curve presents the mean value of eight measurements.

2.3 Measurement of Hygro Expansion Coefficient

As mentioned before, HPL is an orthotropic material. An orthotropic material has different hygro expansion coefficients, β, in different directions. Thus, the hygro expansion coefficient of a High Pressure Laminate should be determined in both the machine and cross direction of the specimen.

Measurements for determining expansion coefficients were done by Perstorp AB. In these measurements, the hygro expansion coefficients were determined for specimens with different thicknesses and specimens with and without an overlay. The scope of this work is focused on 6 mm thick specimens without overlay. This is the reason why, in this chapter only the measurement results for the 6 mm thick specimens without overlay will be presented and interpreted.

2.3.1 Test Conditions

Specimens, 12x120mm, were cut out in each direction and conditioned in ambient air (30 % RH, 20°C). The expansion and contraction of each direction, MD and CD, were measured for the longest size of the specimen, 120 mm. The specimens were placed in two different climatic chambers. The conditions of the chambers are presented in Table 2.11.

Table 2.11 Conditions in the chambers.

Chamber	RH [%]	T[°C]
Dry chamber	0-50	70
Wet Chamber	95	40

As presented in Table 2.11, the temperatures of the chambers were higher than the temperature used when determining the moisture permeability and the sorption isotherm of the HPL. These high temperatures have been chosen in order to reduce the time of measurement.

2.3.2 Results

Measurement results are presented in Figures 2.12 and 2.13. In Figure 2.12, the total contraction in both directions after drying from 30 % to 0 % relative humidity and, in Figure 2.13, the total expansion after wetting from 30% to 95% relative humidity in both directions, are presented. Dashed lines in these figures show the final value of the strain in the longitudinal direction of the specimens.

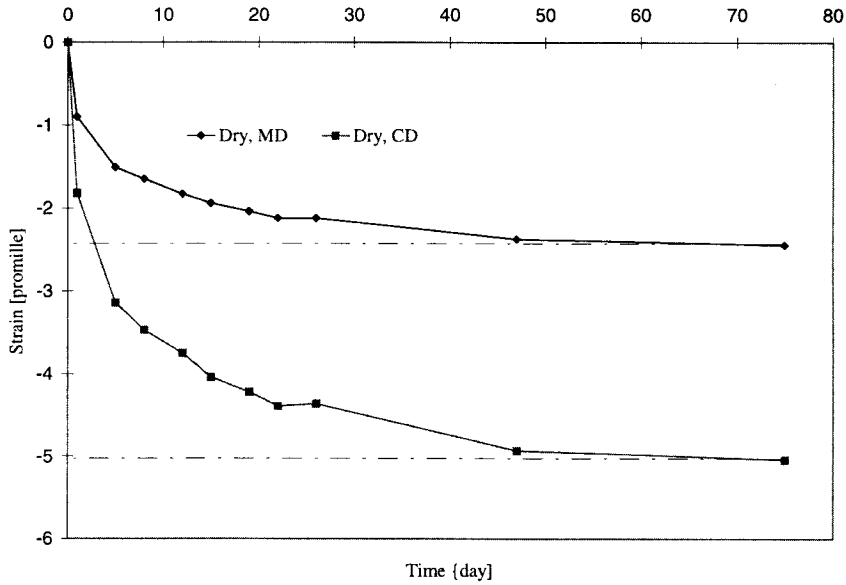

Figure 2.12 Measurement results from the dry chamber. Changes in strain are shown for machine and cross direction of the specimens.

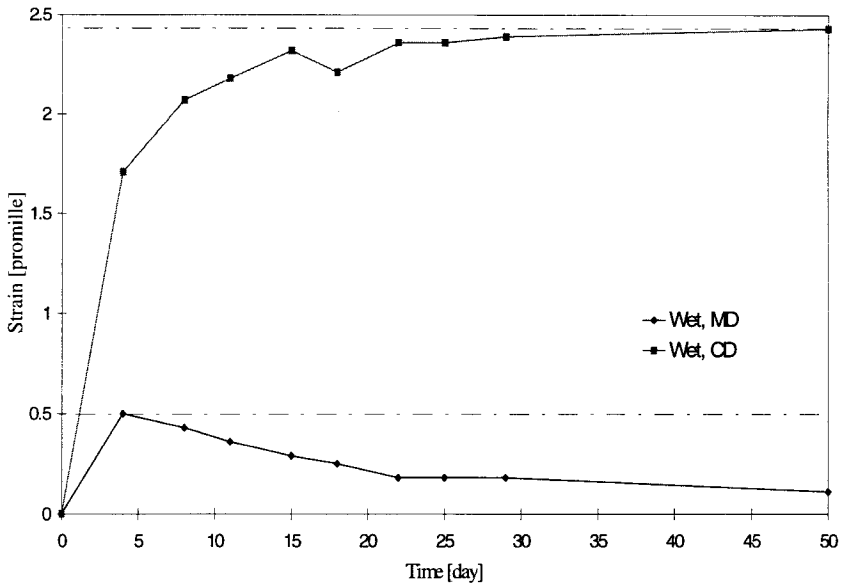

Figure 2.13 Measurement results from the wet chamber. Changes in strain are shown for machine and cross direction of the specimens.

2.3.3 Discussion and Analysis of Measurement Results

The total expansion/contraction of the 6 mm thick specimen has been presented in Figure 2.12-2.13. The maximum expansion/contraction results (dashed lines in figures) are presented in Table 2.12.

Table 2.12 The maximum total strain of the specimens in different directions

	Max. Strain MD [promille]	Max. Strain CD [promille]
Dry	-2.5	-5.0
Wet	+0.5	+2.4

These measurement results indicate that the strain induced by the contraction (drying) of the specimen is always higher than the strain induced by expansion (wetting). This can be explained by a softing of the material (matrix and fibres) during wetting. For instance, the strain induced by expansion in MD, the dominant fibre orientation, is almost close to zero.

The results of the measurement also show that the specimens have different hygro expansion coefficients in the contraction and expansion phases. The contraction of the CD is about two times larger than the contraction of the MD, and in the expansion phase, the expansion of the CD is about five times higher than the MD. These relations between the contraction/expansion of the CD and MD are almost the same for specimens thicker than 4 mm.

The measured total expansion and contraction is related to changes in relative humidity in the order of 30 % and 65 %. For further calculations, hygro expansion/contraction coefficient per percent moisture content mass by mass is needed. By using the measured sorption isotherm, dry density and Equations (2.28), the hygro expansion coefficient can be calculated.

When the free expansion of the specimen is not hindered, the relation between moisture induced strain and the expansion/contraction coefficient, β, can be obtained by using Equations (2.29).

$$\varepsilon_{MD} = (\beta_{MD} + \nu_{MD} \cdot \beta_{CD}) \cdot \Delta u - \nu_{MD} \cdot \varepsilon_{CD} \tag{2.29a}$$

$$\varepsilon_{CD} = (\beta_{CD} + \nu_{CD} \cdot \beta_{MD}) \cdot \Delta u - \nu_{CD} \cdot \varepsilon_{MD} \tag{2.29b}$$

Poisson's ratio and the strain in the machine and cross directions are denoted by ν_{MD}, ν_{CD} and ε_{MD}, ε_{CD}. Here the ν_{MD} and ν_{CD} are the measured Poisson's ratio in

the machine and the cross directions (see Part B, Determination of Mechanical Properties).

Explicit expressions for the hygro expansion/contraction coefficients, β_{MD} and β_{CD}, as functions of ε_{MD} and ε_{CD} can be obtained from the equation system (2.29).

$$\beta_{MD} = \frac{\varepsilon_{MD}}{\Delta u} = \frac{\varepsilon_{MD} \cdot \rho_{dry}}{\Delta w} \tag{2.30a}$$

$$\beta_{CD} = \frac{\varepsilon_{CD}}{\Delta u} = \frac{\varepsilon_{CD} \cdot \rho_{dry}}{\Delta w} \tag{2.30b}$$

Here, the relation in (2.28) has been used.

The hygro expansion and contraction coefficients for MD and CD are calculated by Equation (2.30). The results of these calculations are presented in Table 2.13a.

Table 2.13a Calculated hygro expansion and contraction coefficients for MD and CD

	β_{MD} (x10^{-2})[1/mc %]	β_{CD} (x10^{-2})[1/mc %]
Contraction	4.4	9.0
Expansion	0.7	3.4

The contraction values are obtained by using data from drying from 30 % to zero relative humidity. We assume a constant β-value over this interval. Furthermore, we assume that drying from even higher relative humidities will result in the same β-value. A corresponding assumption is done for β-value obtained for the wetting, 30→95% relative humidity.

The expansion/contraction values presented in Table 2.13a can be used in analyses when only contraction or expansion is under consideration. If contraction and expansion occur at the same time in different surfaces of the HPL, the total expansion/contraction in Table 2.12 is assumed to be related to whole span of the relative humidity, 0-95%, and for each directions. By using this assumption and the measured values, Figures 2.12 and 2.13, the expansion and contraction coefficients are calculated. The results of the calculations are presented in Table 2.13b.

Table 2.13b Calculated hygro expansion/contraction coefficients for MD and CD.

β_{MD} (x 10^{-2})[1/mc%]	β_{CD} (x 10^{-2})[1/mc%]
2.5	6.2

The values in Table 2.13b are used for analyses when expansion and contraction are combined.

2.4 Penetration Depth and Time Scale of Diffusion Process

The penetration depth and the time scale of the sorption and diffusion process can be determined from a one-dimensional analytical solution of Equation (1.2a). In this solution the moisture permeability (δ_v) is assumed to be constant and the sorption curve is linear.

The penetration depth and the time scale of the moisture transport process through the slab can be formulated when the boundary values change from w_0 to w_1.

2.4.1 Step Change of Boundary Moisture Contents

The initial moisture content of the slab, w_0, and moisture changes at the boundaries are shown in Figure 2.14. The solution gives the response to a step change at both boundaries.

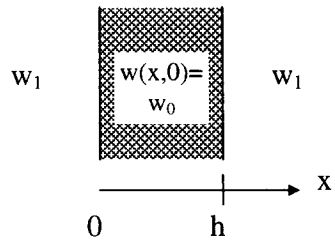

Figure 2.14 Initial moisture content and change at boundaries.

By using the Fourier series technique, the solutions becomes, [4]:

$$w(x,t) = w_1 + \frac{4(w_0 - w_1)}{\pi}\sum_{n=0}^{\infty}\frac{1}{2n+1}\sin\left(\frac{(2n+1)\cdot\pi\cdot x}{h}\right)\cdot e^{-\frac{((2n+1)\pi)^2 Dt}{h^2}} \qquad (2.31)$$

The first term of the Fourier series dominates. The series converges rapidly except for small values of Dt/h^2. A rapid convergens can be obtained by using the error function solution, Equation (2.32):

$$0 \le t \le \frac{h^2}{36D}$$

$$w(x,t) = (w_0 - w_1)\cdot\left(\operatorname{erf}\left(\frac{x}{\sqrt{4Dt}}\right) + \operatorname{erf}\left(\frac{h-x}{\sqrt{4Dt}}\right) - 1\right) + w_1 \qquad (2.32)$$

The vapour diffusivity a is defined by $D = \dfrac{\delta_v \cdot v_s}{dw/d\phi}$.

Equation (2.31) can be rewritten by using the normalised, dimensionless moisture function, F. The dimensionless moisture function, F(x,t) lies in the interval between 0 and 1. At time zero, F is equal to one, which gives w equal to w_0. At infinite time, F is equal to zero, i.e. w will become equal to w_1.

$$F = \frac{w(x,t) - w_1}{w_0 - w_1} = \frac{4}{\pi} \cdot \sum_{n=0}^{\infty} \frac{1}{2n+1} \sin\left(\frac{(2n+1) \cdot \pi \cdot x}{h}\right) \cdot e^{-\frac{((2n+1)\pi)^2 Dt}{h^2}} \qquad (2.33)$$

Let x_p denote the x-coordinate for which F = *p:*

$$F(x_p, t) = p \qquad 0 \le p \le 1$$

The time for which 50% of the difference between the initial moisture value and the final moisture level, F = 0.5, at x_p = h/2, is reached can be calculated by using Equation (2.33).

$$F(h/2, t) = 0.5 \Rightarrow t = \frac{h^2}{10.5\ D} \qquad (2.34)$$

The time, t, in Equation (2.34), gives the time scale for the moisture changes in the slab. After this time, the slab becomes considerably influenced by the new moisture condition of the surface, since half the total change has been reached in the middle of the slab.

By using Equations (2.31) and (2.32), the moisture distribution, due to the step change from 0% to 50% relative humidity in the slab, is calculated for two thicknesses, see Section 2.4.2.

2.4.2 Calculation of the Time Scale for Thick and Thin Specimens

The moisture decline according to Section 2.4.1 was calculated for two thicknesses, namely, 6 mm and 0.17 mm when the moisture condition of the boundaries changed at both sides of the slab from w_0 to w_1. According to the assumptions, the moisture permeability should be constant and the sorption curve should be approximately linear. The constant moisture permeability in these calculations is 1×10^{-8} [m^2/s]and the vapour diffusivity, a, is calculated to 1.27×10^{-12} [m^2/s]. The initial moisture content, w_0, is zero and the moisture boundaries, w_1, change to 72 [kg/m^3], which corresponds to 50% relative humidity in ambient air. It should be mentioned that this boundary condition illustrates the condition during measurement of the sorption isotherm.

The results of these calculations are presented in Figures 2.15 and 2.16. A comparison of these results shows that a 6 mm thick specimen takes about 162

days to reach steady state condition and a 0.17 mm thick sample takes about 3 hours. This is consistent with the dependence of h in the time scale given by Equation (2.34).

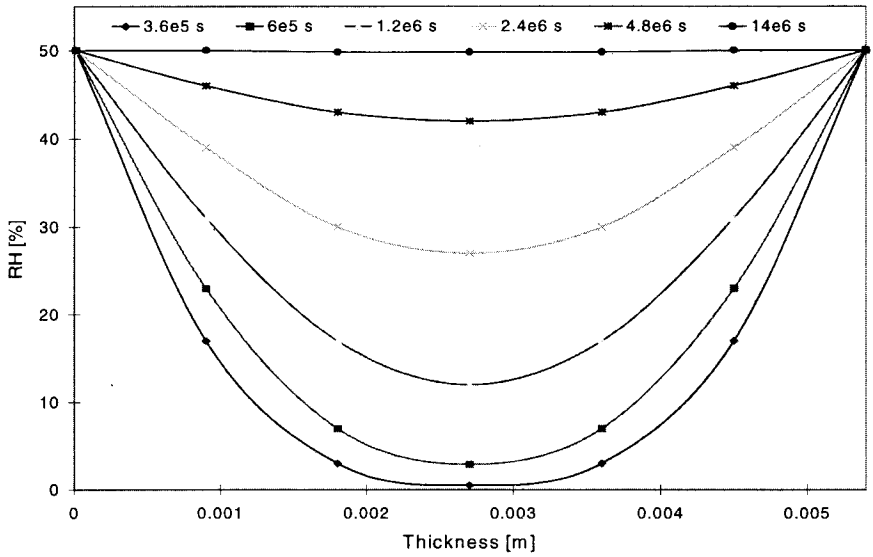

Figure 2.15 Moisture uptake of 50 % moisture difference in a 6 mm thick specimen

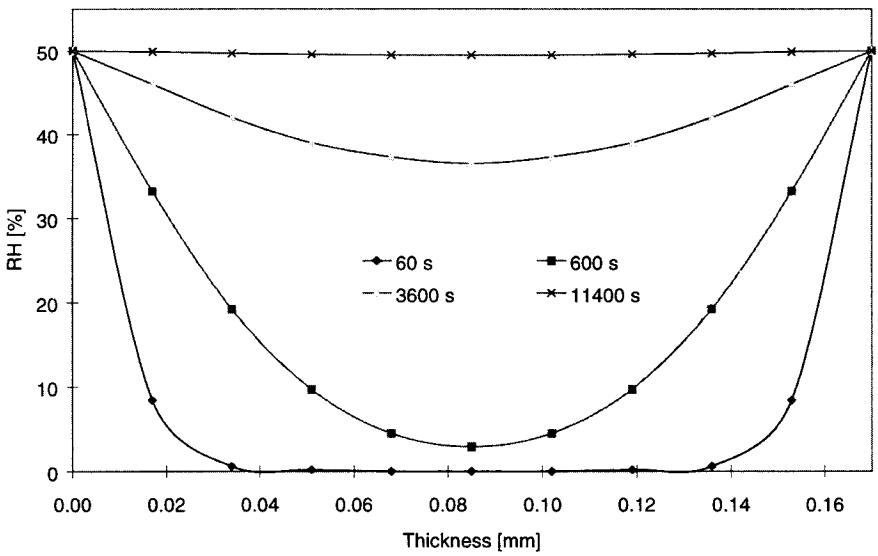

Figure 2.16 Moisture uptake of 50 % moisture difference in a 0.17 mm thick specimen.

3 Numerical Model for the Moisture Flow and the Computer Program

A finite difference method with explicit forward-differences in time is used in the numerical model. For a one-dimensional calculation, a unit area of the cross-section is considered for moisture flows and balances. The slab thickness is divided into a number of N computational cells with the thickness Δx, and the time is discretized using a time step Δt. The numerical solution is based on a moisture balance for each cell and time step, and the moisture content is calculated for the midpoint of each cell. The moisture increase or decrease during a time step for cell i is determined by Equations (3.1-4).

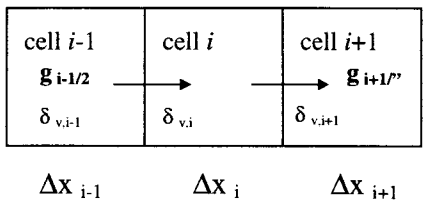

Figure 3.1 Computational cells with the thickness Δx.

$$g_{i-1/2} = \frac{v_{i-1} - v_i}{\frac{\Delta x_{i-1}}{2\delta_{v,i-1}} + \frac{\Delta x_i}{2\delta_{v,i}}} \quad \text{for i = 2 to N} \tag{3.1}$$

$$g_{1/2} = \frac{v_{BL} - v_1}{Z_{v,BL} + \frac{\Delta x_1}{2\delta_{v,1}}} \quad \text{and} \quad g_{N+1/2} = \frac{v_N - v_{BR}}{\frac{\Delta x_N}{2\delta_{v,N}} + Z_{v,BR}} \tag{3.2}$$

The increase in moisture content between two time steps is given by Δw_i.

$$\Delta w_i = \Delta t \cdot (g_{i/2} - g_{i+1/2}) / \Delta x_i \tag{3.3}$$

$$w_i^{New} = w_i^{Old} + \Delta w_i \tag{3.4}$$

Here, g_i is the moisture flow from cell *i-1* to cell *i*. The width, moisture permeability, humidity by volume in cell *i* are denoted by Δx_i , $\delta_{v,i}$, v_i, respectively. The vapour resistance at the boundaries is denoted by $Z_{v,BR}$ and $Z_{v,BL}$.

A PC-program MHPL is developed for the calculation of moisture distribution. The program runs for time being under MS-DOS on PC compatible computers.

The data required by the MHPL are given in a climate data file and an input data file. The climate data file contains the climate data which the HPL is exposed to and the input data file contains the geometry, boundary conditions and material properties of the HPL. For more information about the climate data file, and input data file see Appendix A:2.

3.1 Limitations

The following assumptions and restrictions were made:

- The numerical formulation of the moisture balance only covers the hygroscopic region.

- The sorption isotherm can be simplified by a chain of ten straight lines.

- Variation of the moisture permeability, δ_v , as a function of relative humidity, is often strong when relative humidity is close to 100%. This variation is considered in a numerical calculation by the same simplifications that were used for the sorption isotherm.

3.2 Numerical Validation of MHPL

The evaluation of the MPHL is done by a comparison of the results obtained by MPHL with results obtained by Jam-2. The PC program JAM-2 is developed by Jesper Arfvidsson, Department of Building Physics, Lund University of Technology.

A six millimetre HPL was modelled in both PC-programs. The same measured material properties were used in the modelling. The boundary conditions on left and right-hand side of the HPL were 15% and 95% relative humidity and the initial moisture content was 85 [kg/m^3]. Ten computational cells were used in the modelling and the simulation time was120 days. Moisture content over the cross-section of the HPL was chosen as the output data of the calculations for a comparison of the results. The mean value of the calculated moisture content in the cells after 30, 60, 90 and 120 days is presented in Table 3.1. The moisture content distribution after 60 days over cross- section of the HPL is illustrated in Figure 3.2.

Table 3.1 Comparison of the results obtained by MHPL and JAM-2

w[kg/m^3]				
Time [day]	30	60	90	120
MHPL	136.0	145.2	147.5	147.9
Jam-2	134.6	144.6	147.6	148.2

The difference in the results in Table 3.1 depends mainly on the way the variation of the moisture permeability by relative humidity is described. In Jam-2, this variation is simplified to a number of steps but in MHPL, a chain of ten straight lines is used.

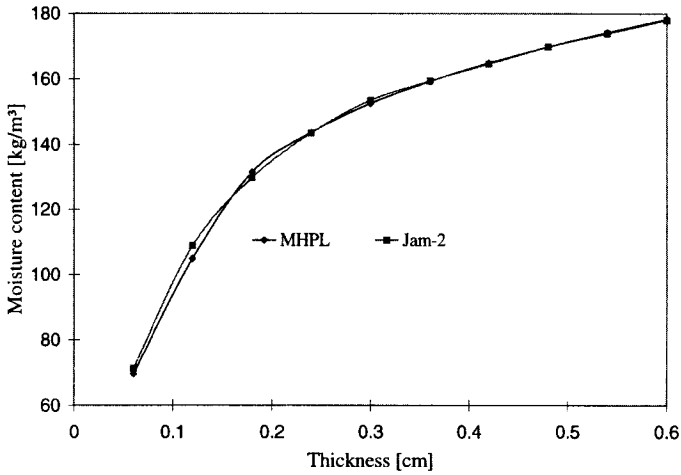

Figure 3.2 The results of calculations, the moisture content distribution over the cross section of the HPL after 60 days.

The results of this comparison indicate that the PC-program MHPL is correctly formulated. In this work, the PC-program MHPL will be used for determining the moisture distribution in High Pressure Laminates.

4 References

[1] H. Nyqvist, Saturated Salt Solutions for Maintaing Specified Relative Humidity, Int. J. Pharm. Tech.& Prod. Mfr. 4(2) 47-48, 1983

[2] Jesper Arfvidsson, Moisture Transport in Porous Media, Byggnadsfysik, Lunds Tekniska Högskola, 1998

[3] Johan Claesson & Carl-Eric Hagentoft, Basic Building Physics, Lund University, Department of Building Physic, June 1994

[4] Carslow, H S, Jaeger, J C, Conduction of Heat in Solids, Oxford University Press, 1959

Part B Mechanical Behaviour and Properties

Part B Mechanical Behaviour and Properties

According to the scope and limitations of this work (see Chapter 4, Scope and Limitations), on a macro mechanical scale of observation, High Pressure Laminates can be considered as a homogeneous and orthotropic material. Furthermore, only the elastic part of the stress/strain relation will be treated here because non-recoverable deformations are not desirable.

The thickness of the HPL plates under observation is less than 6 mm and the smallest width of the plates is larger than 150 mm. Because the ratio of the thickness and the smallest dimension of the HPL does not exceed 1/10, the HPL plates can be classified as thin plates. By limiting the centre deflection (w) of the plate to a fifth of plate thickness, only minor deflections will be considered. The mechanical behaviour can, then, be treated according to the Kirchhoff plate theory for thin plates. Thin plates are straight, plane surface structures which carry external loads two- dimensionally, mostly by internal (bending and torsional) moments and by transverse shears. Statically, plates have simply supported and fixed edges and, in some cases, point supports.

1 Elastic Orthotropic Plate Theory

The theory of elasticity deals with the relationships of external forces, displacements, stresses and strains in elastic bodies. In elastic thin plate theories, the three-dimensional problem is approximated to a two-dimensional one. Two well-known theories for two-dimensional plates have been developed by Gustav Kirchhoff and Eric Reissner. The elastic thin plate theory considers deformations produced by external loads. Through deformations of the loaded object, the external forces are converted into internal forces. The Kirchhoff plate theory, extended to orthotropic plates, is assumed throughout this thesis and will be applied.

1.1 Kirchhoff Plate Theory

The small deflection plate theory, generally attributed to Kirchhoff, is based on the following assumptions:

a) the material of the plate is within the elastic range and it is homogenous and orthotropic, i.e. Hooke's law is valid

b) the thickness of the plate is small when compared with its other dimensions and the deflections are small when compared with plate thickness

c) the slope of the deflected middle surface is small compared to unity

d) the deformation is such that straight lines, initially normal to middle surface, remain straight lines and normal to the middle surface

e) the stresses normal to the middle surface are ignored

To be able to convert external forces into internal forces, relations between deformation and strain are needed, i.e. conditions of compatibility. Furthermore, relations between stress and strain are needed, i.e. constitutive relations. Finally, by using the above assumptions, the equilibrium for a plate can be expressed in terms of its lateral deformation.

1.2 Equilibrium Equation

In the theory of plates, it is customary to deal with internal forces and moments per unit length of the middle surface, see Figure 1.1. Assuming that the plate is exposed to a uniformly distributed load, p_z [N/m^2]. In the plates, the external load p_z, and the external moment M [Nm/m], are carried by lateral shear forces q_x and q_y [N/m], bending moments m_x and m_y [Nm/m], and finally twisting moments m_{xy}, m_{yx} [Nm/m] .

For rectangular plates, the use of the Cartesian coordinate system is the most convenient. The external and internal forces and the deflection components are considered positive when they point in the positive direction of the coordinate axes.

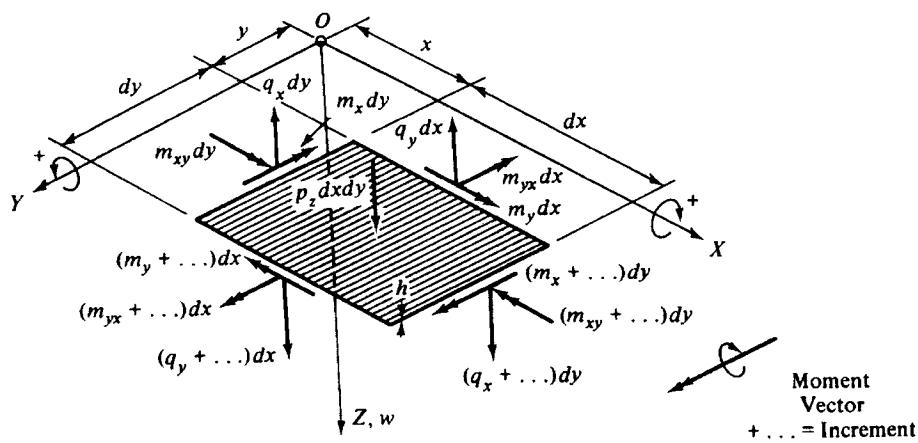

Figure1.1 External and internal forces on the element of the middle surface,[1].

Three of six possible equilibrium equations can be used as follows:

$$\Sigma M_x = 0 \qquad \Sigma M_y = 0 \qquad \Sigma P_z = 0$$

Here, M_x and M_y are the internal and external moments and P_z is all forces in the z-direction.

The sum of the moments around the y-axis, $\Sigma M_x=0$, after neglected terms with more than two differentials gives us:

$$\frac{\partial m_x}{\partial x} + \frac{\partial m_{yx}}{\partial y} = q_x \tag{1.1}$$

and in a similar manner $\Sigma M_y=0$ gives:

$$\frac{\partial m_y}{\partial y} + \frac{\partial m_{xy}}{\partial x} = q_y \tag{1.2}$$

and, finally, the vertical equilibrium, $\Sigma P_z=0$ gives:

$$\frac{\partial q_x}{\partial x} + \frac{\partial q_y}{\partial y} = -p_z \tag{1.3}$$

By substituting Equations (1.1-1.2) into equation (1.3) and knowing that $m_{xy} = m_{yx}$ [2], the equilibrium equation becomes:

$$\frac{\partial^2 m_x}{\partial^2 x} + 2\frac{\partial^2 m_{xy}}{\partial x\,\partial y} + \frac{\partial^2 m_y}{\partial^2 y} = -p_z \tag{1.4}$$

1.3 Constitutive Relation between Stress and Strain

The assumption that the material is in an elastic range permits the use of Hooke's law;

$$\begin{bmatrix} \varepsilon_x \\ \varepsilon_y \\ \gamma_{xy} \end{bmatrix} = \begin{bmatrix} E_x^{-1} & -\nu_{yx}E_y^{-1} & 0 \\ -\nu_{xy}E_x^{-1} & E_y^{-1} & 0 \\ 0 & 0 & G_{xy}^{-1} \end{bmatrix} \begin{bmatrix} \sigma_x \\ \sigma_y \\ \tau_{xy} \end{bmatrix} \tag{1.5}$$

Where the estimated shear modules, G_{xy}, can be expressed as, [1]:

$$G_{xy} \approx \frac{\sqrt{E_x E_y}}{2(1 + \sqrt{\nu_{xy}\nu_{yx}})} \tag{1.6a}$$

By using the elastic symmetry between four of these constants, the following relation is valid:

$$\frac{E_x}{\nu_{xy}} = \frac{E_y}{\nu_{yx}} \tag{1.6b}$$

1.4 Conditions of Compatibility, Relation between Strain and Displacement

By a comparison of a section of the plate before and after deflection, sections I-I and II-II in Figure 1.2, and using assumptions d) and e), from Section 1.1 we can express the relation between strains and displacements.

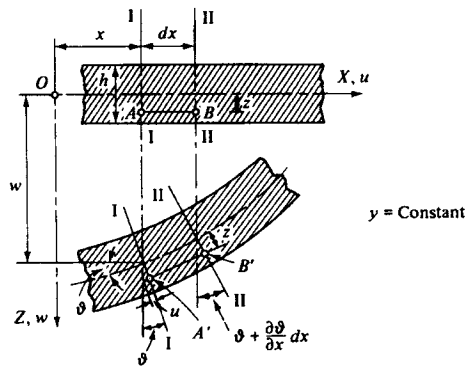

Figure 1.2 Section before (I-I) and after deflection (II-II), [1].

From Figure 1.2, the angle of rotation (ϑ) of lines I-I and II-II, and the in-plane displacements, u and v, can be expressed by Equations (1.7-1.9):

$$\vartheta = -\frac{\partial w}{\partial x} \tag{1.7}$$

$$u = z\vartheta = -z\frac{\partial w}{\partial x} \tag{1.8}$$

In the same manner for y-direction yields:

$$v = -z\frac{\partial w}{\partial y} \tag{1.9}$$

By definition, the strain in the x-direction becomes:

$$\varepsilon_x = \frac{\Delta dx}{dx} = z\frac{d\vartheta}{dx} = -z\frac{\partial^2 w}{\partial x^2} \tag{1.10}$$

similarly

$$\varepsilon_y = -z\frac{\partial^2 w}{\partial y^2} \tag{1.11}$$

The shear strain is defined by the angular distortion in Figure 1.3, thus, we get:

$$\gamma' = \frac{\partial v}{\partial x}, \quad \gamma'' = \frac{\partial u}{\partial y}$$

consequently, the shear strain becomes:

$$\gamma_{xy} = \gamma_{yx} = \gamma' + \gamma'' = \frac{\partial v}{\partial x} + \frac{\partial u}{\partial y} \tag{1.12}$$

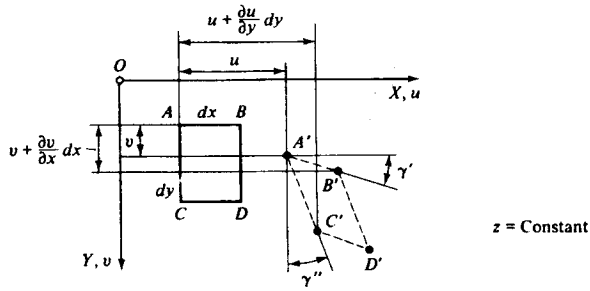

Figure 1.3 Angular distortion, [1].

Finally, the relation between strains and displacements can be written in matrix form:

$$\begin{bmatrix} \varepsilon_x \\ \varepsilon_y \\ \gamma_{xy} \end{bmatrix} = \begin{bmatrix} \frac{\partial}{\partial x} & 0 \\ 0 & \frac{\partial}{\partial y} \\ \frac{\partial}{\partial y} & \frac{\partial}{\partial x} \end{bmatrix} \begin{bmatrix} u \\ v \end{bmatrix} \tag{1.13}$$

1.5 Internal Forces

Internal forces can be expressed in terms of lateral displacement, w. The stress components σ_x , σ_y and τ_{xy} produce bending moments m_x , m_y and the torsional moment m_{xy}.

$$\begin{bmatrix} m_x \\ m_y \\ m_{xy} \end{bmatrix} = \int_{-h/2}^{h/2} z \cdot \begin{bmatrix} \sigma_x \\ \sigma_y \\ \tau_{xy} \end{bmatrix} .dz \qquad (1.14)$$

Here, h is the thickness of the plate. Substituting Equations (1.10-1.11) and (1.6 b) into (1.5), and elimination of strains give:

$$\sigma_x = \frac{-zE_x}{1 - \nu_{xy}\nu_{yx}} \left(\frac{\partial^2 w}{\partial x^2} + \nu_{yx} \frac{\partial^2 w}{\partial y^2} \right) \qquad (1.15\ a)$$

$$\sigma_y = \frac{-zE_y}{1 - \nu_{xy}\nu_{yx}} \left(\frac{\partial^2 w}{\partial y^2} + \nu_{xy} \frac{\partial^2 w}{\partial x^2} \right) \qquad (1.15\ b)$$

$$\tau_{xy} = -2zG_{xy} \frac{\partial^2 w}{\partial x \partial y} \qquad (1.15\ c)$$

The integration of Equation (1.14), by using (1.15 a-c), gives:

$$m_x = -D_x \cdot \left(\frac{\partial^2 w}{\partial x^2} + \nu_{yx} \frac{\partial^2 w}{\partial y^2} \right) \qquad (1.16a)$$

$$m_y = -D_y \cdot \left(\nu_{xy} \frac{\partial^2 w}{\partial x^2} + \frac{\partial^2 w}{\partial y^2} \right) \qquad (1.16b)$$

$$m_{xy} = -2D_{xy} \cdot \frac{\partial^2 w}{\partial x \partial y} \qquad (1.16c)$$

where

$$D_x = \frac{E_x h^3}{12(1-\nu_{xy}\nu_{yx})}, \qquad D_y = \frac{E_y h^3}{12(1-\nu_{xy}\nu_{yx})},$$

$$2D_{xy} = (1 - \sqrt{\nu_{xy}\nu_{yx}})\sqrt{D_x D_y} = G_{xy} \frac{h^3}{6}$$

Finally, the substitution of Equation (1.16) into Equation (1.4) yields the governing differential equation of the plate exposed to lateral loads.

$$D_x \frac{\partial^4 w}{\partial x^4} + 2B \frac{\partial^4 w}{\partial x^2 \partial y^2} + D_y \frac{\partial^4 w}{\partial y^4} = p_z \qquad (1.17)$$

where $B = \frac{1}{2} \cdot (\nu_{xy} D_y + \nu_{yx} D_x + 4D_{xy})$.

Equation (1.17) is a non-homogeneous, fourth-order, partial differential equation. A solution, w(x,y) should simultaneously satisfy the differential equation and the boundary conditions.

1.6 Boundary Conditions

In this thesis, two classical boundary conditions, a fixed edge and a simply supported edge will be treated. Since Equation (1.17) is a fourth order differential equation, two boundary conditions, either for displacements or internal forces, are needed at each boundary. In formulating the boundary conditions, three internal force components: torsional moment, bending moment and transverse shear will be considered. Similarly, the displacement components, lateral displacement and slope, will be used.

1.6.1 Fixed Edge

The displacements (translation and rotation) of the fixed edges are used for the mathematical formulation of this boundary condition. At fixed edges the lateral deflection and the slope of the deflection are zero. Thus, the boundary condition can be written as:

$$w = 0 \qquad \frac{\partial w}{\partial x} = 0 \qquad \text{for } x = 0 \text{ or } x = a \tag{1.18}$$

$$w = 0 \qquad \frac{\partial w}{\partial y} = 0 \qquad \text{for } y = 0 \text{ or } y = b \tag{1.19}$$

1.6.2 Simply Supported Edge

At the simply supported edge, the lateral deflection and the bending moment are zero. Thus,

$$w = 0 \tag{1.20}$$

$$m_x = -D_x\left(\frac{\partial^2 w}{\partial x^2} + \nu_{yx}\frac{\partial^2 w}{\partial y^2}\right) = 0 \text{ for } x = 0 \text{ or } x = a \tag{1.21}$$

$$m_y = -D_y\left(\nu_{xy}\frac{\partial^2 w}{\partial x^2} + \frac{\partial^2 w}{\partial y^2}\right) = 0 \text{ for } y = 0 \text{ or } y = b \tag{1.22}$$

If the simply supported edge is loaded with an external edge moment, M [Nm/m], the boundary conditions, Equations (1.21-1.22), become:

$$m_x = -D_x\left(\frac{\partial^2 w}{\partial x^2} + \nu_{yx}\frac{\partial^2 w}{\partial y^2}\right) = M_x \tag{1.23}$$

$$m_y = -D_y(\nu_{xy}\frac{\partial^2 w}{\partial x^2} + \frac{\partial^2 w}{\partial y^2}) = M_y \qquad (1.24)$$

1.7 Simultaneous Bending and Stretching

Equation (1.17) is based on the assumption that no in-plane forces act on the middle surface of the plate. However, in-plane forces arise, for instance, when displacements of the plate, due to moisture or temperature variations, parallel to its middle surface are hindered by supports. The effect of the in-plane forces (membrane forces) n_x ,n_y and n_{xy} on deflection can be superimposed with a fictitious lateral load if the membrane forces are known. The fictitious load, p_z^* , is calculated from Equation (1.25). The following sign convention for membrane forces is used: compression is positive and tension negative. Here, it should be mentioned that the moisture and temperature variation through the thickness of the plate do not produce in-plane shear forces, i.e. n_{xy} is zero.

$$p_z^* = n_x\frac{\partial^2 w}{\partial x^2} + n_y\frac{\partial^2 w}{\partial y^2} + 2n_{xy}\frac{\partial^2 w}{\partial x \partial y} \qquad (1.25a)$$

The corresponding moisture induced fictitious load becomes:

$$p_z^* = n_x\frac{\partial^2 w}{\partial x^2} + n_y\frac{\partial^2 w}{\partial y^2} \qquad n_{xy}= 0 \qquad (1.25b)$$

The governing differential equation (1.17) can, then, be rewritten as:

$$D_x\frac{\partial^4 w}{\partial x^4} + 2B\frac{\partial^4 w}{\partial x^2 \partial y^2} + D_y\frac{\partial^4 w}{\partial y^4} = p_z + p_z^*(w) \qquad (1.26)$$

here p_z* is a function of w, n_x and n_y.

1.8 Solution of the Governing Differential Equation

Equation (1.17) is a fourth-order, non-homogeneous and linear differential equation of the elliptic type. The exact solution of this equation for isotropic plates is available for simple plate geometry, load and boundary conditions. If these conditions are more complex, numerical and approximative methods are the only approaches that can be used.

The combination of orthotropic material, moisture induced deformations and boundary conditions makes this mathematical model complex. Owing to this,

numerical methods will be used for the solution of Equation (1.17). In Chapter 3, Part B, the numerical technique used is formulated.

2 Measurement of Mechanical Properties

Generally, an elastic, orthotropic, three-dimensional body has nine independent elastic properties (elastic constants). The number of elastic constants can be reduced to five if a two-dimensional body is under consideration, [3]. As mentioned before, an HPL has machine and cross directions as orthotropic axes. In this chapter, the x-coordinate is assigned to the Machine Direction (MD) and the y- coordinate is assigned to the Cross Direction (CD). Thus, for High Pressure Laminates, the elastic constants are:

E_{MD} Young's modulus in the machine direction,

E_{CD} Young's modulus in the cross direction,

ν_{MDCD} Poisson's ratio, for cross direction tension, giving machine direction contraction,

ν_{CDMD} Poisson's ratio, for machine direction tension, giving cross direction contraction,

G shear modulus in the plane of the plate,

As mentioned in Chapter 1, the following relation exists:

$$\frac{E_{MD}}{\nu_{MDCD}} = \frac{E_{CD}}{\nu_{CDMD}}$$

There is no other relation between these constants, and, in particular, there is no relation between the shear modulus and Young's modulus. But the shear modulus, G, can be estimated by Equation (1.6a).

These five elastic constants must be known in order to investigate moisture induced deformation. Since adequate and accurate mechanical material data were not available, the mechanical properties of the High Pressure Laminates had to be determined by experimental investigation.

2.1 Measurement of the Elastic Constants

The elastic constants are measured by two methods, namely: the tension test and the modal test. These measurements are carried out for three relative humidity levels 32, 50 and 95 %. These measurements define the influence of moisture content on the elastic constants.

The dynamic measurements (modal test) were carried out by Daniel Larsson at the Department of Structural Engineering, Unit for Dynamics in Design, Chalmers University of Technology. More information about this testing method is available in [4].The static measurements (tension test) were carried out by The Swedish National Testing and Research Institute. In addition to determining the elastic properties, the ultimate stress/strain and the reaction of HPL due to loading and unloading were determined during the static tests [5].

The dynamic test, which is a non-destructive test method, gives the elastic constants, particularly the shear modulus, which are required. In according with the limitations, only the elastic range of the stress/strain relation will be considered. This means that the elastic stress/strain level is needed, too. For this reason, the static tests were carried out. The objective of the static tests are to determine the ultimate stress/strain level and the elastic constants. The results of the static tests are used, then, to calculate moisture induced deformations and the results of the dynamic tests are used to verify the static tests.

2.2 Samples and Tests

All samples were conditioned for about four months at various relative humidities. The dimension of the samples in the modal test was about 5.4x100x200 mm and in the tension test 5.4x15x100 mm. The samples in the tension tests were prepared from the modal test samples. The samples which were used to determine the ultimate stress levels, were not conditioned for a specific relative humidity.

All tensile tests were performed at 23°C, with a displacement speed of 0.5 mm/min with an Instron 1195 tensile testing machine. A Kyowa 0°/90° strain gage and an MTS 632.17c-20 extensometer were used to measure strains.

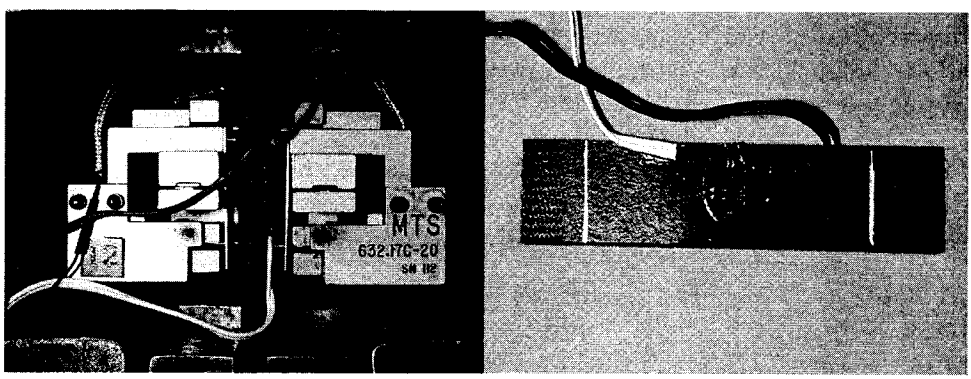

Picture 1 Extensometer and strain gages applied to test specimen.

2.3 Results

The measurement results, the elastic constants E_{MD}, E_{CD}, ν_{MDCD}, ν_{CDMD} and G, are presented in Tables 2.1-2.3.

Table 2.1 The results obtained by statical tests for determining elastic constants at different relative humidity levels.

RH [%]	E_{MD} [GPa]	E_{CD} [GPa]	ν_{CDMD}	ν_{MDCD}	G [GPa]*
32	17.68	12.37	0.250	0.347	5.712
50	17.45	12.23	0.250	0.346	5.644
95	15.74	10.90	0.243	0.347	5.082

* Estimated value according to Equation (1.6a)

Table 2.2 The results obtained by dynamic tests to determine elastic constants at different relative humidity levels.

RH [%]	E_{MD} [GPa]	E_{CD} [GPa]	ν_{CDMD}	ν_{MDCD}	G [GPa]
32	20.10	15.80	0.26	0.33	5.95
50	19.50	13.89	0.24	0.34	5.90
95	18.00	13.40	0.25	0.33	5.10

A comparison of the results of Young's modulus, from static- and modal tests, shows that the results from the dynamic test are between 10-20 % higher than the static test results. This deviation is not alarming because this level of difference is observed and discussed in [3]. The deviation of calculated shear modulus obtained from the static test from the measured shear modulus by the dynamic test is between 1-5 %.

Poisson's ratios in both test methods are almost in the same range in the different relative humidities. This means that the relative humidity level has a minor influence on the Poisson's ratio of the specimens.

2.3.1 Determination of the Elastic Stress/Strain Level

To be able to determine the elastic stress/strain level, a fracture test was done. The results of this test are shown in Figure 2.1 and Table 2.3.

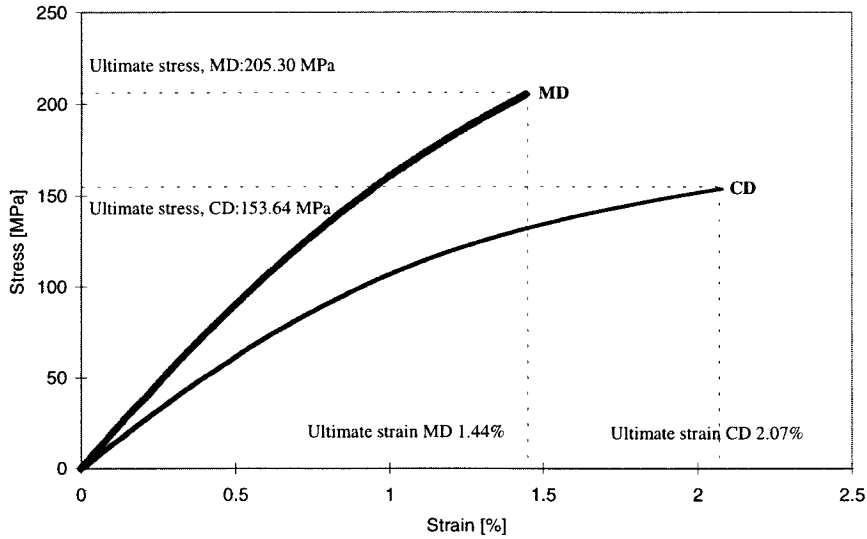

Figure 2.1 The ultimate stress/strain level in Machine- and Cross Directions.

Table 2.3 The ultimate stress/strain levels determined by statical test.

Direction	Stress [MPa]	Strain [%]
MD	205.30	1.44
CD	153.64	2.07

These results are used in the design of further tests for determining the elastic range. Two strain levels, 0.3 and 0.6%, were chosen as the elastic range in both the machine- and cross direction. Samples were conditioned in 32, 50 and 95% relative humidity. In these tests, the specimens were loaded up to the chosen strain levels, 0.3 and 0.6%, and then unloaded. When the specimen was fully unloaded, the remaining deformations were measured. The results of these measurements are shown in Table 2.4.

Table 2.4 Remaining strain in MD and CD after unloading.

Relative humidity [%]	Maximum strain [%]	Remaining strain [%], MD	Remaining strain [%], CD
32	0.6	0.010	0.012
32	0.3	0.004	0.003
50	0.6	0.010	0.011
50	0.3	0.003	0.003
95	0.6	0.015	0.015
95	0.3	0.005	0.008

According to Table 2.4 in both strain levels, 0.3 and 0.6%, at least 97% of the strain at all relative humidity levels, in both the machine and cross direction are recovered.

3 Numerical Treatment of Elastic PDE and Developed Computer Program

In this section, the governing partial differential equation (PDE) of the plate subjected to lateral loads is approximated by using the finite difference expression of fourth and mixed derivatives. A computer program is developed in order to solve the algebraic equation systems which are obtained by a finite difference formulation of the plate equation.

3.1 Numerical Formulation of the Elastic PDE: Finite Difference Method

One available numerical method for solving Equation (1.17) is the Finite Difference Method (FDM). In the finite difference technique, the derivatives appearing in the governing Partial Differential Equation (PDE) are replaced by appropriate finite difference approximations which transform the PDE into solvable algebraic equations.

Our scheme for solving these equations will be to replace the derivatives with difference quotients at some selected points. We can write the difference equation corresponding to each point at the intersections (nodes) of a grid work that subdivides the region of interest at the point where the function values are unknown. Solving these equations with iterative methods gives values for the function at each node which approximates the true value.

There are three methods for the approximation of derivatives with FDM : forward difference, central difference and backward difference. Since central differences are more accurate than both forward or backward differences, central differences are used in both interior nodes (interior region) and boundary nodes.

3.1.1 Discretization of Differential Equations

Equation (1.17) is approximated using the central difference method. The approximation of the fourth and mixed derivatives in the central difference method can be signed as follows:

$$\left.\frac{\partial^4 w}{\partial x^4}\right|_{i,j} = \frac{1}{\Delta x^4}\left(w_{i-2,j} - 4w_{i-1,j} + 6w_{i,j} - 4w_{i+1,j} + w_{i+2,j}\right)$$

$$\left.\frac{\partial^4 w}{\partial y^4}\right|_{i,j} = \frac{1}{\Delta y^4}\left(w_{i,j-2} - 4w_{i,j-1} + 6w_{i,j} - 4w_{i,j+1} + w_{i,j+2}\right)$$

$$\left.\frac{\partial^4 w}{\partial^2 x \partial^2 y}\right|_{i,j} = \frac{1}{\Delta x^2 \Delta y^2}(w_{i-1,j-1} - 2w_{i-1,j} + w_{i-1,j+1} - 2w_{i,j-1} +$$
$$4w_{i,j} - 2w_{i,j+1} + w_{i+1,j-1} - 2w_{i+1,j} + w_{i+1,j+1})$$

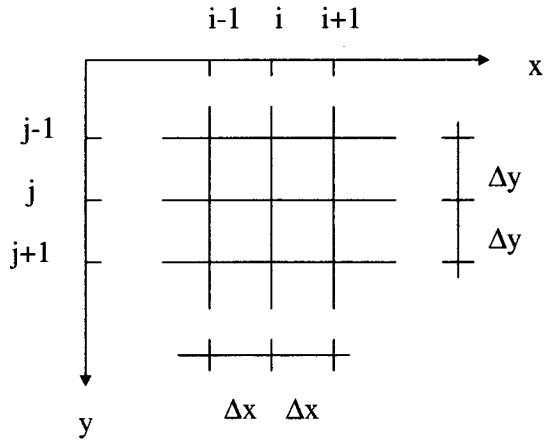

Figure 3.1 Finite difference mesh.

Introduction of the relations of derivatives into the differential Equation (1.17) gives :

$$D_x[w_{i-2,j} - 4w_{i-1,j} + 6w_{i,j} - 4w_{i+1,j} + w_{i+2,j}] + 2B[w_{i-1,j-1} - 2w_{i-1,j} + w_{i-1,j+1} - 2w_{i,j-1} + 4w_{i,j} - 2w_{i,j+1} + w_{i+1,j-1} - 2w_{i+1,j} + w_{i+1,j+1}] + D_y[w_{i,j-2} - 4w_{i,j-1} + 6w_{i,j} - 4w_{i,j+1} + w_{i,j+2}] = (p_z + p_z^*)_{ij} \quad (3.1)$$

The value of the p_z^* , according to Equation (1.25b), is also approximated by the finite difference method. The fictitious load, p_z^*, is calculated for each new field of the w and is used in Equation 3.1.

The value of w(x,y) at node (i,j), w(i,j), becomes:

$$w_{i,j} = -\{D_x[w_{i-2,j} - 4w_{i-1,j} - 4w_{i+1,j} + w_{i+2,j}] + 2B[w_{i-1,j-1} - 2w_{i-1,j} + w_{i-1,j+1} - 2w_{i,j-1} - 2w_{i,j+1} + w_{i+1,j-1} - w_{i+1,j} + w_{i+1,j+1}] + D_y[w_{i,j-2} - 4w_{i,j-1} - 4w_{i,j+1} + w_{i,j+2}] - (p_z + p_z^*)_{i,j}\}/(6D_x + 6D_y + 8B) \quad (3.2)$$

where D_x , D_y and B are given by Equations (1.16-1.17).

By using Equation (3.2) the lateral deflection can be calculated in the interior nodes (interior region). To calculate the lateral deflection at the nodes close to

the boundary and on the boundary nodes, we need to introduce fictitious nodes outside the region of interest.

3.1.2 Discretization of Boundary Conditions

The equations for the boundary conditions for fixed edge and simply supported plates according to Chapter 1.6 are also discertized. The boundary of a simply supported plate is treated for two cases, namely: the ordinary simply supported edge and the simply supported edge loaded by moment.

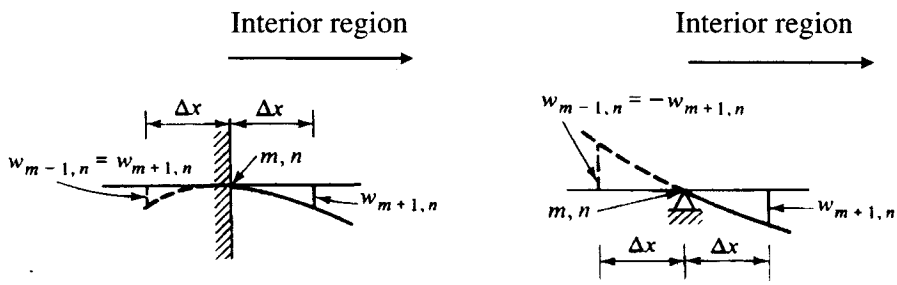

a) Fixed b) Simple support

Figure 3.2 Representation of the boundary conditions by the use of nodes in the interior region of the boundary, and fictitious nodes outside the plate region.

a) Fixed Edges

The discretized expression of Equations (1.18-1.19), for fixed edges which are parallel to the y-axis, gives:

$$w_{m,n} = 0 \tag{3.3 a}$$

$$\left.\frac{\partial w}{\partial x}\right|_{m,n} \approx \frac{w_{m+1,n} - w_{m-1,n}}{2\Delta x} = 0 \Rightarrow w_{m+1,n} = w_{m-1,n} \tag{3.3 b}$$

Similarly, for edges parallel to the x- axis:

$$w_{m,n} = 0 \tag{3.4 a}$$

$$\left.\frac{\partial w}{\partial y}\right|_{m,n} \approx \frac{w_{m,n+1} - w_{m,n-1}}{2\Delta y} = 0 \Rightarrow w_{m,n+1} = w_{m,n-1} \tag{3.4 b}$$

Fictitious grid points are introduced in order to express boundary conditions by a central difference.

b) Ordinary Simply Supported Edges

The discretized expression of Equations (1.20-1.22) for simply supported edges which are parallel to the y-axis, gives:

$$w_{m,n} = 0 \tag{3.5a}$$

$$-D_x\left(\frac{\partial^2 w}{\partial x^2} + \nu_y \frac{\partial^2 w}{\partial y^2}\right) = 0 \Rightarrow w_{m+1,n} = -w_{m-1,n} \tag{3.5b}$$

Similarly, for edges parallel to the x- axis:

$$w_{m,n} = 0 \tag{3.6a}$$

$$-D_y\left(\nu_x \frac{\partial^2 w}{\partial x^2} + \frac{\partial^2 w}{\partial y^2}\right) = 0 \Rightarrow w_{m,n+1} = -w_{m,n-1} \tag{3.6b}$$

c) Simply Supported Edges Loaded by Edge Moment

In this case, the displacement, w, is equal to zero such as an ordinary simply supported edge and the FDM expression of Equations (1.23-1.24) gives

- Edges parallel to the y- axis:

$$\frac{\partial^2 w}{\partial x^2} + \nu_y \frac{\partial^2 w}{\partial y^2} = -\frac{M_x}{D_x} \Rightarrow w_{m+1,n} = -w_{m-1,n} - \frac{M_x}{D_x} \tag{3.7}$$

- Edges parallel to the x-axis:

$$\nu_x \frac{\partial^2 w}{\partial x^2} + \frac{\partial^2 w}{\partial y^2} = -\frac{M_y}{D_y} \Rightarrow w_{m,n+1} = -w_{m,n-1} - \frac{M_y}{D_y} \tag{3.8}$$

3.1.3 Solution of the Governing PDE by an Iterative Method

As opposed to the direct method of solving a set of equations by elimination, an iterative method is used for simplicity. The large number of equations, and the chosen method for solving them, require the development of a computer program.

In numerical calculations carried out by computers it is always important to minimise the time required for the execution. For this reason, the dominant method used is the Gauss-Seidel iteration method. In the Gauss-Seidel method, an initial approximation of w(i,j) is required. A zero value for w is a natural choice. Substituting these values on the right hand-sides of the set of equations, Equation (3.2), results in a new set of approximations. These new values, in each trial, are substituted into the right-hand sides and give us a new approximation.

To reduce the calculation time, a relaxation method is used. Relaxation is an iteration method which is more rapidly convergent than Gauss-Siedel. The method was named after a British engineer, Richard Southwell, and has been applied to a wide range of problems. In the over-relaxation method we start the iteration with the same initial set of values ,$w^{initial}(i,j)=0$. The equations will give suggestions for new values which we denote by, w′(i,j). Let us rename the $w^{initial}(i,j)$ to $w^{old}(i,j)$, then, the new approximation will be

$$w^{new}(i,j)= w^{old}(i,j) + R \,.\, (w'(i,j)- w^{old}(i,j))$$

$$i: 1.....N_x,\ j: 1.....N_y$$

where R is an over-relaxation factor. The optimised over-relaxation factor lies typically between 1.8 and 1.95. The new value of the unknown variable, $w_{i,j}^{new}$ is used directly for calculating of the new value of other nodes.

This process is repeated until the successive values of each of the variables are sufficiently alike, which means $|w'(i,j) - w^{old}(i,j)| \le \varepsilon$ for all *i* and *j*. Where ε is close to zero and can be chosen by the user.

3.1.4 About the Computer Program

A computer program, MecHPL, has been implemented in a Windows environment. The program codes are written in Borland Pascal codes and Borland Delphi is used for the user interface. The program can be run on any PC with a Pentium processor.

The plate under consideration can be described by a rectangular grid. Arbitrary orthotropic material properties, boundary conditions and numerical conditions can be specified. The bearing condition of the edge is limited to simply supported and fixed, loading is limited to uniform lateral force and edge moment.

Using these input data and the computer program MecHPL, the deflection of each grid point can be calculated by the iterative method explained above. When the deflection of each grid point is known, internal forces, such as moment and shear forces can be calculated. The calculation results are stored in files for further analysis.

3.2 Evaluation of the Mechanical Program

The results obtained by the mechanical computer program, MecHPL, should be numerically validated by a comparison with existing table values and/or with results obtained by established and validated mechanical programs. An evaluation of the MecHPL is carried out in two steps. In the first step, comparisons concern elastic isotropic plates and, in the second step, an orthotropic plate loaded by edge moment is considered. Geometry, material properties and the boundary conditions of the plate will be explained during each step. By using the results of this validation, the optimal number of discritization points and calculation time can be determined.

3.2.1 Isotropic Plate

An isotropic rectangular plate, 0.6 x 0.6 x 0.006 m, is considered. The material properties of the plate are: Young's modulus, E = 20 GPa and Poisson's ratio,ν = 0.3. The plate is subjected to a uniformly distributed load, p_z, of 1000 Pa. Four bearing conditions, according to Table 3.1 and Figure 3.3, are chosen.

The values calculated by MecHPL will be compared with the table values from [6]. The deflection (w) and moments in the centre of plate, M_{xs}, M_{ys} [Nmm], and the edge moment in the centre of the bearing, M_{ysv}, M_{xsv} [Nmm] when the edge is fixed, are presented in Table 3.2-Table 3.5. It is known that when the plate has a symmetric boundary and geometry, the moment M_{xs} is equal to M_{ys}.

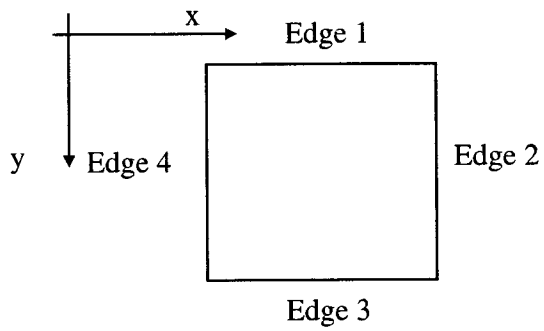

Figure 3.3 Coordinates and edge number of the plate.

Table 3.1 Bearing condition of the plate. SS signs Simply Supported edge and F signs Fixed edge.

	edge			
	1	2	3	4
Case 1	SS	SS	SS	SS
Case 2	F	F	F	F
Case 3	F	SS	F	SS
Case 4	SS	SS	SS	F

In these calculations, the lateral deflection is the primary variable. This means that a correctly calculated deformation field leads to correctly calculated internal forces.

Table 3.2 Case 1. Comparison of the results calculated by MecHPL for different mesh densities and table values. All four edges of the plate are simply supported.

Table value		Calculated value			
		Node 20x20		Node 30x30	
w [mm]	M_{xs} [Nm]	w	M_{xs}	w	M_{xs}
1.329	17.208	1.330	17.205	1.330	17.200

Table 3.3 Case 2. Comparison of the calculated results of different mesh densities and table values. All four edges of the plate are fixed.

Node	Table Value	Calculated value			
		20x20	30x30	40x40	60x60
w[mm]	0.417	0.423	0.418	0.417	0.416
M_{xs}[Nm]	8.244	8.279	8.261	8.254	8.249
M_{xvs}[Nm]	-18.540	-18.238	-18.372	-18.420	-18.449

Table 3.4 Case 3. Comparison of the calculated results of different mesh densities and table values. Two parallel edges are simply supported and the other two edges of the plate are fixed.

Node	Table Value	Calculated value			
		20x20	30x30	40x40	60x60
w[mm]	0.627	0.637	0.632	0.630	0.629
M_{xs}[Nm]	8.748	8.866	8.818	8.801	8.789
M_{ys}[Nm]	11.952	11.973	11.970	11.969	11.969
M_{yvs}[Nm]	-25.164	-24.87	-25.022	-25.074	-25.117

Table 3.5 Case 4. Comparison of the calculated results of different mesh densities and table values. Three edges are simply supported and the fourth edge of the plate is fixed.

Node	Table Value	Calculated value			
		20x20	30x30	40x40	60x60
w[mm]	0.912	0.919	0.915	0.914	0.913
M_{xs}[Nm]	12.168	12.244	12.219	12.210	12.200
M_{ys}[Nm]	14.148	14.093	14.101	14.102	14.103
M_{xvs}[Nm]	-30.240	-29.809	-30.024	-30.099	-30.152

In the above evaluation cases, the ratio between the length and width of the plate is equal to unity. To be sure that the program is capable of calculating the deflection of an other ratio between the length and width, the deformation of a simply supported plate with a length to width ratio equal to two is calculated. Material properties and loading are the same as before. The results of this calculation are represented in Table 3.6.

Table 3.6 Comparison of the calculated results and table values. All four edges of the plate are simply supported. The dimensions of the plate are 0.6 x 0.3 x 0.006 m, i.e. the ratio of the length to width is equal to two.

Table value		Calculated value			
		Mesh 20x20		Mesh 30x30	
w [mm]	M_{xs} [Nm]	w	M_{xs}	w	M_{xs}
0.207	4.176	0.207	4.169	0.207	4.171

Table 3.6 shows that the deviation of the results obtained by MecHPL from the table values is less than 0.5%, which means that plates with various widths and lengths can be handled by MecHPL.

3.2.2 Isotropic Plate Loaded with Edge Moment

Two parallel edges of a simply supported plate with the same geometry (0.6 x 0.6 x 0.006 m) and material properties as in Section 3.2.1 are exposed to edge moments, 100 Nm/m. The calculated values will be compared with the table values from [1]. Results of the comparison, which are deflection and moment at the centre of the plate, are presented in Table 3.7.

Table 3.7 Comparison of the calculated results with a table value for a simply supported plate exposed to edge moment.

Table value		Calculated value			
		Mesh 20x20		Mesh 30x30	
w [mm]	M_{xs} [Nm]	w	M_{xs}	w	M_{xs}
0.335	2.560	0.335	2.574	0.335	2.567

Table 3.7 shows that the difference between tabulated and calculated values obtained by MecHPL is less than 0.5 % for a mesh with 20x20 nodes. Thus, the MecHPL program is capable of calculating the deflection of plates loaded by edge moments, too.

3.2.3 Orthotropic Plate Loaded by Edge Moment

An orthotropic rectangular plate with the dimensions 0.6 x 0.3 x 0.006 m, is considered. The material properties of the plate are: Young's moduli, E_{MD} = 17 GPa, E_{CD}=12 GPa, and Poisson's ratio,ν_{MD} = 0.350, ν_{CD} = 0.247 . The plate is loaded by edge moments. The bearing conditions and edge moments are presented in Figure 3.4 and Table 3.8.

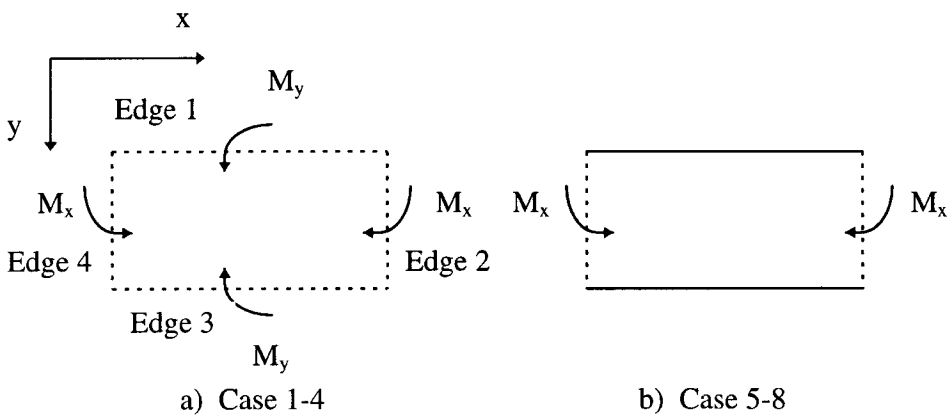

a) Case 1-4 b) Case 5-8

Figure 3.4 Bearing condition of the plates. Dashed line denotes simply supported edges with edge moment and fixed edges are marked with solid lines.

A positive moment produces tension in the layers located at the bottom part of the structure. This sign convention is maintained for the plates.

Table 3.8 Bearing condition of the orthotropic plate. SS signs Simply Supported edge and F signs Fixed edge. Material properties A and B are presented in Table 3.9.

Case	M_x	M_y	Edge1	Edge2	Edge3	Edge4	Material
1	1	2	SS	SS	SS	SS	A
2	2	1	SS	SS	SS	SS	A
3	1	2	SS	SS	SS	SS	B
4	2	1	SS	SS	SS	SS	B
5	1	2	F	SS	F	SS	A
6	2	1	F	SS	F	SS	A
7	1	2	SS	F	SS	F	B
8	2	1	SS	F	SS	F	B

Table 3.9 Mechanical properties for materials A and B

	E_{MD}[MPa]	E_{CD}[MPa]	ν_{MD}	ν_{CD}	G[MPa]
Material A	17	12	0.350	0.247	5.5
Material B	12	17	0.247	0.35	5.5

The calculated results obtained by MecHPL are compared with calculated ones obtained by an established and validated mechanical program. The chosen program is Ansys computer software for mechanical engineering. Ansys is based on Finite Element Modelling (FEM) and is a mechanical CAE tool which helps in building a complete finite element model, including physical and material properties, loads and boundary conditions. Here, it should be mentioned that the model in both programs contains, 30x30 nodes.

Table 3.10 Results calculated by MecHPL for the cases defined in Table 3.8.

Case	w[mm]	M_x^{max}[Nmm]	M_x^{min}[Nmm]	M_y^{max}[Nmm]	M_y^{min}[Nmm]
1	0.075	1.064	0.737	1.934	0.366
2	0.047	1.822	0.369	1.025	0.563
3	0.059	0.972	0.512	1.966	0.497
4	0.036	1.764	0.252	1.133	0.786
5	0.0083	1.845	-0.307	0.491	-0.869
6	0.0403	0.755	-1.700	1.918	-0.420
7	0.0083	1.816	-0.303	0.701	-1.239
8	0.0356	0.5164	-1.199	1.938	-0.425

Table 3.11 Results calculated by Ansys for the cases defined in Table 3.8.

Case	w[mm]	M_x^{max}[Nmm]	M_x^{min}[Nmm]	M_y^{max}[Nmm]	M_y^{min}[Nmm]
1	0.075	1.053	0.737	1.933	0.367
2	0.047	1.819	0.369	1.021	0.561
3	0.059	0.967	0.517	1.965	0.501
4	0.036	1.758	0.255	1.126	0.788
5	0.0083	1.845	-0.298	0.490	-0.875
6	0.0409	0.750	-1.703	1.919	-0.412
7	0.0083	1.815	-0.299	0.700	-1.246
8	0.0358	0.5196	-1.201	1.939	-0.422

A comparison of the results, w, M_x and M_y, in Tables 3.10, 3.11, shows that the deviation of results obtained by MecHPL and Ansys, is less than 0.5 %. Figure 3.5 shows the calculated deflections which are almost exactly matched.

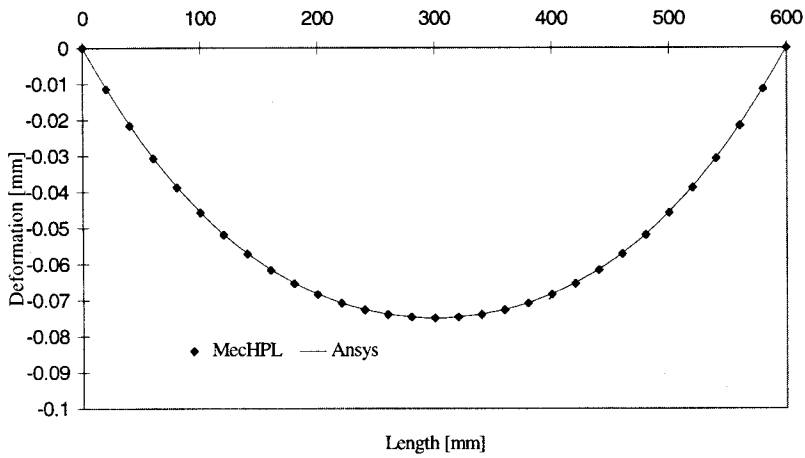

Figure 3.5 Results, lateral deflection (w) in centre of the plate , obtained from MecHPL compared with results from Ansys

3.2.4 Optimal Number of Discritization Points and Calculation Time

The choice of the number of discritization points depends on the user's demand on calculation time and accuracy. Higher accuracy, which is obtained from a denser mesh, requires a longer calculation time.

A comparison of the calculated values obtained by MecHPL with tabulated values or the results obtained by Ansys, shows that there are some deviations. The deviation level varies with type of boundary condition. For each mesh, there is a deviation in the calculated results. For instance, 20x20 discritization

points gives a deviation less than 1% when compared with tabulated values. The calculation time for this case was less than two minutes. By increasing the number of the discritization points to 30x30, the deviation decreases to 0.5% and the calculation time increases to seven minutes. Finally, the deviation of the results obtained by a mesh with 40x40 points is about 0.25% and the calculation time is about 45 minutes, which is sex times longer than for the 30x30 mesh.

It should be mentioned here that the choice of relaxation factor, R, affects the calculation time. The recommended relaxation factor lies between 1.8 and 1.95. In the above mentioned example the relaxation factor is equal to 1.8, by choosing a more optimal relaxation factor, normally a higher one, the calculation time becomes shorter.

3.3 Conclusion

MecHPL is capable of calculating the deflections in thin isotropic and orthotropic plates exposed to a uniformly distributed load with an arbitrary length and width. The program can also handle edges loaded with an edge moment. The boundary condition of the plate can either be simply supported or fixed edges. Simultaneous bending and stretching of the plates can be handled by the program if the normal forces are known.

A 30x30 mesh with a relaxation factor equal to 1.8 is a suitable choice for the calculating of deformation of plates with dimensions 0.6x0.6x0.006 m^3.

3.4 References

[1] Rudolph Szilard, Theory and Analysis of Plates, 1974, ISBN 0-13-913426-3

[2] Timoshenko and Goodier, Theory of Elasticity, McGrow-Hill, 1969

[3] Lekhiskii, S.G., Theory of Elasticity of an Anisothropic Elastic Body, Holden-Day, San Fransisco, 1963

[4] Daniel Larsson, Mechanical Characterization of Engineering Materials by Modal Testing, Doctoral thesis, Chalmers University of Technology, 1997

[5] B. Adl-Zarrabi, Determination of the Mechanical Properties of High Pressure Laminate with Various Moisture Content, Department of Building Physic, Chalmers University of Technology, Report 902, R-98.2

[6] Bares, Tables for the Analysis of Plates, Slabs and Diaphragms, Based on the Elastic Theory, 1964

Literature

- L.R. Calcute,The Analysis of Laminated Composite Structures, Department of Structural Research, Southwest Research Institute, San Antonio, Texas, 1969

- *Eric Reissner,Reflection on the Theory of Elastic Plates, Appl Mech Rev vol 38, no 11, Nov 1985*

- Curtis F. Gerald and Patrick O. Wheatly, Applied Numerical Analysis, California Polytechnic State University, 1994

- Wolfgang Hackbusch, Iterative Solution of Large Sparse Systems of Equations, Applied Mathematical Science 1995

- Wolfgang Hackbusch, Elliptic Differential Equations, Theory and Numerical Treatment, Us, 1992

- *Eric Reissner, The Effect of Transvese Shear Deformation on the Bending of Elastic Plates, Journal of Applied Mechanics, 1945*

- F.S. Shaw, An Introduction to Relaxation Methods, 1953, US

- Ulrika Wendt, Adaptive Modelling of Plates in Bending and Shear, Licentiate thesis, Chalmers University of Technology, Sweden, 1994

Part C Transient Hygro-elasticity

Part C Transient Hygro-elasticity

The non-uniform distribution of moisture in a material causes expansion and/or contraction, which leads to a state of internal stresses and strains. The coupling between these stresses/strains and moisture diffusion represents a complex physical phenomenon. In this chapter, moisture induced stress/strain, which leads to lateral deformations of a plate, will be treated.

According to the assumptions and limitations of this work, the stress/strain gradient has a negligible influence on the moisture diffusion process. Thus, moisture distribution can be determined independently of the stress analysis. It should be mentioned that the influence of moisture on mechanical material properties is taken into account in the calculations of moisture induced deformation. Furthermore, it is assumed that the moisture induced deformations are in the elastic range. Thus, the stress field resulting from the non-uniform distribution of moisture can be superimposed on that resulting from the field of external loading. Finally, isothermal conditions and one-dimensional transient moisture diffusion over the thickness of the HPL plates are considered.

By using these assumptions and limitations, treated in Part A and Part B, moisture induced deformation of HPL plates will be determined. The boundary conditions of the plates are: free to deform, simply supported edges and fixed edges. In the case of plates with fixed edges and simply supported edges, the calculations of the moisture induced forces and deformations are obtained by using the superposition principle.

1 Addition of Hygro-stresses to the PDE of Plates Exposed to Non-uniform Moisture Distribution through the Thickness

The governing partial differential equation, Equation (1.17) in Part B will be completed below with the influence of the non-uniform moisture distribution over the cross section of the HPL plates. It should be noted that this moisture distribution will not contribute to the shear strain components.

By substituting Equations (1.8, 1.9 and 1.13) into Equations (1.15a-b) in Part B, the orthotropic stress-strain relationships, without moisture influence, can be rewritten as:

$$\sigma_x = \frac{E_x}{1 - \nu_{xy}\nu_{yx}}(\varepsilon_x + \nu_{yx}\varepsilon_y) \tag{1.1a}$$

$$\sigma_y = \frac{E_y}{1 - \nu_{xy}\nu_{yx}}(\varepsilon_y + \nu_{xy}\varepsilon_x) \tag{1.1b}$$

Moisture induced stresses can be superimposed on Equation (1.1).

$$\sigma_x = \frac{E_x}{1-\nu_{xy}\nu_{yx}}(\varepsilon_x + \nu_{yx}\varepsilon_y - (\beta_x + \beta_y\nu_{yx})\cdot\Delta u) \tag{1.2a}$$

$$\sigma_y = \frac{E_y}{1-\nu_{xy}\nu_{yx}}(\varepsilon_y + \nu_{xy}\varepsilon_x - (\beta_y + \beta_x\nu_{xy})\cdot\Delta u) \tag{1.2b}$$

where u is the moisture content mass by mass and Δu is equal to $u-u_0$, where u_0 is the initial moisture content of the material. The parameters β_x and β_y are the moisture expansion coefficients in the x-direction (MD) and the y-direction (CD).

The resultant moment (m) and the axial force (n) acting on the plate due to non-uniform moisture distribution can be calculated by substituting Equations (1.2a) and (1.2b) into Equation (1.14) in Part B:

$$m_x = \int_{-\frac{h}{2}}^{\frac{h}{2}} \frac{E_x}{1-\nu_{xy}\nu_{yx}}(\varepsilon_x + \nu_{yx}\varepsilon_y - (\beta_x + \beta_y\nu_{yx})\cdot\Delta u)\cdot z\,dz \tag{1.3a}$$

$$m_y = \int_{-\frac{h}{2}}^{\frac{h}{2}} \frac{E_y}{1-\nu_{xy}\nu_{yx}}(\varepsilon_y + \nu_{xy}\varepsilon_x - (\beta_y + \beta_x\nu_{xy})\cdot\Delta u)\cdot z\,dz \tag{1.3b}$$

$$n_x = \int_{-\frac{h}{2}}^{\frac{h}{2}} \frac{E_x}{1-\nu_{xy}\nu_{yx}}(\varepsilon_x + \nu_{yx}\varepsilon_y - (\beta_x + \beta_y\nu_{yx})\cdot\Delta u)\,dz \tag{1.4a}$$

$$n_y = \int_{-\frac{h}{2}}^{\frac{h}{2}} \frac{E_y}{1-\nu_{xy}\nu_{yx}}(\varepsilon_y + \nu_{xy}\varepsilon_x - (\beta_y + \beta_x\nu_{xy})\cdot\Delta u)\,dz \tag{1.4b}$$

Equations (1.3) and (1.4) can be written as:

$$m_x = m_x^i - m_x^m \tag{1.5a}$$

$$m_x^i = \int_{-\frac{h}{2}}^{\frac{h}{2}} \frac{E_x}{1-\nu_{xy}\nu_{yx}}(\varepsilon_x + \nu_{yx}\varepsilon_y)\cdot z\,dz \tag{1.5b}$$

$$m_x^m = \int_{-\frac{h}{2}}^{\frac{h}{2}} \frac{E_x}{1-\nu_{xy}\nu_{yx}}(\beta_x + \beta_y\nu_{yx})\cdot\Delta u\; z dz \tag{1.5c}$$

$$m_y = m_y^i - m_y^m \tag{1.6a}$$

$$m_y^i = \int_{-\frac{h}{2}}^{\frac{h}{2}} \frac{E_y}{1-\nu_{xy}\nu_{yx}}(\varepsilon_y + \nu_{xy}\varepsilon_x) \cdot z \, dz \tag{1.6b}$$

$$m_y^m = \int_{-\frac{h}{2}}^{\frac{h}{2}} \frac{E_y}{1-\nu_{xy}\nu_{yx}}(\beta_y + \beta_x\nu_{xy}) \cdot \Delta u \, z dz \tag{1.6c}$$

Here, m^i corresponds to the internal moments and m^m corresponds to the moisture induced moments. These moments are not dependent of x,y. This means that Equation (1.4) in Part B remains unchanged. The moisture induced moments enter in the boundary condition only. See Equation (1.18) in this part.

In a similar manner the axial forces become:

$$n_x = n_x^i - n_x^m, \qquad n_y = n_y^i - n_y^m$$

where n^i designates internal axial forces and n^m designates the moisture induced axial forces.

$$n_x^m = \int_{-\frac{h}{2}}^{\frac{h}{2}} \frac{E_x}{1-\nu_{xy}\nu_{yx}}(\beta_x + \beta_y\nu_{yx}) \cdot \Delta u \, dz \tag{1.7a}$$

$$n_y^m = \int_{-\frac{h}{2}}^{\frac{h}{2}} \frac{E_y}{1-\nu_{xy}\nu_{yx}}(\beta_y + \beta_x\nu_{xy}) \cdot \Delta u \, dz \tag{1.7b}$$

Axial forces and moments induced by moisture are formulated in Equations (1.5-1.7). As mentioned before, the superposition principle will be used. These moisture induced forces and moments are superimposed on a plate with a uniform moisture condition, considering the modification of boundary conditions.

1.1 Dimensionless Moisture Induced Moment Factor

In Equations (1.5-1.6), the integration terms include material parameters and the difference in the moisture content over the thickness of the plate. By assuming that the material parameters of the plate, β, ν and E are not dependent on the moisture content variation in the material, the dimensionless moisture induced moment factor, I, can be introduced:

$$I = \frac{1}{h^2} \int_{-\frac{h}{2}}^{\frac{h}{2}} \Delta u \, z dz \tag{1.8}$$

By introducing this factor into Equation (1.5c) we get:

$$m_x^m = C_x \cdot I \tag{1.9}$$

Here, C_x [Nm/m] is a constant, depending on material properties and the thickness of the plate. The constant, C_x has the same dimension as the moment.

$$C_x = \frac{E_x}{1 - \nu_{xy}\nu_{yx}} (\beta_x + \beta_y \nu_{yx}) \cdot h^2 \tag{1.10}$$

In a similar manner, m_y^m becomes:

$$m_y^m = C_y \cdot I \tag{1.11a}$$

$$C_y = \frac{E_y}{1 - \nu_{xy}\nu_{yx}} (\beta_y + \beta_x \nu_{xy}) \cdot h^2 \tag{1.11b}$$

The dimensionless moisture induced moment factor can be used for simplified calculations in the design of HPL applications. This factor gives an indication of the level of the moisture induced moment, i.e., the magnitude of the moisture induced moment for different thicknesses and different moisture content differences. However, it should be mentioned that these calculations neglect the influence of the moisture content on the material properties, for instance, elastic modulus. The difference between the results obtained by simplified calculations and the results of a more accurate calculation, for instance with the PC-program MHPL, could be about 20%.

In Chapter 2, the nature of the moisture induced moment factor, and the use of the factor will be demonstrated.

1.2 Free to Deform Plate

In an orthotropic free to deform plate exposed to a moisture gradient through the thickness of the plate, the plate is physically free to deform at the boundaries. Nevertheless the individual laminae of the plate cannot expand freely due to the restriction of the continuity, thus, their free expansion/ contraction prevents and causes deformations. The form of the deformation is shown in Figure 1.1.

The magnitude of the displacement at the midpoint on the plate, δ, can be calculated from Equation (1.12).

$$\delta \approx R \cdot (1 - \cos(\frac{L}{2R})) \qquad (1.12)$$

where R is the radius of the plate curvature and L is the length of the plate.

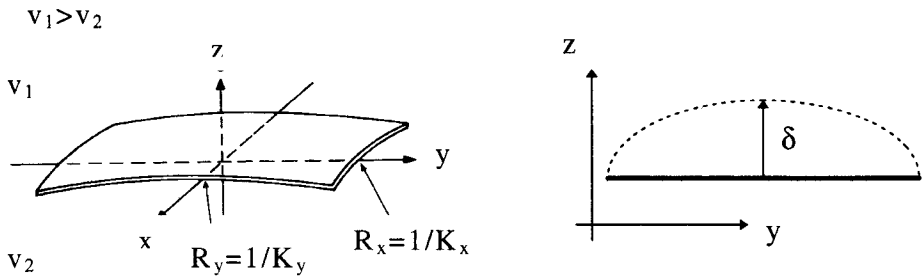

Figure 1.1 The state of deformation is expressed by the curvatures K_x and K_y. R_x and R_y are the radii of the plate curvatures. v_1 and v_2 are the humidity by volume of the ambient air.

In a free to deform plate, i.e., no external forces and moments are in action $m_x=0$, the moisture induced moments should be in balance with the internal moments, $m_x^i = m_x^m$ (self-equilibrated). Thus, to calculate the curvature, Equations (1.5) and (1.6), using equations (1.9) and (1.10), can be rewritten as:

$$\int_{-\frac{h}{2}}^{\frac{h}{2}} (\varepsilon_x + \nu_{yx}\varepsilon_y)\, z\, dz = h^2 \cdot (\beta_x + \beta_y \nu_{yx}) \cdot I \qquad (1.13a)$$

$$\int_{-\frac{h}{2}}^{\frac{h}{2}} (\varepsilon_y + \nu_{xy}\varepsilon_x)\, z\, dz = h^2 \cdot (\beta_y + \beta_x \nu_{xy}) \cdot I \qquad (1.13b)$$

Here, we have assumed constant values for β_x, β_y, ν_{xy} and ν_{yx} ,i.e., they are not dependent on the moisture content variation of the material.

Equations (1.10-1.11) in part B, can be rewritten as:

$$\varepsilon_x = -z \frac{\partial^2 w}{\partial x^2} = z K_x \qquad (1.14a)$$

$$\varepsilon_y = -z\frac{\partial^2 w}{\partial y^2} = z\,K_y \tag{1.14b}$$

where K_x and K_y are the curvature of the orthotropic plate with respect to the x- and y-directions.

Substituting Equation (1.14) into (1.13) gives:

$$(K_x + \nu_{yx}\,K_y)\int_{-\frac{h}{2}}^{\frac{h}{2}} z^2\,dz = h^2\cdot(\beta_x + \beta_y\nu_{yx})\cdot I \tag{1.15a}$$

$$(K_y + \nu_{xy}\,K_x)\int_{-\frac{h}{2}}^{\frac{h}{2}} z^2\,dz = h^2\cdot(\beta_y + \beta_x\nu_{xy})\cdot I \tag{1.15b}$$

The integration of Equations (1.15a) and (1.15b) gives:

$$K_x + \nu_{yx}\,K_y = \frac{12}{h}\cdot(\beta_x + \beta_y\nu_{yx})\cdot I \tag{1.16a}$$

$$K_y + \nu_{xy}\,K_x = \frac{12}{h}\cdot(\beta_y + \beta_x\nu_{xy})\cdot I \tag{1.16b}$$

By substituting Equation (1.16a) into (1.16b), the curvatures K_x and K_y can be calculated.

$$K_x = \frac{12\cdot\beta_x\cdot I}{h} \tag{1.17a}$$

$$K_y = \frac{12\cdot\beta_y\cdot I}{h} \tag{1.17b}$$

Using these curvatures, the centre deformation of the plate can be determined by Equation (1.12).

Equation (1.17) demonstrates that the curvature of the plate is proportional to the expansion/contraction coefficients of the material and the moisture induced moment factor, I. The elastic properties of the plate have no influence on the deformation of a free to deform plate.

1.3 Simply Supported and Fixed Boundary

Moisture stresses are produced if the free expansion is restricted by certain boundary conditions. The moisture induced moment should be in balance with internal and external moments according to the equilibrium equation, Equation

(1.4) in Part B. This means that the equilibrium equation should be fulfilled at all parts of the plate. In the absence of external loads and by substituting Equations (1.5a) and (1.6a) into Equation (1.4) in Part B and by omitting the index, i, for simplification, we get:

$$\frac{\partial^2 m_x}{\partial^2 x} + 2\frac{\partial^2 m_{xy}}{\partial x\,\partial y} + \frac{\partial^2 m_y}{\partial^2 y} = 0 \qquad (1.18)$$

Since the moisture induced moments, m_x^m and m_y^m, are neither dependent on x nor on y, Equation (1.18) is the same as the equilibrium equation of a plate with uniform moisture distribution. This indicates that the plate problem exposed to the non-uniform moisture distribution over a cross-section of the plate can be reduced to the plate problem of uniform moisture distribution. However, the boundary condition of the plate should be modified.

1.3.1 Modification of the Boundary Condition

If the free expansion of the plate is to be hindered, the plate have to be exposed to normal forces, n, [N/m], see Figure 1.2. In the thin plate theory, these forces have to be transferred to the middle surface of the plate. The normal forces can be transformed to the middle surface as a result of normal forces and the moment induced by these forces.

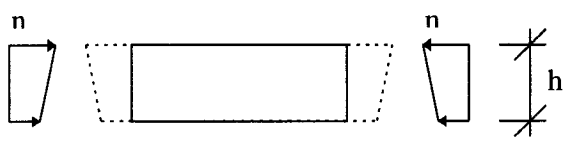

Figure 1.2 The plate should be exposed to normal forces, if free expansion is to be hindered.

In a fixed edge plate, the edge of the plate is exposed to the resultant of the normal forces, which prevent normal strains. These normal forces are equal to moisture induced normal forces, according to Equation (1.7). As long as the normal forces are known, the influence of the normal forces on the lateral deflection can be treated according to Chapter 1.7 in Part B. The moment induced by the transformation of the normal forces is equal to the moisture induced moment absorbed by the fixed boundary. Thus, the lateral deflection of the fixed edge plate is the deflection of a plate with a uniform moisture distribution, loaded by a transverse load, p_z^*, which is a function of n_x^m and n_y^m according to Equation (1.25b) in Part B.

In a simply supported plate the normal forces can be treated as explained for a fixed edge plate, but a simply supported plate cannot bear the moment induced

by the transformation of the normal forces. Therefore the boundary condition of the plate should be modified by a edge moment equal to the moisture induced moment, according to Equations (1.21-1.24) in Part B, Chapter 1.6. Thus, the lateral deflection of a simply supported plate exposed to a non-uniform moisture condition, can be calculated by a plate with a uniform moisture distribution exposed to edge moment and transverse load.

Finally, by these modifications Equation (1.18) can be rewritten as:

$$\frac{\partial^2 m_x}{\partial^2 x} + 2\frac{\partial^2 m_{xy}}{\partial x \partial y} + \frac{\partial^2 m_y}{\partial^2 y} = p_z^* \qquad (1.19)$$

Figure 1.3 illustrates the modification of boundary conditions, fixed- and simply supported edges, for a plate which is exposed to uniform moisture distribution over the cross-section of the plate. The external load, p_z^*, corresponds to the influence of moisture induced normal forces, and, m^m corresponds to the moisture induced moment.

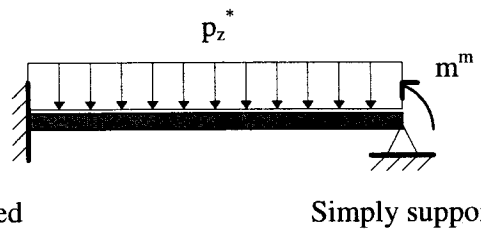

Figure 1.3 Modification of boundary conditions, fixed and simply supported edges.

2 Nature of the Moisture Induced Moment

The aim of this chapter is to determine the variation of the dimensionless moisture induced moment factor, I, by using analytical solutions for a plate which is exposed to step-change or periodic variations in the surrounding climate. In order to obtain analytical solutions, the moisture permeability and the slope of the sorption curve are assumed to be constant in the humidity range of interest.

Figure 2.1 shows the thin plate under observation. The humidity by volume on the left-hand side of the plate is constant and on the right-hand side it can change periodically or as a step-change.

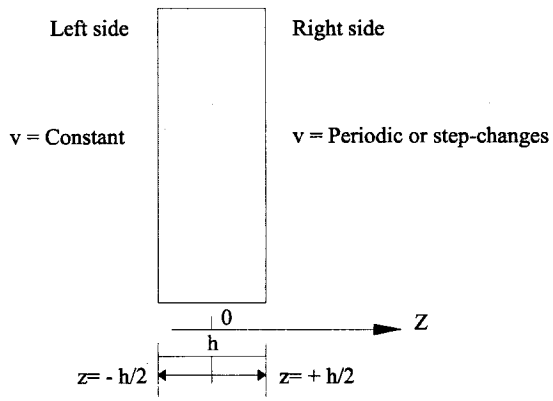

Figure 2.1 The geometry and the boundary condition of the plate.

The linearization of the sorption curve will be used in determining the dimensionless moisture induced moment factor, introduced in Section 1.1, Equation (1.8). The sorption curve is linearized around $\phi = \phi_0$ according to Equation (2.1).

$$w - w_o = \frac{v - v_0}{v_s(T)} \cdot \left.\frac{dw}{d\phi}\right|_0 = \frac{\Delta v}{v_s(T)} \cdot \left.\frac{dw}{d\phi}\right|_0 \tag{2.1}$$

Equation (1.8) can be rewritten as:

$$I = \left.\frac{dw}{d\phi}\right|_0 \frac{1}{v_s(T)} \frac{1}{\rho h^2} \int_{-\frac{h}{2}}^{\frac{h}{2}} \Delta v \cdot z dz \tag{2.2}$$

2.1 Step-change of the Moisture

Assume that the plate under consideration has the following initial condition:

$$v = v_0 \qquad -h/2 \le z \le h/2 \qquad \text{for} \qquad t \le 0$$

Suddenly, at time zero, the humidity on the right-hand side of the plate is changed to v_1:

$$v_{BR} = v_1 \quad z = +h/2 \quad \text{for} \quad t > 0$$
$$v_{BL} = v_0 \quad z = -h/2 \quad \text{for} \quad t \ge 0$$

The variation of the I-factor due to the step-change (v_1-v_0) is given by [1]:

$$I = \left.\frac{dw}{d\phi}\right|_0 \frac{1}{v_s(T)} \frac{v_1 - v_0}{\rho} \cdot f^0\left(\frac{\sqrt{Dt}}{h}\right) \tag{2.3}$$

$$D = \frac{\delta_v \cdot v_s(T)}{dw \,/\, d\phi} \tag{2.4}$$

Where, $\sqrt{Dt}$, is the penetration depth. It is defined by the case of a very thick plate exposed to a step change on one of its sides. At the depth $\sqrt{Dt}$ from the exposed side, half the step in humidity by volume has been reached, i.e., v is equal to $(v_1+v_0)/2$. The value of the dimensionless function, f^0 in Equation (2.3), is presented in Table 2.1.

Table 2.1 Values for the $f^0(\alpha)$. In Equation (2.3), α corresponds to $\frac{\sqrt{Dt}}{h}$.

α	0	0.02	0.04	0.06	0.08	0.1	0.12	0.14	0.16	0.18
f^0	0	0.011	0.021	0.030	0.039	0.046	0.053	0.059	0.065	0.069

α	0.2	0.25	0.3	0.35	∞
f^0	0.073	0.079	0.082	0.083	0.083

An equilibrium of the plate with ambient air is reached approximately when $\sqrt{Dt} = h \cdot 0.35$. This corresponds to a time, t, equal to $h^2 \cdot D^{-1} \cdot 0.35^2$.

2.2 Periodical change of Moisture

For this case, the right-hand side of the plate is exposed to a periodical moisture variation in time, i.e., a periodic variation in the humidity by volume, with the

amplitude of v_A, varying around a constant value v_0. On the left-side of the plate a constant humidity by volume is maintained.

$$v_{BL} = v_o, \quad z=-h/2$$

$$v_{BR} = v_0 + v_A \cdot \sin(\frac{2\pi t}{t_p}) \qquad z = h/2$$

The variation of the dimensionless moisture induced moment factor due to the periodical variation is obtained from [1].

$$I(t) = I_A \cdot \sin\left(\frac{2\pi(t - t_{lag})}{t_p}\right) \tag{2.5}$$

where I_A and t_{lag} can be expressed as:

$$I_A = \frac{dw}{d\phi}\bigg|_0 \frac{1}{v_s(T)} \frac{v_A}{\rho} \cdot \left|\hat{I}_0\left(\frac{d_p}{h}\right)\right| \tag{2.6}$$

$$t_{lag} = -\frac{t_p}{2\pi} \cdot \arg\left(\hat{I}_0\left(\frac{d_p}{h}\right)\right) \tag{2.7}$$

and finally periodic penetration depth can be expressed as:

$$d_p = \sqrt{\frac{D \cdot t_p}{\pi}} \tag{2.8}$$

The absolute value and phase for the complex-value function $\hat{I}_0$ are presented in Table 2.2.

Table 2.2 Absolute value and phase for the complex-value function $\hat{I}_0$. In Equations (2.6) and (2.7) β corresponds to d_p / h

β	$\lvert\hat{I}_0(\beta)\rvert$	$-\frac{1}{2\pi}\arg(\hat{I}_0(\beta))$
0	0	0.125
0.02	0.007	0.122
0.04	0.014	0.118
0.06	0.020	0.115
0.08	0.026	0.111
0.10	0.032	0.107
0.12	0.038	0.104
0.14	0.043	0.100
0.16	0.049	0.095
0.18	0.054	0.090
0.20	0.059	0.084
0.25	0.070	0.067
0.30	0.076	0.052
0.35	0.079	0.040
0.40	0.080	0.032
0.50	0.082	0.021
0.60	0.083	0.015
0.75	0.083	0.0094
1.0	0.083	0.0053
1.5	0.083	0.0024
2.0	0.083	0.0013

2.3 Moisture Induced Moments, Hindered Free Expansion

The variation of the moisture induced moment, due to step and periodical moisture changes, in a plate in which free expansion is hindered can be calculated approximately by substituting Equations (2.3) and (2.6) into Equations (1.9-1.11).

Any variation of the moisture induced moment depends on the variation of the dimensionless moisture induced moment factor, I. In the next section, a few examples are presented in order to illustrate the calculation of the dimensionless moisture induced moment factor and the moisture induced moment.

The calculation of the moisture induced moment can be used when designing the HPL for different applications. However, it should be noted that the

calculated moment is only an approximation, since simplified moisture data are used. For more accurate analyses, the MHPL program should be used.

2.3.1 Calculation of Dimensionless Moment Factor, a Few Examples

In this section two examples are presented. In the first example, the moisture condition is changed step wise and, in the second one, the moisture condition is changed periodically, see Sections 2.1 and 2.2.

Example 1: Calculation using an isotropic plate with a thickness of 0.006 m and following material properties exposed to a step-change in humidity, i.e. from 30% to 50% relative humidity.

$E = 20$ GPa, $\nu = 0.3$, $\beta = 5 \cdot 10^{-2}$[1/mc%], $\delta_v = 2.4 \cdot 10^{-8}$ m^2/s, $dw/d\phi = 150$ kg/m^3, $T = 20$ °C, $v_s(T) = 17.28 \cdot 10^{-3}$ kg/m^3, $v_1 - v_0 = 3.46 \cdot 10^{-3}$ kg/m^3, $\rho = 1383$ kg/m^3

The following calculations will be performed:

a. Calculation of the moisture induced moment.
b. Calculation of the time until the steady-state condition is approximately reached.

c. Calculation of the maximum centre deformation of a free to deform plate with a length of 3 m.

a. Formula (2.3) is used for the calculation of the factor, I. First $\sqrt{Dt}/h$ is calculated for each time step, then f° is determined using Table 2.1. When the factor, I, is calculated, the moisture induced moment can be calculated by using Equations (1.9-1.11). Results of the calculation are shown in Figure 2.2.

b. The time which is required to reach an approximately steady-state condition then becomes:

$$t = (0.35)^2 \cdot \frac{h^2}{D} = 0.1225 \frac{0.006^2 \cdot 150}{2.4 \cdot 10^{-8} \cdot 17.28 \cdot 10^{-3}} = 1.6 \cdot 10^6 \text{s}$$

The time corresponds to 22 days. In Figure 2.3 the calculated dimensionless moisture induced moment factor, I, is shown in great details. The approximated time for steady-state is presented. If the moisture permeability is 10 times lower, the time will be increased to about 220 days.

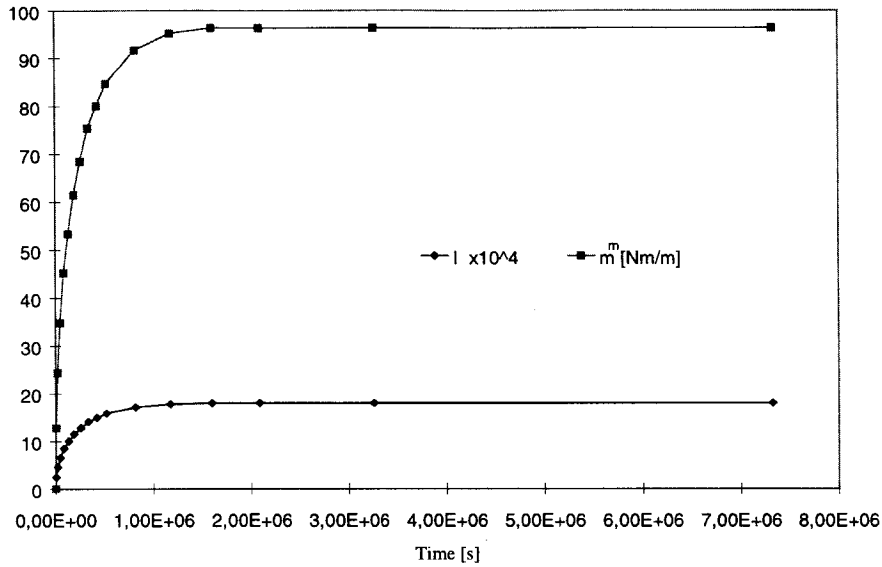

Figure 2.2 The calculated dimensionless moment factor, I, and the moisture induced moment, m^m.

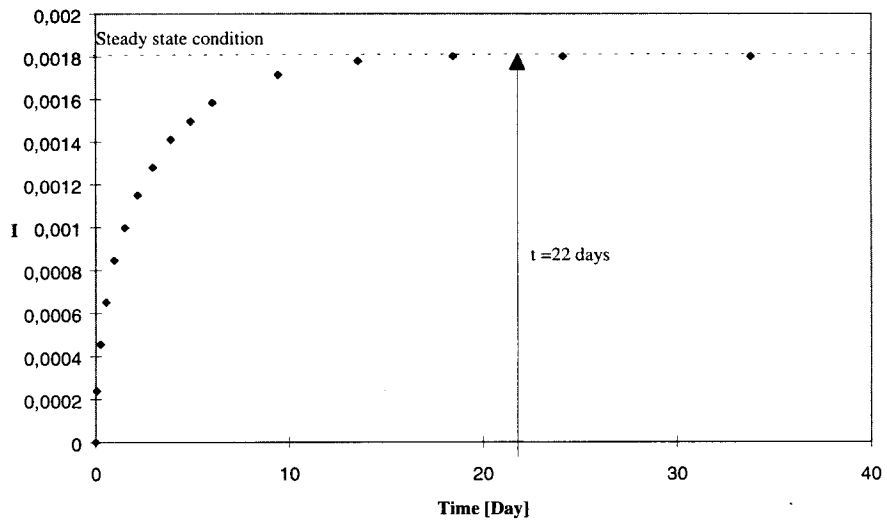

Figure 2.3 The calculated dimensionless factor, I, and the approximate time to reach steady-state.

c. Equations (1.17) and (1.8) give:

$$K = \frac{12\beta}{h} . I = \frac{12 \cdot 5 \cdot 10^{-2}}{0.006} 0.0018 = 0.18 \ 1/m$$

The factor, I, is equal to 0.0018 when the steady-state condition is reached.

$$R = \frac{1}{K} = 5.56 \text{ m}$$

Using Equation (1.12), the maximum deformation of the plate can be calculated:

$$\delta = 5.56 \cdot (1 - \cos(\frac{3}{2 \cdot 5.56}) = 0.2 \text{ m}$$

Example 2: A plate with the same material properties as in Example 1 is exposed to periodical moisture changes. The time period, t_p, is 24 hours and the amplitude of the variation, v_A, is 5 g/m^3. The amplitude of the dimensionless factor, I_A, and the time lag between the variation in humidity and the factor, I, are of interest.

Using Equations (2.4) and (2.8) we get moisture diffusivity, D, and periodic penetration depth, d_p, according to:

$$D = \frac{\delta_v \cdot v_s(T)}{dw \ / \ d\phi} = \frac{2.4 \cdot 10^{-8} \cdot 17.28 \cdot 10^{-3}}{150} = 2.76 \cdot 10^{-12} \text{ m}^2/\text{s}$$

$$d_p = \sqrt{\frac{D \cdot t_p}{\pi}} = \sqrt{\frac{2.76 \cdot 10^{-12} \cdot 24 \cdot 3600}{\pi}} = 0.276 \text{mm}$$

$$\frac{d_p}{h} = \frac{2.76 \cdot 10^{-4}}{0.006} = 0.046$$

The amplitude and phase of the dimensionless function, $\hat{I}_0$, is obtained by using Table 2.2.

$$\left| \hat{I}_0(0.046) \right| = 0.016$$

$$-\frac{1}{2\pi} \arg(\hat{I}_0(0.046)) = 0.117$$

Using Equations (2.6)-(2.7) the amplitude, I_A, and time lag, t_{lag} become:

$$I_A = \frac{dw}{d\phi}\bigg|_0 \frac{1}{v_s(T)} \frac{v_A}{\rho} \cdot \left| \hat{I}_0\left(\frac{d_p}{h}\right) \right| = \frac{150 \cdot 5 \cdot 10^{-3}}{17.28 \cdot 10^{-3} \cdot 1383} \cdot 0.016 = 5.02 \cdot 10^{-4}$$

$$t_{lag} = -\frac{1}{2\pi} \arg\left(\hat{I}_0\left(\frac{d_p}{h}\right) \right) \cdot t_p = 0.117 \cdot 24 \cdot 3600 = 10109 \text{ s} = 2.81 \text{ hours}$$

A schematic sketch of the calculated variables is presented in Figure 2.4.

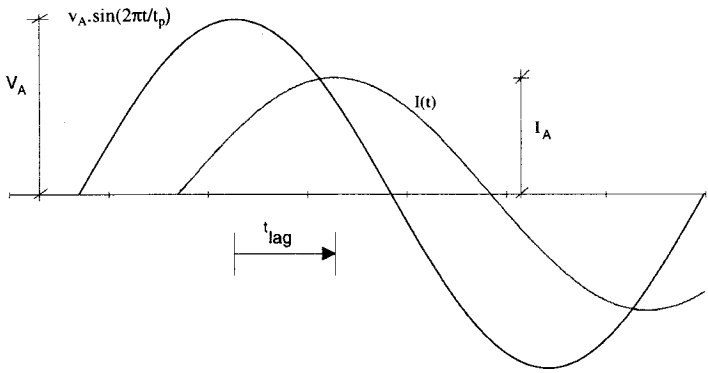

Figure 2.4 A sketch of the relation between I(t) and the periodic part of v(t).

The deformation at the centre of the plate, δ, will vary with time. It will change signs and the maximum magnitude is, then given by I_A, $5.02.10^{-4}$. Using Equations (1.17) and (1.18), periodical variation of the deformation will obtain the following extreme values.

$$\delta = \pm 0.056 \text{ m}$$

2.4 Moisture Induced Moment in HPL

The dimensionless moisture induced moment factor is calculated by the PC-program MHPL, first by using simplified moisture properties, such as material properties in Example 1 in Section 2.3.1, and then by using measured moisture properties as in Part A and B. The initial relative humidity of the plate and the relative humidity of the ambient air are 30 % for both cases.

The relative humidity on the right-hand side of the plate is changed from 30% to 50 %, for instance step-change, which corresponds to a change in the humidity by volume of 3.46×10^{-3} kg/m^3. For the second case, the plate is exposed to a periodical change as presented in Section 2.3.1. The moisture permeability and slope of the sorption isotherm for both cases are chosen by using the measured moisture permeability and sorption isotherm curve according to Part A.

The results of these calculations which deal with the step- and periodical changes are shown in Figures 2.5-2.6. Theses figures show that the maximum deviation of the factor, I, calculated by simplified and measured moisture properties is about 10 % after the steady-state condition. A ten percent deviation

seems to be acceptable. However, it should be observed that the moisture permeability of the HPL is almost constant in the relative humidity range of 30-50 %. This means that the deviation depends only on the difference between the measured slope of the sorption isotherm curve and the simplified one in this range. If the step change in the relative humidity of the ambient air takes place at higher relative humidity ranges, the deviation will increase, since moisture permeability varies strongly at higher relative humidities and, in addition, the slope of the sorption curve will increase.

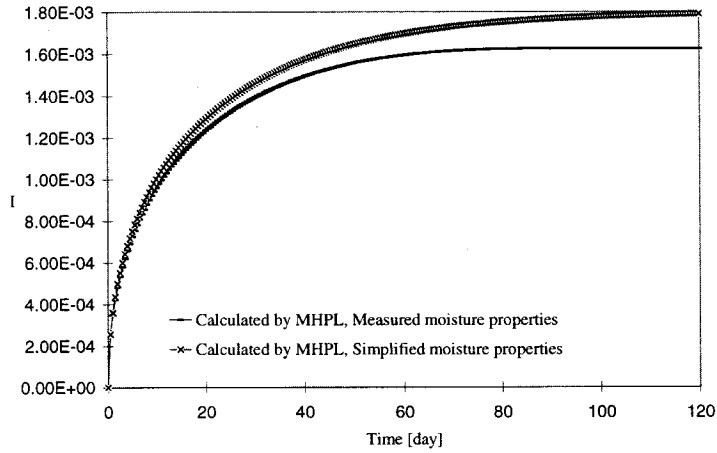

Figure 2.5 Factor I is calculated with the PC-program MHPL for the step-change at boundary humidity. The simplified moisture properties, according to Example 1 in Section 2.3.1, and the measured moisture properties are used as input data.

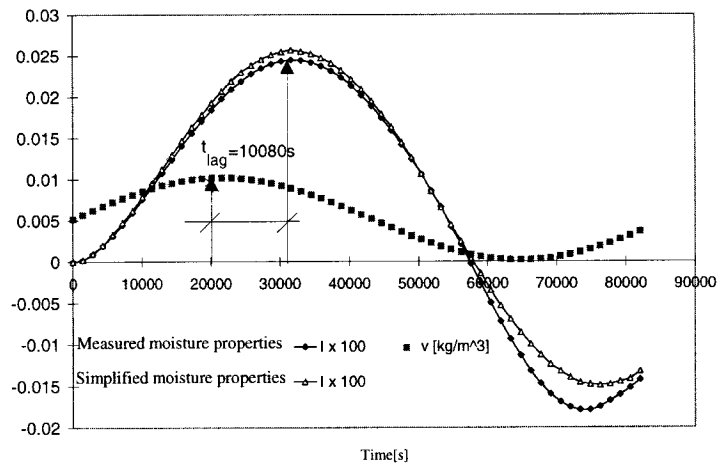

Figure 2.6 Factor I is calculated with the PC-program MHPL for periodical changes of the boundary humidity. The simplified and measured moisture properties are used as input data.

3 Calculation of Deformation in a Simply Supported Plate

In this section, the deformation of an orthotropic, simply supported plate loaded by edge moments will be calculated. The aim of these calculations is to provide benchmarks for some fundamental cases. These calculations are done by using the dimensionless moisture induced moment factor and the mechanical computer program, MecHPL.

A rectangular and simply supported plate loaded by edge moments, see Figure 3.1, is under consideration. Edges parallel to the x-axis are loaded by m_y^m, and edges parallel to the y-axis are loaded by m_x^m. The solution will be proportional to any of these moments. It will also depend on the ratio of these moments, that is on the ratio E_x/E_y, see Equations (1.9) to (1.11).

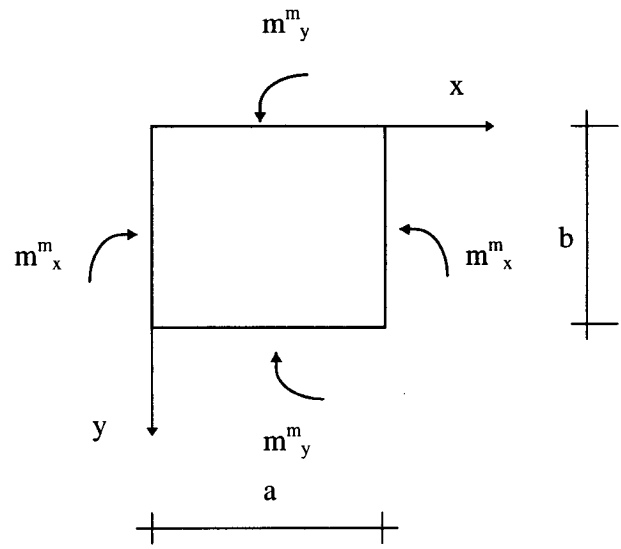

Figure 3.1. A simply supported plate, width (a) and length (b), loaded by edge moments.

By assuming that the ratio of the elastic modulus, E_x/E_y, and of the expansion coefficients, β_x/β_y, are known, the deformation of the plate due to edge moments can be calculated using scaling technique.

$$w = \ell \cdot w'(x/a, y/b) \tag{3.1}$$

Here, w' is a dimensionless function defined by the ratios a/b, E_x/E_y and β_x/β_y. The parameter ℓ has the dimension of a length. It is defined by:

$$\ell = \sqrt{\frac{m_x^m \cdot m_y^m}{D_x \cdot D_y}}\, a \cdot b \qquad (3.2a)$$

By substituting Equations (1.9-1.11) into Equation (3.2a) and using the expression of the D_x and D_y in Part B, Equation (3.2a) can be rewritten as:

$$\ell = 12 \cdot I \cdot \frac{a \cdot b}{h} \sqrt{(\beta_x + \beta_y \cdot \nu_{yx}) \cdot (\beta_y + \beta_x \cdot \nu_{xy})} \qquad (3.2b)$$

The deduction of Equation (3.1) is presented in Appendix C1.

The moisture induced deformation of an arbitrary simply supported plate can be calculated by Equation (3.1), if w' is known.

3.1 Calculation of Dimensionless Function, w'

The deformation, w, of the simply supported plate, with a fixed Poisson's ratio ν_{xy}=0.35 and ν_{yx}=0.25, is calculated by MecHPL for nine fundamental cases, according to Table 3.1, using specified values for the edge moments. The nine fundamental dimensionless deformations, w', are then determined from the relation in Equation (3.1).

Table 3.1 Nine fundamental cases

	Case 1	Case 2	Case 3	Case 4	Case 5	Case 6	Case 7	Case 8	Case 9
E_x / E_y	0.5	0.5	0.5	1	1	1	2	2	2
β_x / β_y	0.5	0.5	0.5	1	1	1	1	1	1
a / b	0.5	1	2	0.5	1	2	0.5	1	2

The result of the calculation for Case 1, in graphical form, is presented in Figure 3.2. The results for the other eight cases are presented in Appendix C2. Furthermore, the centre deformation of the plate for all cases is presented in Table 3.2.

Table 3.2 Calculated centre deformation of the plates.

w'_{centre} ($\times 10^{-2}$)								
Case 1	Case 2	Case 3	Case 4	Case 5	Case 6	Case 7	Case 8	Case 9
-5.34	-8.23	-6.98	-5.58	-7.47	-5.91	-5.54	-7.34	-5.61

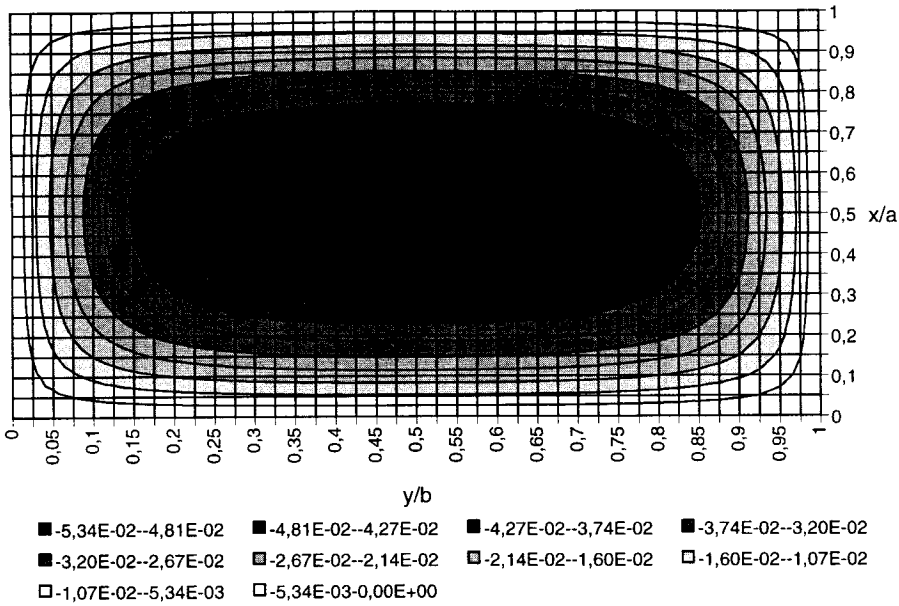

Figure 3.2 Calculated iso-curves for w′, Case 1.

Here should be mentioned that in Table 3.1, the relation between Young's moduli and Poisson's ratio, see Equation (1.6.b) in Part B, is not fulfilled. However, these calculations are not sensitive to deviation of the relation.

3.2 An Example for Calculation of Deformation

Example: An orthotropic simply supported plate with a thickness of 6 mm and the following material properties, is exposed to moisture induced moments m_x^m and m_y^m. Assume, that factor 'I' is equal to $6.8.10^{-3}$. The moisture induced deformation is to be calculated.

E_x=10 GPa	β_x=0.005 [1/mc%]	a = 0.4 m
E_y=20 GPa	β_y=0.010 [1/mc%]	b = 0.8 m
ν_{xy}=0.35	ν_{yx}=0.25	

The moisture induced moment can be calculated by using Equations (1.9-1.11).

$$m_x^m = \frac{E_x \cdot (\beta_x + \beta_y \nu_{yx}) \cdot h^2}{1 - \nu_{xy}\nu_{yx}} \cdot I =$$

$$\frac{10 \cdot 10^9 \cdot (0.005 + 0.010 \cdot 0.25)}{1 - 0.25 \cdot 0.35} \cdot 0.006^2 \cdot 6.8 \cdot 10^{-3} = 20.12 \text{ Nm/m}$$

$$m_y^m = \frac{20\cdot 10^9\cdot(0.010+0.005\cdot 0.35)}{1-0.25\cdot 0.35}\cdot 0.006^2\cdot 6.8\cdot 10^{-3} = 63.04 \text{ Nm / m}$$

D_x and D_y can be calculated using Equation (1.16) in Part B.

$$D_x = 197.26 \text{ Nm} \qquad D_y = 394.52 \text{ Nm}$$

When D_x , D_y and moisture induced moments are known, the length ℓ in Equation (3.2a) can be calculated.

$$\ell = \sqrt{\frac{m_x^m\cdot m_y^m}{D_x\cdot D_y}}.a\cdot b = \sqrt{\frac{20.12\cdot 63.04}{197.26\cdot 394.52}}\cdot 0.4\cdot 0.8 = 4.08\cdot 10^{-2}\text{m}$$

The relations of the material properties of the plate in this example, are the same as the relations in Case 1 in Table 3.1. Thus, w'_{centre} is equal to $-5.34.10^{-2}$, see Table 3.2. By using Equation (3.1) the centre deformation of the plate can be determined.

$$w_{centre} = \ell\cdot w'(0.5,0.5) = 4.08\cdot 10^{-2}\cdot(-5.34\cdot 10^{-2}) = -2.18 \text{ mm}$$

Here, it should be mentioned that the above calculation procedure, including Figure 3.2, can be used for the calculation of deformation at any arbitrary point of the plate. For instance, the deformation of the point, x/a =0.2, y/b=0.5, becomes:

$$-0.032\cdot 10^{-2} \geq w'(0.2,0.5) \geq -0.0374\cdot 10^{-2}$$

Using Equation (3.1), the deformation of the point becomes:

$$-1.31 \geq w(0.2,0.5) \geq -1.53 \text{ mm}$$

4. Validation Tests

A series of tests are made to validate the simulation model. In the first measurement, the plate is free to deform and, in the second test series the plates are simply supported. The moisture conditions will be explained in the description of each measurement. The deformation of the centre of the plates is measured and the measurement results obtained from the tests will be compared with the calculated ones.

4.1 The Free to Deform Plate, Measurement of Deformation

A specimen of HPL was sealed to a climate box in such a way that the free expansion of the plate was not hindered. This specimen was made from the same HPL batch that was used for the determination of the hygro- and mechanical properties. The area of the specimen was 0.2x 0.3 m^2 and the thickness of the plate was about 0.006 m. The box was placed in a climate chamber. The relative humidity of the climate chamber was constant, 50 % , and the temperature was about 20 °C. Inside the box, the relative humidity was 11%, which was sustained by using saturated salt (Lithium chloride). The centre deformation of the plate was measured by a dial gauge. The resolution of the dial gauge was 0.01 mm and it was mounted to a steel plate in order to stabilised the position of the dial gauge.

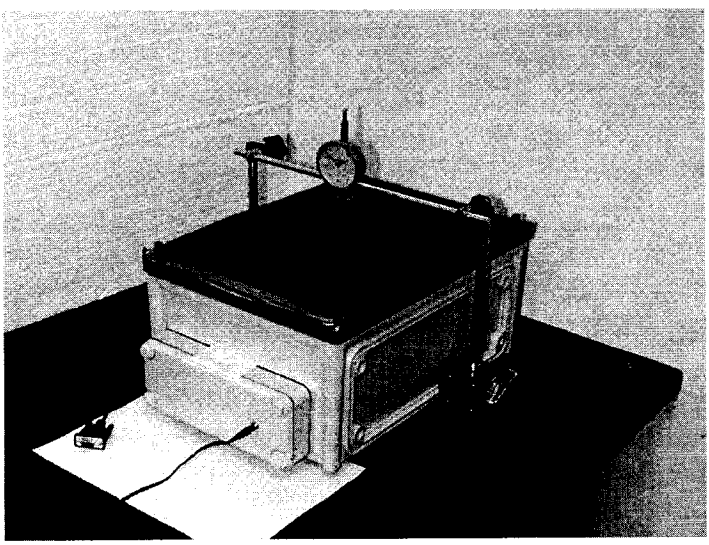

Picture 1 Test arrangement for measurement of deformation.

The dial gauge was calibrated by a micro meter instrument, Mitutoyo. The

micro meter had an accuracy of 0.005 mm. Calibration results indicated that the accuracy of the dial gauges was equal to 0.01 mm.

The relative humidity in the climate box was measured by a moisture sensor, TinyTag, for confirmation of the condition of the saturated solution. To reduce the surface vapour resistance between the specimen and the conditioned air, a fan was mounted in the climate box. The time interval between two measurements was less or equal to one day.

4.1.1 Results and Discussion

The centre deformation of the plate during the measured time, about 160 days, is presented in Figure 4.1.

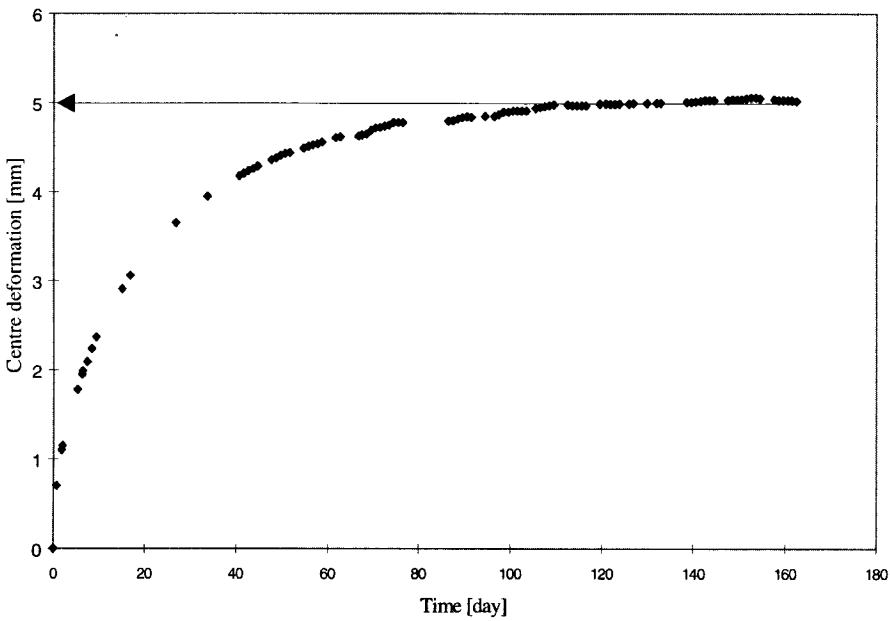

Figure 4.1 The measured centre deformation of the free to deform plate.

Results show that when the steady-state moisture condition in the specimen is reached, the deformation is about 5 mm. This deformation level is the maximum deformation of the plate during measuring time. Furthermore, results show that the centre deformation of the plate is about half of the maximum deformation already after 10 days. This means that the deformation initially increases more rapidly than toward the end of the measuring time.

The maximum deformation , 5 mm, is about eight times larger than the

thickness of the plate. This level of deformation, large deformation, cannot be handled by MecHPL when the plate is simply supported. Furthermore, this level of deformation is not desired in the application of High Pressure Laminates under observation. Therefore, a shorter measuring time must be used when the plate is simply supported.

4.2 Deformation of the Simply Supported Plate

4.2.1 General Description of the Test Arrangement

In order to determine the deformation of a simply supported plate, a special climate box was made. This special climate box contained two climate chambers, a door and a moveable steel frame. The function of the steel frame was to hinder the free expansion of the plate when the plate was fastened to the frame. The coupling between the plate and the steel frame was made in order to reach the simply supported condition. The tightness of the climate box was tested by the use of smoke ampoules.

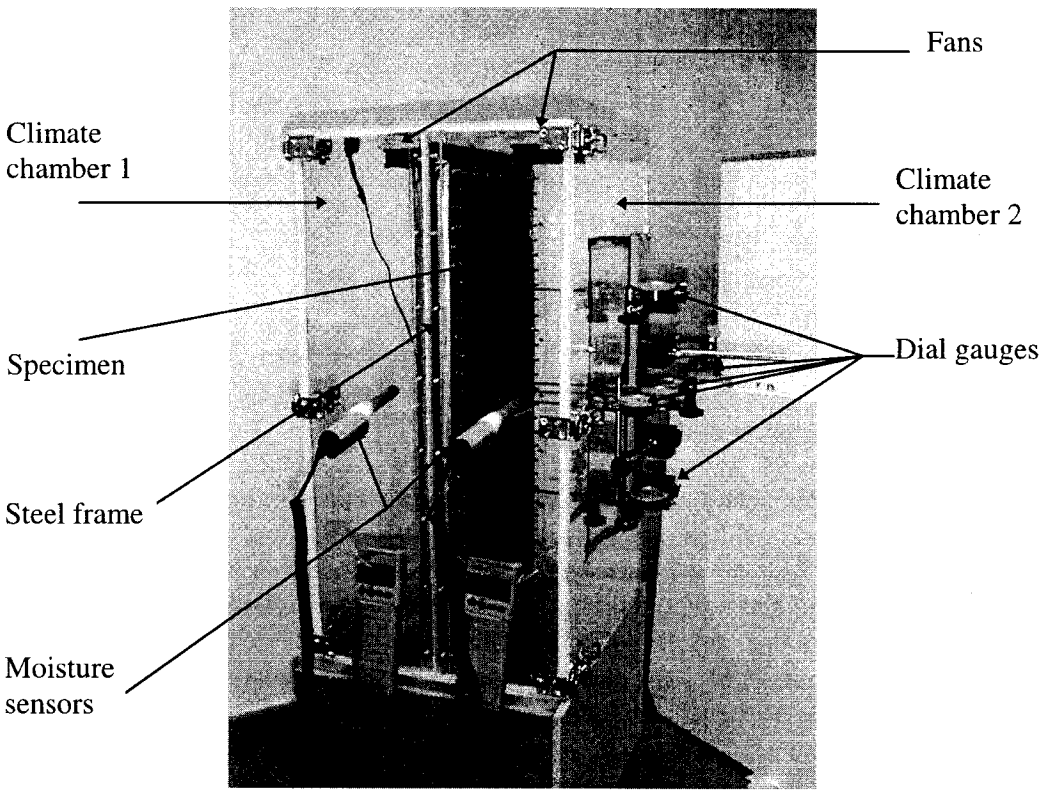

Picture 2 Test arrangement and climate box for simply supported plate.

The edges of the specimens, four edges, were fastened to the movable steel frame. The joint between the steel frame and the edges of the specimens hindered the free expansion but they could not take up moments.

The deformation of the specimen was measured by five dial gauges. The location of the measurement points is shown in Figure 4.2. Dial gauge 3 was placed in the centre of the plate and the other dial gauges were placed in middle of the distance between dial gauge 3 and the edges of the plate. The purpose of placing dial gauges 1,2,4 and 5 was to determine and control the shape of the deformation curve.

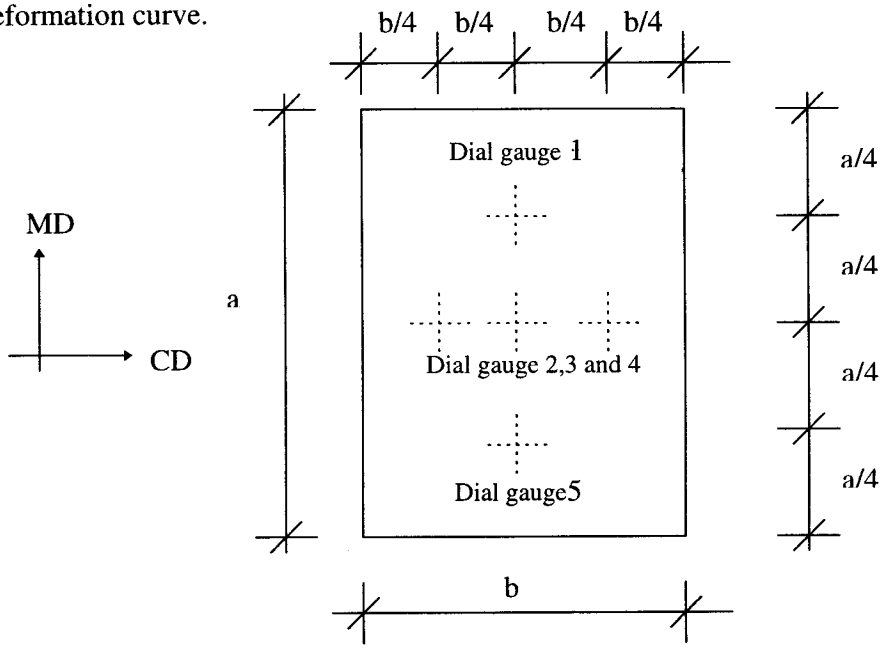

Figure 4.2 The location of the dial gauges.

In each climate chamber a moisture sensor and a fan were located. The relative humidity in the climate box was measured by the moisture sensor, Vaisala. The purpose of locating a moisture sensor in each climate chamber, in addition to confirming the condition of the saturated solution, was to register the essential climate data for further calculations. The fans were mounted in the climate chambers in order to reduce the surface vapour resistance between the specimen and the conditioned air in the chambers.

The climate box was placed in the same climate chamber as explained in the measurement of the deformation of the free to deform plate, see Section 4.1.

4.2.2 Simply Supported Plate, Dynamic Moisture Loading

A six millimeter specimen, was mounted to the steel frame and placed in the climate box, see Section 4.2.1. The area of the specimen was about 0.63x0.35 m^2. Here, it should be mentioned that this specimen was not from the same batch from which material properties of HPL were determined.

The initial relative humidity of climate chambers 1 and 2 was 50%. A tank of sodium chloride, sustaining 75% relative humidity, was placed in climate chamber 1, and another tank of lithium chloride, sustaining 11% relative humidity, in climate chamber 2. The relative humidity and temperature in both chambers were measured continuously.

The deformations of the specimen were measured for six hours and the measuring interval was 30 minutes. After six hours, the tank in climate chamber 1 was placed in chamber 2 and vice versa. The specimen was exposed to this new condition for 6 more hours. After that, the specimen was exposed to 50% relative humidity in both climate chambers. The measured relative humidities and temperatures in the chambers, during the first 12 hours, are presented in Figures 4.3 and 4.4. These measured climate data were used in the climate file required by the computer program MHPL.

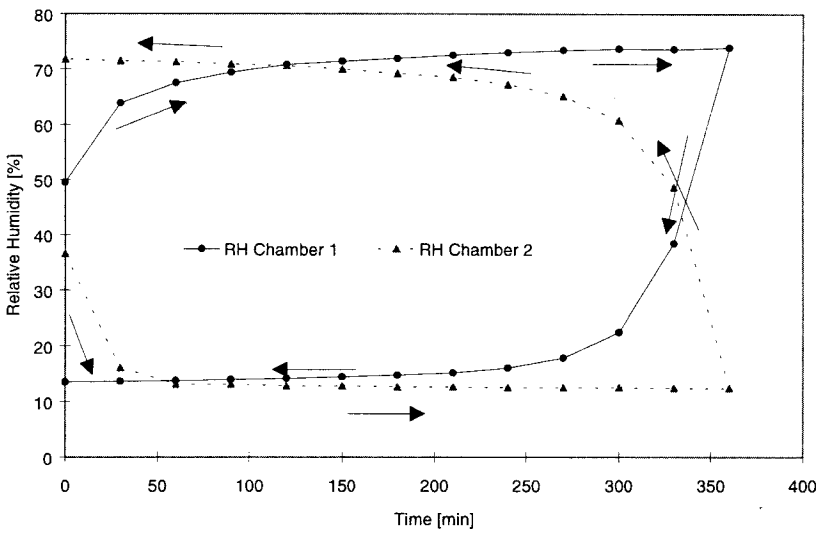

Figure 4.3 Sequence of the relative humidity in the chambers during 6+6 hours.

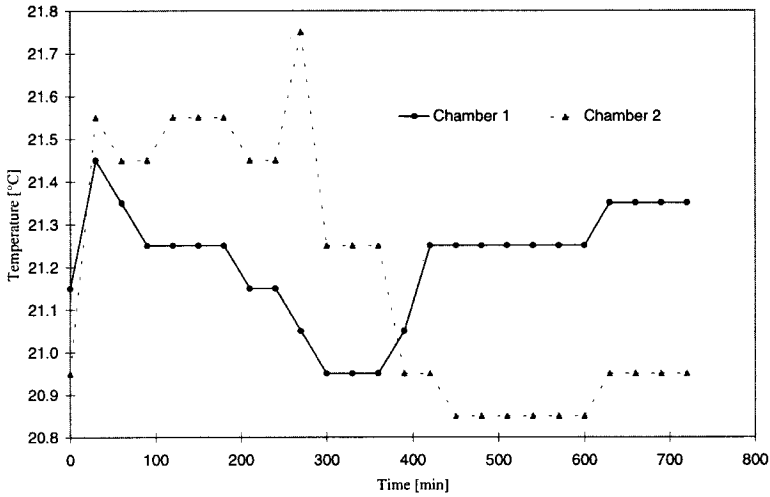

Figure 4.4 The measured temperature in the chambers.

4.2.2.1 Results and Discussion

The results of this test are presented in Figures 4.5 and 4.8. Figure 4.5 shows the results of the first 12 hours and Figure 4.8 shows results there after 50% relative humidity in both chambers.

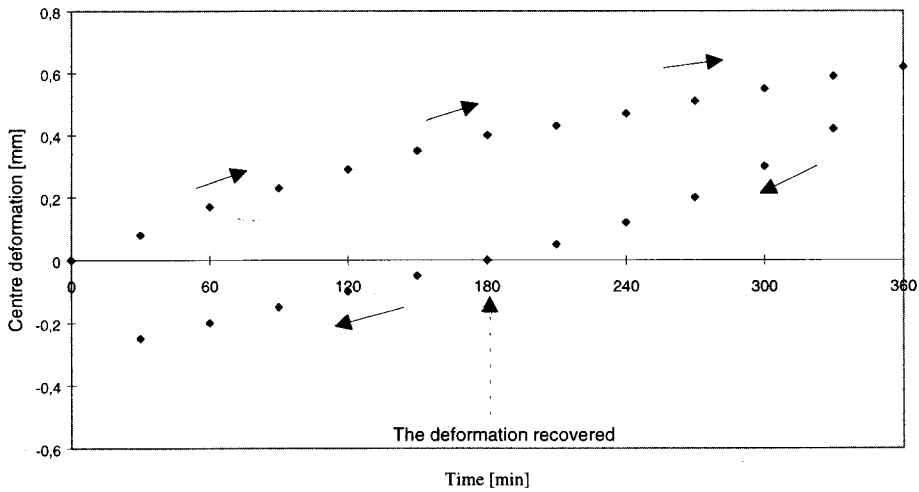

Figure 4.5 The centre deformation of the specimen during the first 12 hours.

As Figure 4.5 shows, the centre deformation of the specimen after 360 minutes is about 0.62 mm, which is about 1/10 of the thickness. After changing the moisture conditions in the climate chambers the deformation is recovered after

180 minutes, which means that the deformation, 0.62 mm, is recovered twice as fast. This phenomena is explained in the following paragraph.

Assume that the initial relative humidity of the specimen and the chambers is 50%. Furthermore, assume that the temperature is constant, for instance, T=20 °C. This means that the initial gradient of humidity by volume over the cross-section of the specimen is equal to zero, $\Delta v_{initial} = 0$. By changing the initial relative humidities in the chambers to 75% and 11%, the relative humidity of the surface layers of the specimen will change. The specimen is exposed to this gradient for 6 hours which means that the first layers, say with the thickness Δh, on both sides of the specimen have enough time to become temporarily balanced with the relative humidities in the chambers, see Figure 4.6.

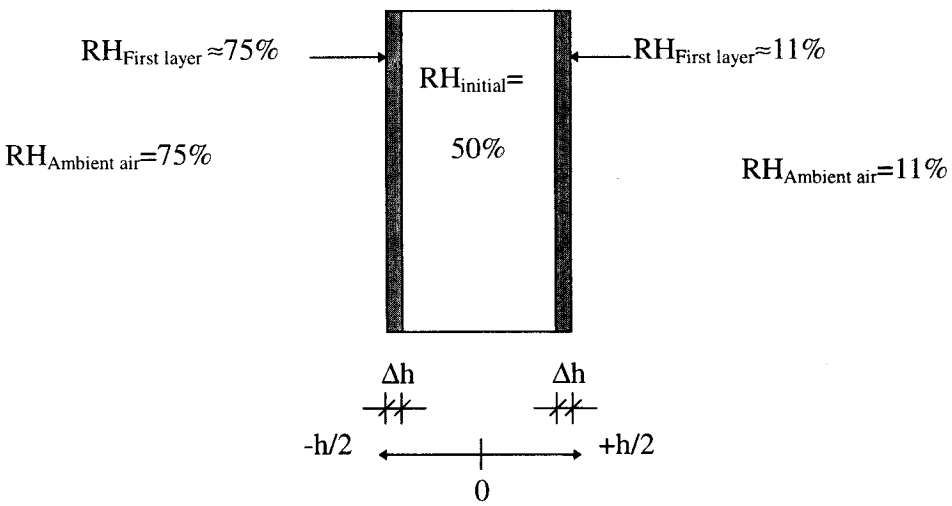

Figure 4.6 The first layers of the specimen are temporarily balanced with the relative humidity of the ambient air in the chambers after 6 hours.

The dimensionless moisture induced moment factor, I, for the condition presented in Figure 4.6, becomes:

$$I_1 \sim \int_{h/2}^{-h/2} \Delta v \cdot z \cdot dz = \int_{-h/2}^{-h/2+\Delta h} (0.75-0.50)\cdot v_s(T)\cdot z \cdot dz + \int_{h/2-\Delta h}^{h/2} (0.11-0.50)\cdot v_s(T)\cdot z \cdot dz =$$

$$0.25 \cdot v_s(T)\cdot(-\frac{h}{2})\cdot \Delta h - 0.39 \cdot v_s(T)\cdot(\frac{h}{2})\cdot \Delta h = -0.32 \cdot v_s(T)\cdot h \cdot \Delta h$$

When the relative humidity is changed again, the specimen is exposed to the moisture conditions illustrated in Figure 4.7.

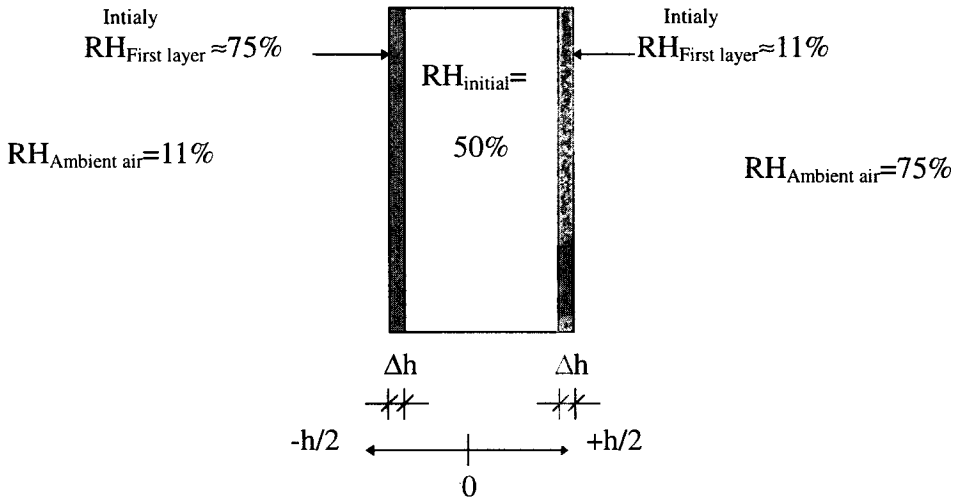

Figure 4.7 Moisture condition of the ambient air and the material directly after swapping the relative humidities in the chambers.

The dimensionless moisture induced moment factor, I, for the conditions presented in Figure 4.7, becomes:

$$I_2 \sim \int_{h/2}^{-h/2} \Delta v \cdot z \cdot dz = \int_{-h/2}^{-h/2+\Delta h} (0.11-0.50) \cdot v_s(T) \cdot z \cdot dz + \int_{h/2-\Delta h}^{h/2} (0.75-0.50) \cdot v_s(T) \cdot z \cdot dz =$$

$$-0.39 \cdot v_s(T) \cdot (-\frac{h}{2}) \cdot \Delta h + 0.25 \cdot v_s(T) \cdot \frac{h}{2} \cdot \Delta h = +0.32 \cdot v_s(T) \cdot h \cdot \Delta h$$

The dimensionless moisture induced moment factor, I_1, after 6 hours, is equal to $-0.32 \cdot v_s \cdot h \cdot \Delta h$. After swapping the relative humidity in the chambers, the dimensionless moisture induced factor, I_2, becomes $+0.32 \cdot v_s \cdot h \cdot \Delta h$. The difference between I_2 and I_1 becomes $+0.64 \cdot v_s \cdot h \cdot \Delta h$. This means that after swapping the relative humidity in the chambers the specimen is exposed to twice as large a moisture induced moment in the opposite direction. Thus, deformation after swapping the relative humidity changes, is recovered approx. twice as fast.

The results of the measured centre deformation of the specimen after 12 hours, when the relative humidity in both chambers is 50%, is shown in Figure 4.8. Figure 4.8 shows that the centre deformation is zero after about 7 days and rises

to a constant level, which is about 0.1 mm although the relative humidity in both chambers is 50%.

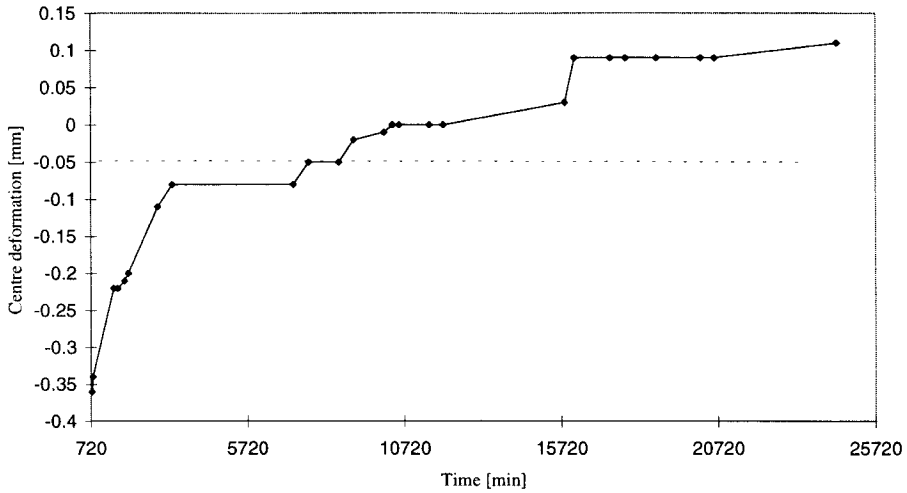

Figure 4.8 The centre deformation of the specimen, dial gauge 3, when the relative humidity in both chambers is equal to 50%.

Measured deformations by dial gauges 1 and 5 are shown in Figure 4.9 and dial gauges 2 and 4 in Figure 4.10. The measured deformations for dial gauges 1 and 5 and dial gauges 2 and 4 are almost the same, which indicates that the specimen is deformed symmetrically; see position of the dial gauges in Figure 4.2. This means that the deformation is symmetrical as indicated in Figure 1.1.

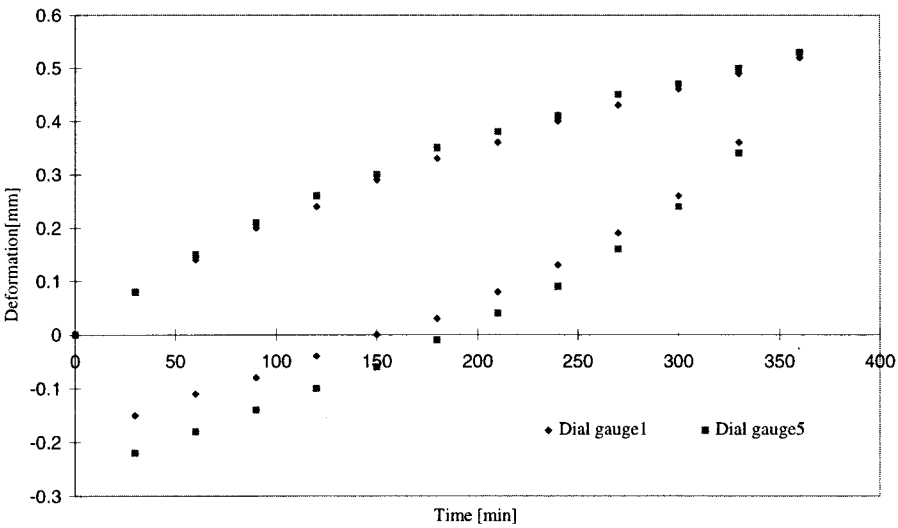

Figure 4.9 Measured deformation by dial gauges 1 and 5.

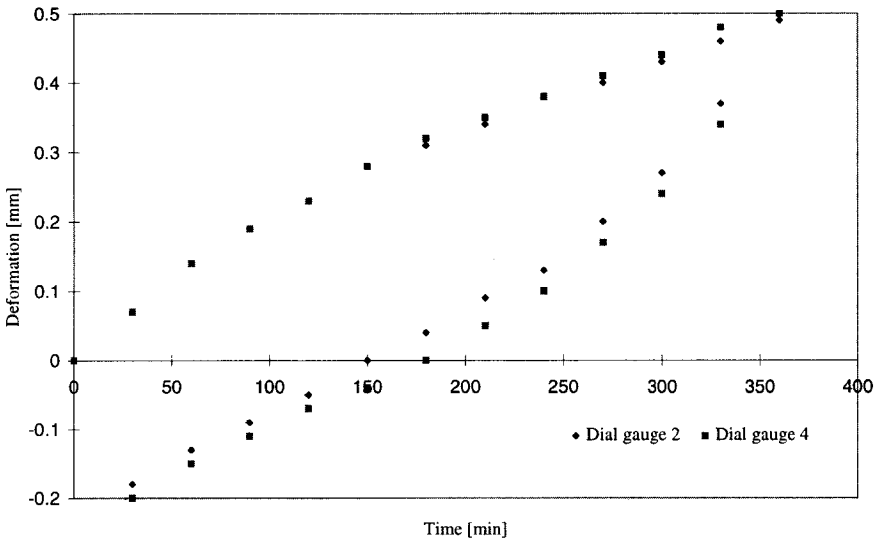

Figure 4.10 Measured deformation by dial gauges 2 and 4.

These gauges shown the same behaviour after 12 hours as the middle gauge.

4.2.3 Simply Supported Plate, Constant Humidity

Three six millimeter thick specimens were investigated. One of the specimens, Specimen 1, is taken from the same batch from which the material properties were determined, and the two others were from the second batch.

The test arrangement was the same as the test arrangement in Section 4.2.2 , except for the moisture condition in the chambers. In these tests, a constant humidity gradient over the entire measuring time was used. In one of the chambers, the specimens were exposed to about 100% relative humidity and in the other chamber to 11%. This means that the difference humidity by volume is constantly about 15.4 g/m^3 over the specimen.

According to the limitation and assumption, the hygrocopic range, up to 95% RH, was under observation and consequently the material properties were determined for this range. Using a relative humidity around 100% in this test exceeded the limitation of this work. However, these tests can be considered as a check for the possibility to apply the measured material properties in calculations up to this level, 100%, of the relative humidity.

The results of these tests are shown in Figure 4.11. The results show that the maximum deformation of Specimen 1 after 20 days is about 10 mm, which is 17 times larger than the thickness of the plate. According to the assumption of this

work, the theory of the thin plate pertains to deformations up to 1/5-1/10 of the thickness of the plate. Because of this restriction, a time period should be found during which the deformation is at least less than 1.2 mm.

Figure 4.12 presents the first 2750 minutes (about 2 days) of the total testing time for Specimen 1.

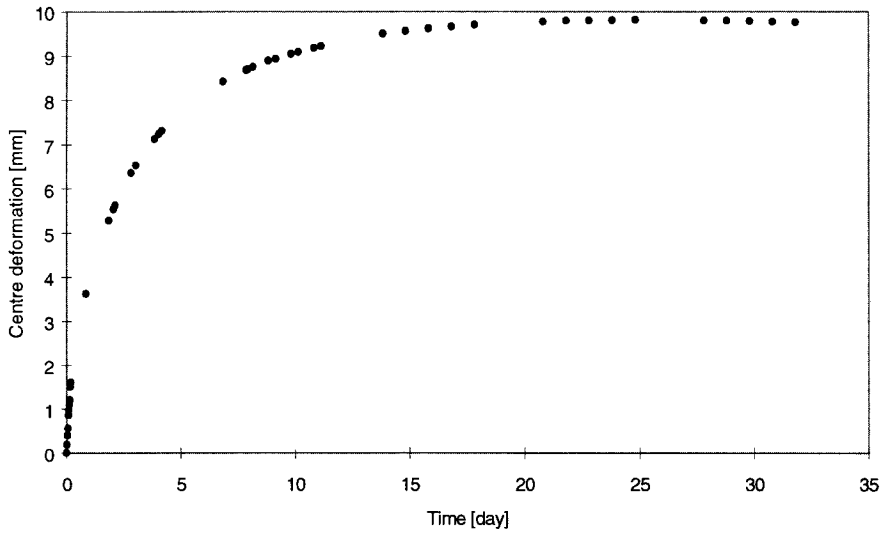

Figure 4.11 The deformation of Specimen 1 during 33 days.

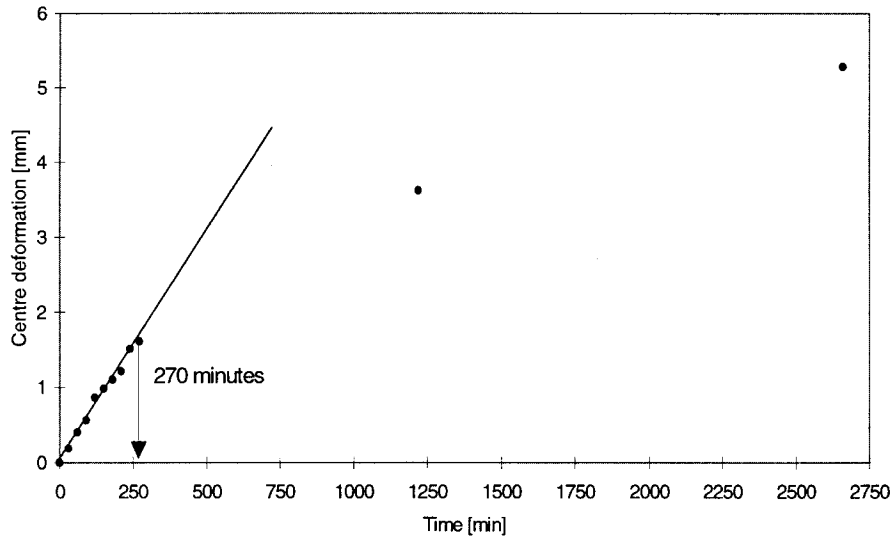

Figure 4.12 The deformation of Specimen 1 during the first 2 days.

Figure 4.12 indicates that the linear relation between time and deformation expired after about 270 minutes. Furthermore, the measured centre deformation for 270 minutes is larger than the limitation of this work, 1.2 mm. Thus, for this reason the time period of at least 270 minutes could be defined as the maximum time period for which the theoretical models are valid, for a simply supported plate exposed to the described moisture boundary conditions.

The deformation of the two other specimens were measured for a period of 6 hours with a measuring time interval of 30 min. The results of these tests are presented in Figure 4.13.

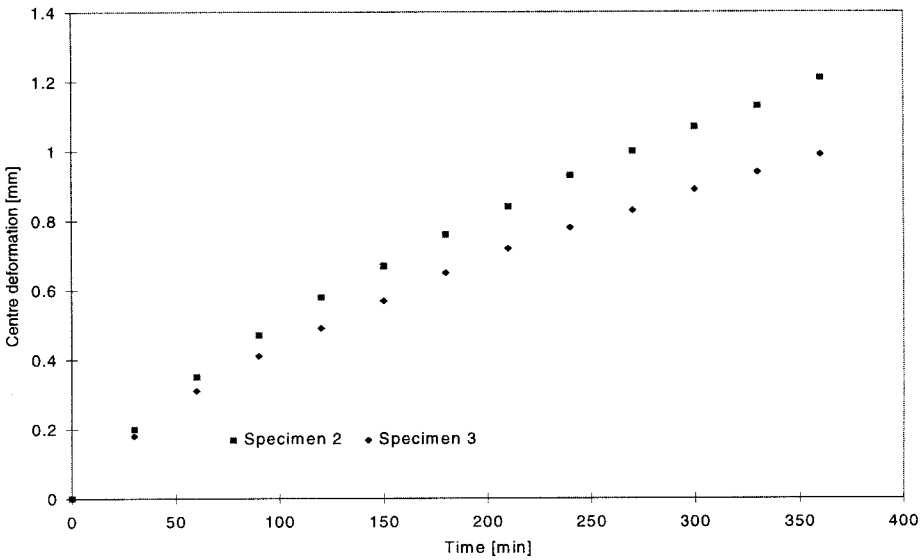

Figure 4.13 The deformation of Specimens 2 and 3 over a period of 6 hours.

5. Calculated Results in Comparison with Measurement Results

In this chapter, the calculated results for a free to deform plate and a simply supported plate in Chapter 5 are compared with the measurement results in Chapter 4. The input data for the calculations are the measured properties which are presented in Part A and Part B.

5.1 The Free to Deform Plate

The measured deformation, presented in Section 4.1, and the calculated deformation of the free to deform plate are presented in Figure 5.1.

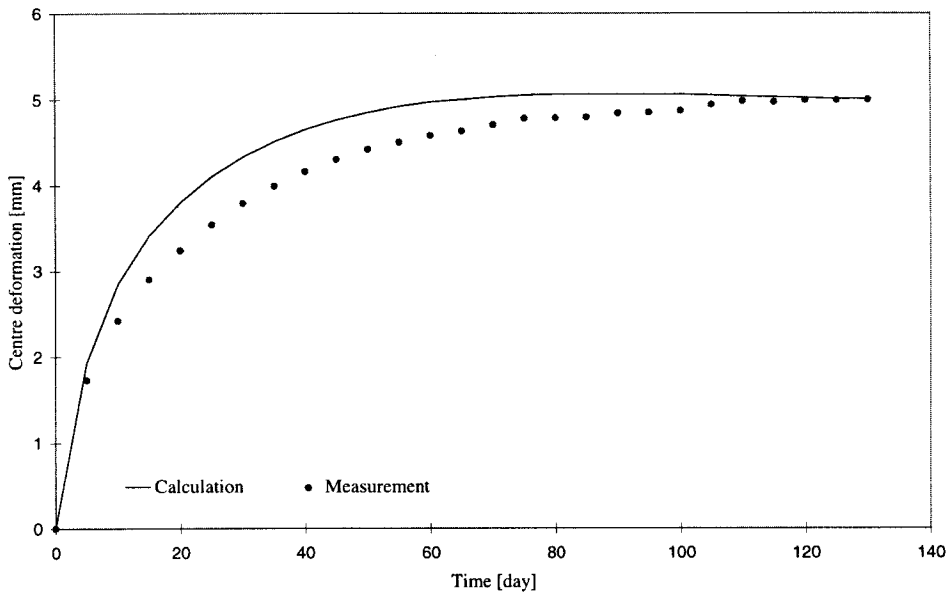

Figure 5.1 Comparison of the calculated and measured deformation for the free to deform plate.

Figure 5.1 shows that the deviation of results after a long time at approximately steady-state condition, is close to zero. The maximum deviation between the calculated and measured deformation in relation to the maximum measured deformation, $(w_{measured}-w_{calculated}) / w^{max}_{measured}$, is less than 11% for a time period of 120 days. This deviation have several causes, for instance, a variation in the material property of the paper, the influence of two-dimensional treatment and the production process parameters.

5.2 Simply Supported Plate, Dynamic Moisture Loading

The calculated and measured deformation of the simply supported specimen which is exposed to dynamic moisture loading is presented in Figure 5.2.

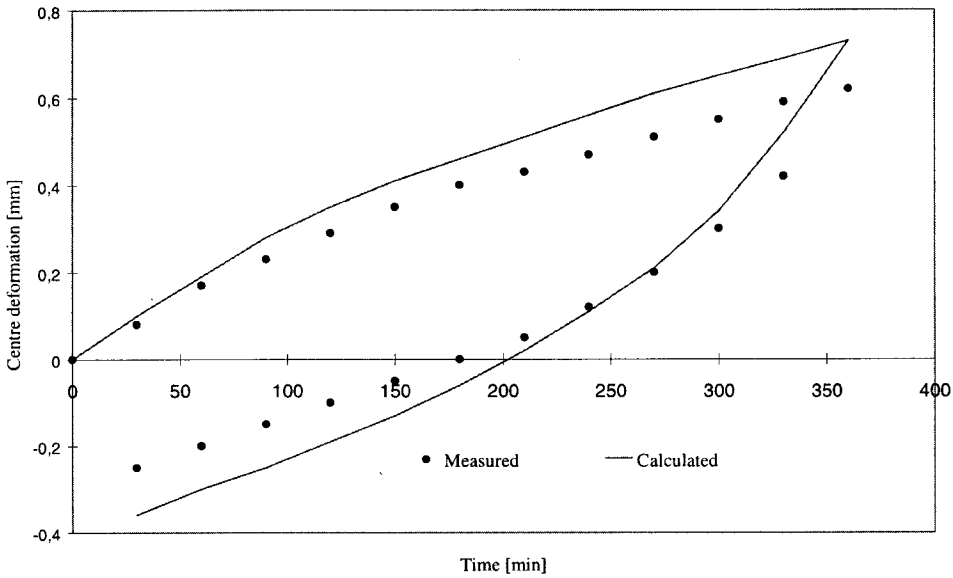

Figure 5.2 Comparison of the calculated and measured deformation for a simply supported specimen exposed to dynamic loading.

The maximum deviation of the results on the positive side of the deformation axes in relation to the maximum measured deformation is about 17 %, which is in the same deviation range as on the free to deform plate. On the negative side of the deformation axes, the maximum deviation of the results is about 20% of the maximum measured deformation.

Another possible reason for this deviation, in addition to the parameters mentioned for the free to deform plate, see Section 5.1, is the simulation of the boundary condition. One possibility is that the boundary condition of the test is not fully simply supported.

5.2.1 Simply Supported Plate, Constant Humidity

The measured deformation of the specimens which were exposed to 100% relative humidity on one side and 11% relative humidity on the other side, are compared with the results obtained by the PC-program MecHPL. The results of the comparison for Specimen 1 are shown in Figure 5.3 and the results for Specimens 2 and 3 are presented in Figure 5.4.

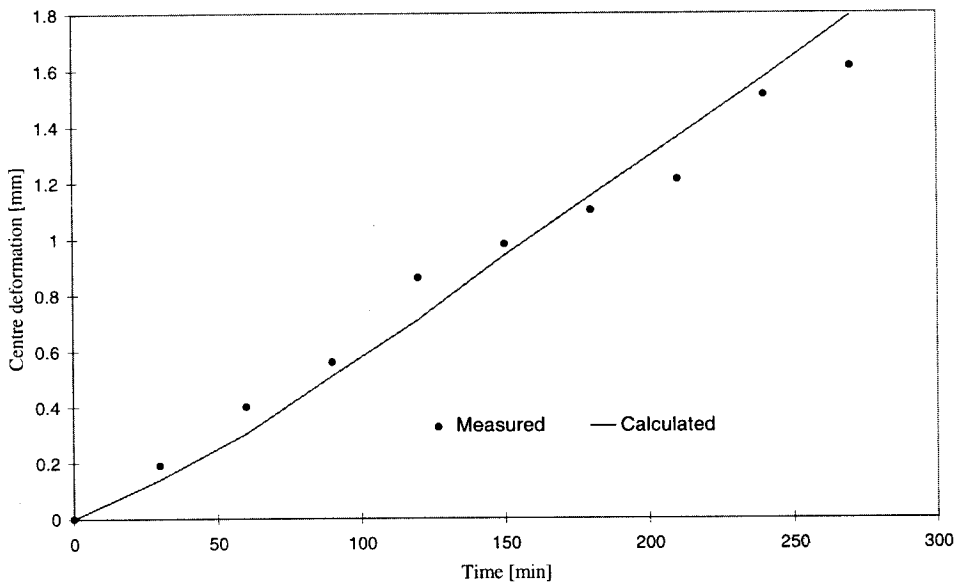

Figure 5.3 Comparison of the calculated and measured deformation for simply supported specimen exposed to constant humidity difference.

The results of the comparison, shown in Figure 5.3, indicate that even by using the measured material properties up to 95% relative humidity, it is possible to get satisfactory results for a plate which is exposed to 100% relative humidity. Here, it should be mentioned that Specimen 1 was taken from the same batch from which the material properties were determined.

The results of the comparison of Specimens 2 and 3, shown in Figure 5.4, deviate much more than expected. The maximum deviation is about 30% between measured and calculated deformation for the first 270 minutes of the measurement. This could be because these two specimens are from different batch than the one used for determination of material properties and that the material properties of the specimens in higher relative humidities than 95%, differ form the measured ones. However, to be able to predict and determine the deformation of paper based High Pressure Laminates, it is necessary to determine the variation of the material properties which HPLs are made of.

Furthermore, if the HPLs are going to be exposed by relative humidities close to 100% relative humidity, the material properties should be determined for this level, too.

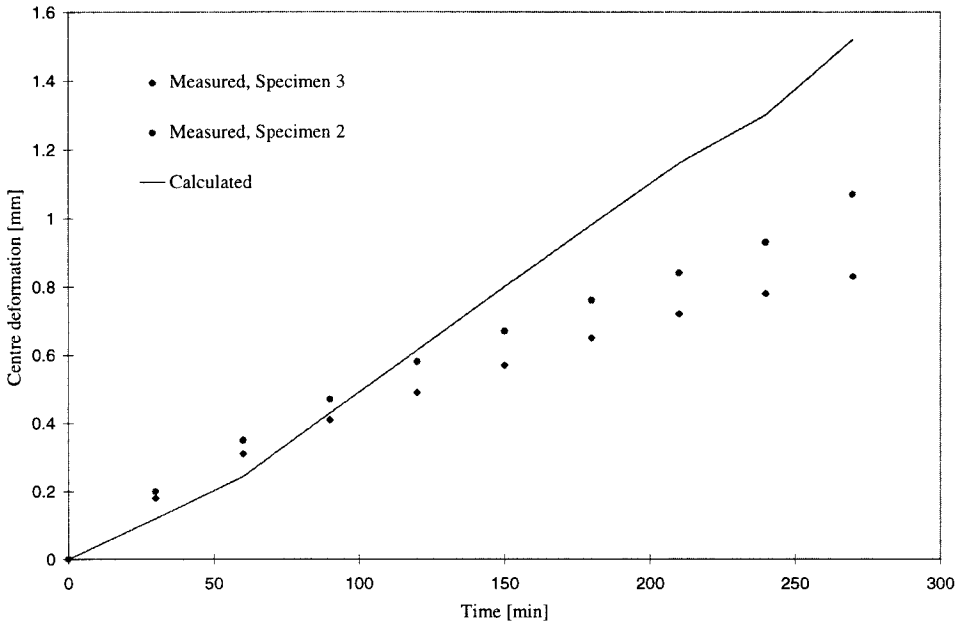

Figure 5.3 Comparison of the calculated and measured deformation of simply supported specimen exposed to static loading.

5.3 Conclusion and Further Research

It is not possible to draw conclusive conclusions regarding measurements and calculations from this limited number of tests, although the following observations can be made.

A comparison of the results of a free to deform plate, indicates that the analytical formulation of the problem is correct and that the moisture induced deformation can be calculated by Equation (1.12).

However, the number of tests is not sufficient when the plate is simply supported, although the results indicate that couplings of the PC-programs are at least able to predict elastic moisture induced deformation. Maximum differences up to 30% have been observed. These differences appear when the specimens are not taken from the batch which is used for the determination of material properties. This indicates that the material properties of two different batches of HPL can vary strongly. It is possible that the material properties of each component of the HPL before production processes i.e., impregnation,

high temperature and mechanical pressure, do not differ so much. But after production processes due to different degrees of the impregnation and the position of the HPL in the press device, the material properties of batches can be very different.

The PC-programs MHPL and MecHPL are based on theoretical models and each model has its specific limitations. Two basic limitations in the MHPL are that the stress/strain gradient has no influence on the diffusion processes and that the moisture distribution in the HPL follows Fick's law. As long as these limitations are valid, the results obtained by the MHPL can be used in any other mechanical model. The MecHPL is based on the Kirchhoff plate theory. This theory considers elastic and small deformations of thin plates. There are a number of programs which are able to perform an equivalent analysis to the MecHPL. MecHPL could be considered as a base for some special analyses which the existing programs in a PC-environment are not able to perform.

At this stage, the comparison of the measured and calculated results is generally satisfactory.

5.3.1 Future Research

There is much further work to do concerning the determination of moisture induced deformation. Future research work can be divided into model development and determination of the material properties.

- ***Model development***

The theoretical model presented in this work has two parts, namely, a moisture transport model and a mechanical model. Each of these models has their limitations.

The mechanical model is limited to a small and elastic range of deformations because non-recoverable deformations are not desired. This model can be completed so that large deformations can be handled. However, large deformations are not desired in construction such as flooring and interior walls, but the treatment of large deformations is interesting from a theoretical point of view. Furthermore, a large deformation model can be used for other HPL applications where, a higher level of deformation is acceptable.
The mechanical model can be supplemented with other kinds of boundary conditions, i.e., using point supports in the mounting of HPLs is interesting in practical point of view.

The model of moisture transport would be based on Fick's law although it is known that the transport of moisture in polymers does not completely behave

according to Fick's law. An investigation into moisture transport in polymers and their influence on the moisture transport process in HPL and adding any eventual deviation from Fick's law to the model can be an interesting task.

By using these models, the PC-programs MHPL and MecHPL have been developed. These programs can be executed separately. Future work would be an integration of these programs into a single one.

Finally, in this work the core of the HPL has been under consideration, the models should be completed to be able to treat the influence of the overlays.

- ***Determination of Material Properties***

Accurate properties of the material, are essential to any kind of calculations. There is a large amount of work which could be done concerning the material properties of High Pressure Laminates. HPL contains paper and polymer. The material properties of the polymer can be determined almost without any variations. But, on the other hand, properties of the paper can vary strongly from one batch to another. It is important to determine the variation interval of the paper properties.

Determining the variation interval of the material properties of HPL after production processes can be another future task.

Expansion and contraction coefficients are of major importance, because these coefficients are coupled coefficients between moisture transport and the mechanical behaviour of the HPL. Special attention should be paid to determining these coefficients.

Finally, the material properties of overlay should be determined, if the influence of the overlay is to be investigated.

6 Dimension Stable Material

In this chapter, some improvements of the material and the geometry of a plate, in order to get a better dimension stability, are discussed. It should be noted that all material properties are inter connected and changing one property will affect the other properties.

6.1 Improving Dimensional Stability

- The curvatures of a free to deform plate and the moisture induced moment in a simply supported plate are proportional to the expansion/contraction coefficients. By using Equations (1.9) and (1.17a), it can be found that if expansion/contraction coefficients, β_x and β_y , are equal to zero, the curvatures of the free to deform plate and the moisture induced moment in a simply supported plate become zero, too. This means that by reducing the expansion/contraction coefficients, the material becomes more dimension stabile. A reduction of the expansion/ contraction coefficients of HPL is possible by a modification of the paper and impregnation substances.

- The moisture induced deformations of a free to deform plate and a simply supported plate can be calculated by Equations (1.12) and (3.1), respectively. These equations indicate that the E-modulus of the plate has no influence on the moisture induced deformation. However, the ratio of the E-modulus in the orthotropic directions should be known for the calculation of moisture induced deformations.

- In Equation (2.2), Δv is equal to the difference between the initial humidity by volume of the material and the new humidity of the material after changes in the relative humidity of the ambient air. The relation of the moisture content by volume and the relative humidity of the material is determined by the sorption curve. The moisture capacity of a material is defined by the slope of the sorption curve ($dw/d\phi$), a large slope gives a higher moisture capacity, i.e., a higher Δw. A larger Δw leads to a larger moisture induced moment. This means that by reducing the moisture capacity of the substances in a material, a more dimensionally stable material is obtained.

- Finally, by reducing the moisture diffusion coefficient, the time scale of the deformation becomes longer. However, the changes of the moisture diffusion coefficient have no influence on the maximum deformation of the structure when steady-state condition is reached, see Example 1, last paragraph, in Section 2.3.1.

6.2 Some Geometrical Observations

The dimensions of the plate are other factors which have an influence on the magnitude of the moisture induced moment and forces. There are relations between thickness, length and the width of the plate at which moisture induced moments and forces are minimum.

In Equation (3.1), deformation of the simply supported plate is expressed. Substituting Equations (3.2b) and (2.3) into Equation(3.1) gives:

$$w = \left.\frac{dw}{d\phi}\right|_0 \frac{1}{v_s(T)} \frac{v_1 - v_0}{\rho} \cdot f^0\left(\frac{\sqrt{Dt}}{h}\right) \cdot \frac{a \cdot b}{12 \cdot h} \sqrt{(\beta_x + \beta_y \cdot \nu_{yx}) \cdot (\beta_y + \beta_x \cdot \nu_{xy})} \cdot w' \quad (6.1)$$

By assuming that all other variables in this equation, except f^0 and the thickness of the plate, h, are constants, it can be found that the deformation of the plate, w, is proportional to f^0 and inversely proportional to the thickness of the plate, h.

$$w \sim f^0\left(\frac{\sqrt{Dt}}{h}\right) \cdot \frac{1}{h} \quad (6.2)$$

The function f^0 depends on the thickness of the plate and the value of this function, which varies between zero and 0.083, is presented in Table 2.1. If $(Dt)^{0.5}/h$, α-value, is equal to 0.2 for a particular thickness, h_p, then the function f^0 is equal to 0.073. In the same way, the f^0 function for a twice as thick plate, $2h_p$, becomes 0.046.

Substituting these values into Equation (6.2), indicates that the deformation of the plate, w, with double thickness, $2h_p$, is about three times smaller than the thinner plate. This means that the deformation of the plate becomes three time smaller by doubling the thickness. When steady-state condition is reached, α is equal to ∞ and f^0 is equal to 0.83, the deformation of the thinner plate will be twice as large as than the thicker plate.

Deformations of the plate are proportional to the width and length of the plate, see Equation (3.2). In an orthotropic plate it is difficult to choose the optimum relation between the length and width of the plate unless a number of calculations is executed. Calculations of this type are done in Chapter 3. By using the table values and figures in this chapter, the designer is able to determine the optimum relation between the width and length of the plate in the construction.

7 References

[1] C.E.Hagentoft, B.A.Zarrabi, The Moisture Moment Factor, Paper to be submitted to Nordic Journal of Building Physics

Appendix

Appendix A:1

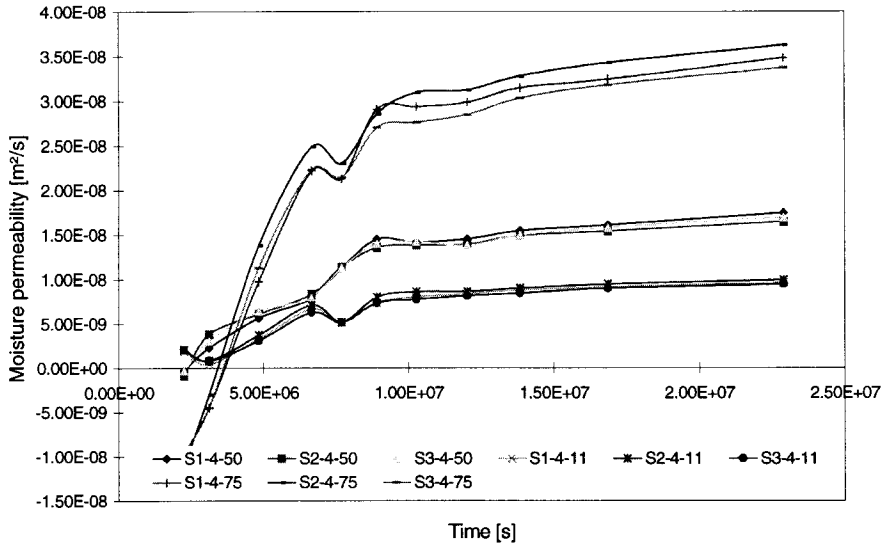

Figure A.1 Measured moisture permeability for 4 mm specimens at different relative humidity difference.

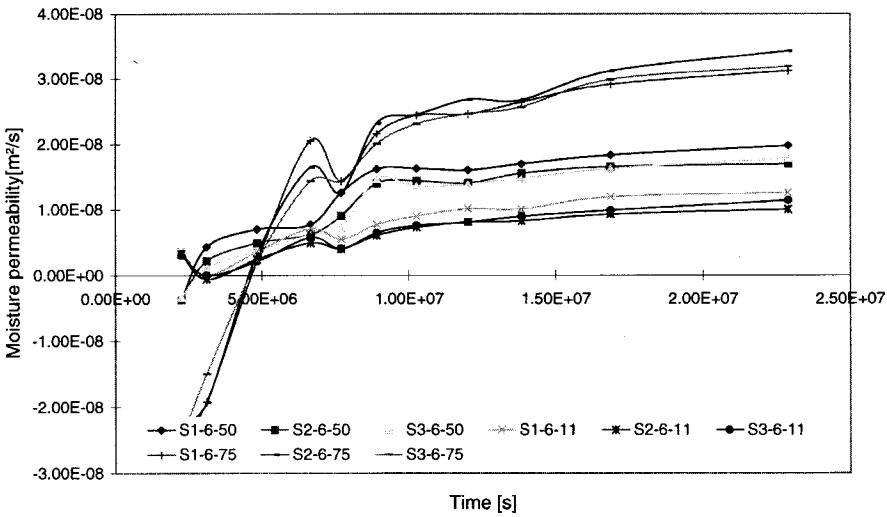

Figure A.2 Measured moisture permeability for 6 mm specimens at different relative humidity difference.

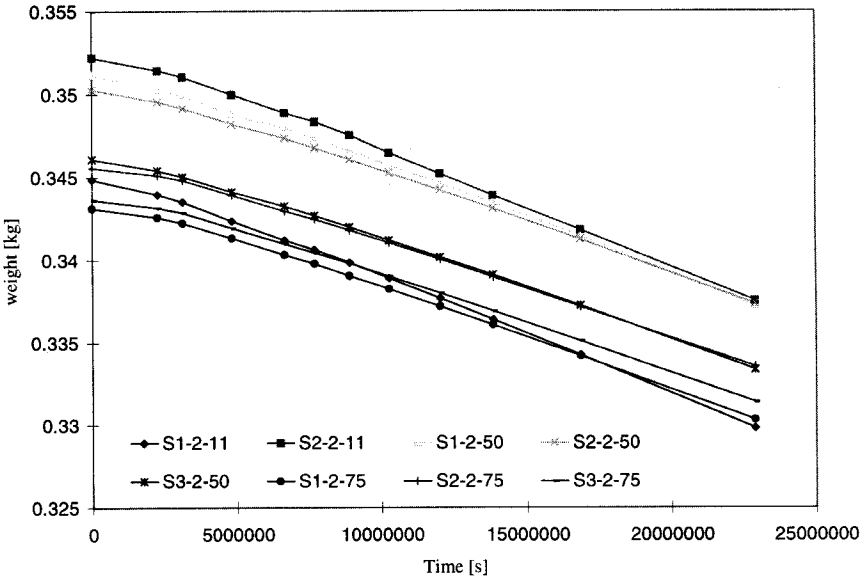

Figure A3 Weight change of the 2 mm thick specimen.

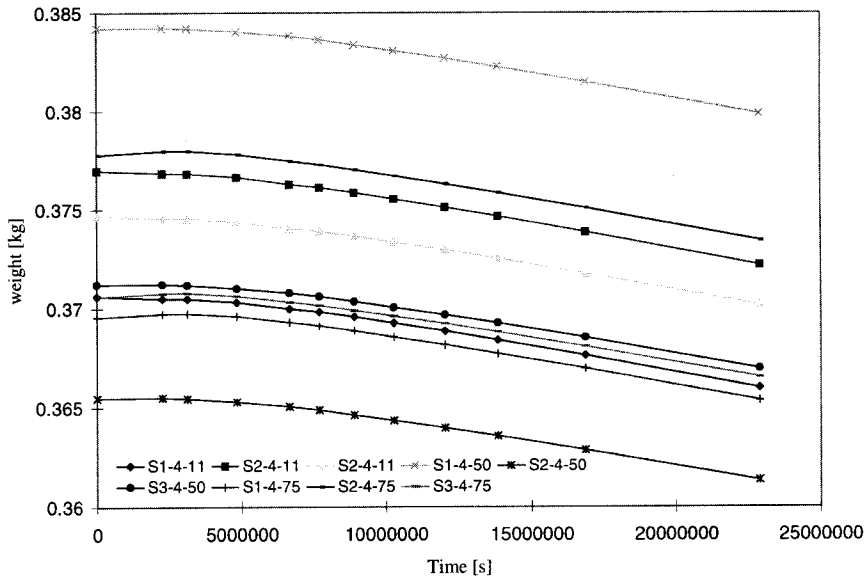

Figure A4 Weight change of the 4 mm thick specimen.

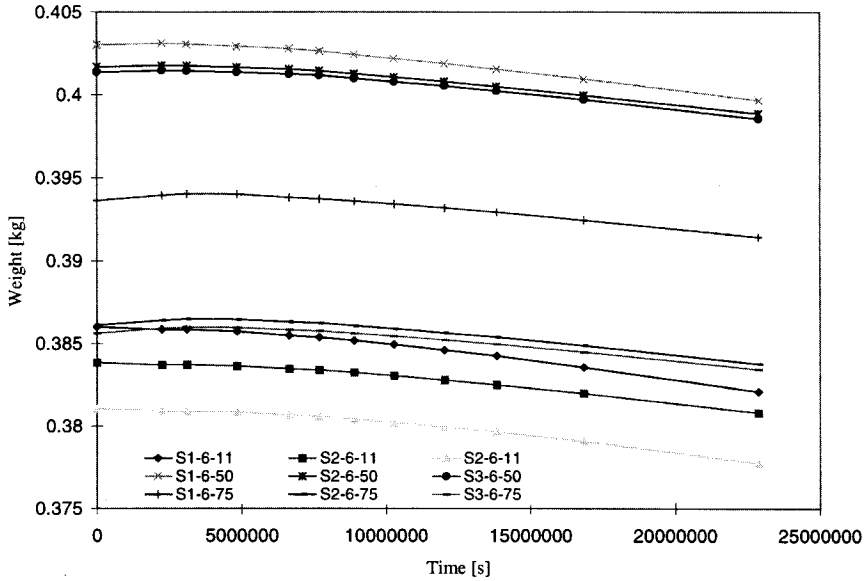

Figure A5 Weight change of the 6 mm thick specimen.

Appendix A:2

The PC-program MHPL is a modification of the PC-program 1D-HAM. MHPL needs a climate file and a input data file. In the climate file, boundary conditions, moisture and temperature, should be explained. The input data file consist of the geometry and the material properties of the object under consideration. The content of these two files are described in following paragraphs.

Climate data

The climate data are given in a special ASCII-file. The first line must contain the number, $N_{climate}$, of climate data sets that follows. This number must not exceed the number 8 762. This number is larger than the number of hours of the year (8 760). Each data set, each line, has the following structure:

$t^1(s)$ T_l^1 T_r^1 υ_l^1 υ_r^1

. . . .

. . . .

. . . .

$t^{N_{climate}}(s)$ $T_l^{N_{climate}}$ $T_r^{N_{climate}}$ $\upsilon_l^{N_{climate}}$ $\upsilon_r^{N_{climate}}$

The time t is the time of the year in seconds. The index l refers to the left side and the index r refers to the right one.

Input data

The data required by MHPL are given in an input data file. The construction is divided into a number of layers with different properties. This file must contain the following data:

Name of output files	Name of output files without extension
Text 1	Arbitrary string of text that will be written together with the output data
Name of climate file	Name of file, includes the path if necessary
t_{start}	Start time of simulation (s)
t_{stop}	Stop time of simulation (s)
$t_{first\ print\ time}$	Time for first output (s)
$t_{print\ interval}$	Print interval (s)

N_{layer}	Number of different layers in the wall (-)
$d_1 \ldots . d_{N\ layer}$	Width of each layer, from left to right (m)
$N_{cell(1)} . N_{cell(N\ layer)}$	Number of computational cells in each layer, from left to right
$\lambda_1 \ldots . \lambda_{N\ layer}$	Thermal conductivity for each layer, from left to right (W/mK)
$C_1 \ldots . C_{N\ layer}$	Volumetric heat capacity of each layer, from left to right (J/m^3K)
$T_1(0) \ldots . T_{N\ layer}(0)$	Start temperature of each layer, from left to right (C)
$NPsor_{(1)} \ldots . NPsor_{(N\ layer)}$	Number of points for approximation of the sorption curve for each layer
$Wsor_1 \ldots . Wsor_{NPsor(1)}$	
.....	
.....	Values of the moisture content by volume W for each layer (kg/m^3)
$Wsor_1 \ldots . Wsor_{NPsor\ (N\ layer)}$	
$RHsor_1 \ldots . RHsor_{Nsor(1)}$	
.....	
.....	Values of the relative humidity for each value moisture content for each layer (%)
$RHsor_1 \ldots . RHsor_{Nsor\ (N\ layer)}$	
$Ndiff_{(1)} \ldots . Ndiff_{(N\ layer)}$	Number of values which indicate relation between diffusion coefficient and relative humidity for each layer
$D_1 \ldots . D_{Ndiff\ (1)}$	
.....	
.....	Values of the diffusion coefficient for each layer (m^2/s)
$D_1 \ldots . D_{\ Ndiff\ (N\ layer)}$	
$RHdiff_1 \ldots . RHdiff_{\ (Ndiff\ 1)}$	
.....	
.....	Values of the relative humidity for each diffusion coefficient for each layer (%)
$RHdiff_1 \ldots . RHdiff_{Ndiff\ (N\ layer)}$	
$W_1(0) \ldots W_{N\ layer}(0)$	Start moisture content of each layer, from left to right (kg/m^3)
$D_1(0) \ldots D_{N\ layer}(0)$	Start value of diffusion coefficient of each layer, from left to right (m^2/s)
d_{al} , d_{al}	Thickness of surface air layer (film) at the left and right side (m)
λ_{al} , λ_{ar}	Thermal conductivity of left and right surface films (W/mK)
D_{al} , D_{ar}	Value of D_V for the left and right surface films (m^2/s)

$T_{ref}, T_{min}, T_{max}, v_{max}$	Reference temperature (°C) for convective heat flow, estimated minimum and maximum temperature (°C), and maximum relative humidity by volume (kg/m^3) in the construction
Switch	Equal to 1 if annual cyclic values of the climate data should be use Else the value is equal to 0.

Appendix C 1: Deduction of Equation (3.1)

Assume E_x, E_y, ν_{xy}, ν_{yx}, α and β are independent of the moisture condition in the material, Equation (1.5c) in Part C can be rewritten:

$$m_x^m = \frac{E_x(\beta_x + \beta_y \nu_{yx})}{1-\nu_{xy}\nu_{yx}} \int_{-\frac{h}{2}}^{\frac{h}{2}} \Delta u \, z \, dz = \frac{E_x \cdot (\beta_x + \beta_y \nu_{yx})}{1-\nu_{xy}\nu_{yx}} \cdot h^2 \cdot I \quad (1a)$$

In a similar manner Equation (1.6c) in Part C becomes:

$$m_y^m = \frac{E_y \cdot (\beta_y + \beta_x \nu_{xy})}{1-\nu_{xy}\nu_{yx}} \cdot h^2 \cdot I \quad (1b)$$

By using Equations (1a-b), we find that the ratio of the moisture induced moments is not dependent of the moisture variation.

$$\frac{m_x^m}{m_y^m} = \frac{E_x}{E_y} \cdot \frac{\beta_x + \beta_y \nu_{yx}}{\beta_y + \beta_x \nu_{xy}} \quad (2)$$

- Dimensionless formulation of the govering differential equation in Part B

Assume

$$x = x' \cdot a \quad \text{and} \quad y = y' \cdot b \quad (3)$$

where 'a' and 'b' are the length and the width of the plate.

The derivatives become from Equation (3):

$$\frac{\partial}{\partial x} = \frac{1}{a}\frac{\partial}{\partial x'} \quad \text{and} \quad \frac{\partial}{\partial y} = \frac{1}{b}\frac{\partial}{\partial y'} \quad (4)$$

Assume that the function (5) is a solution to Equation (1.17) in Part B.

$$w = \sqrt{\frac{m_x^m \cdot m_y^m}{D_x \cdot D_y}} \cdot a \cdot b \cdot w'(x/a, y/b) = \ell \cdot w'(x/a, y/b) \quad (5)$$

where ℓ [m] is a constant and w' is a dimensionless function.

Substitution of (5) into the governing differential equation, Equation (1.17) in Part B, gives:

$$D_x \frac{\ell}{a^4} \frac{\partial^4 w'}{\partial x'^4} + \frac{2 \cdot B \cdot \ell}{a^2 b^2} \frac{\partial^4 w'}{\partial x'^2 \partial y'^2} + D_y \frac{\ell}{b^4} \frac{\partial^4 w'}{\partial y'^4} = 0 \qquad (6)$$

Equation (6) can be rewritten as:

$$\frac{D_x}{D_y} \frac{b^4}{a^4} \frac{\partial^4 w'}{\partial x'^4} + \frac{2 \cdot B}{a^2 b^2} \frac{b^4}{D_y} \frac{\partial^4 w'}{\partial x'^2 \partial y'^2} + \frac{\partial^4 w'}{\partial y'^4} = 0 \qquad (7)$$

where

$$\frac{D_x}{D_y} = \frac{E_x \cdot h^3}{12(1 - \nu_{xy} \cdot \nu_{yx})} \cdot \frac{12(1 - \nu_{xy} \cdot \nu_{yx})}{E_y \cdot h^3} = \frac{E_x}{E_y} \qquad (8)$$

$$\frac{B}{D_y} = 0.5(\nu_{xy} D_y + \nu_{yx} D_x + 4 G_{xy} \frac{h^3}{12}) \cdot \frac{1}{D_y} = \qquad (9a)$$

or

$$= 0.5(\nu_{xy} + \nu_{yx} \nu_{xy} \frac{E_x}{E_y} - 2\sqrt{\frac{E_x}{E_y}} \cdot (\frac{1 - \nu_{yx} \nu_{xy}}{1 + \sqrt{\nu_{yx} \nu_{xy}}}))$$

The constants in the partial differential equation Equation (7), are dependent on E_x/E_y , ν_{xy} and ν_{yx}. If E_x/E_y , ν_{xy} and ν_{yx} are fixed, Equation (7) can be rewritten as:

$$\frac{E_x}{E_y} \frac{1}{(a / b)^4} \frac{\partial^4 w'}{\partial x'^4} + \frac{2}{(a / b)^2} \frac{B}{D_y} \frac{\partial^4 w'}{\partial x'^2 \partial y'^2} + \frac{\partial^4 w'}{\partial y'^4} = 0 \qquad (10)$$

where $0 \le x' \le 1$ $0 \le y' \le 1$

Equation (10) indicates that solution of w' depends on E_x/ E_y, a/b and the Poisson's ratios. The boundary conditions will of course also govern the solution.

Appendix C2

Calculation results of the dimensionless parameter, w', in graphical form for case 1-9 in Table3.1.

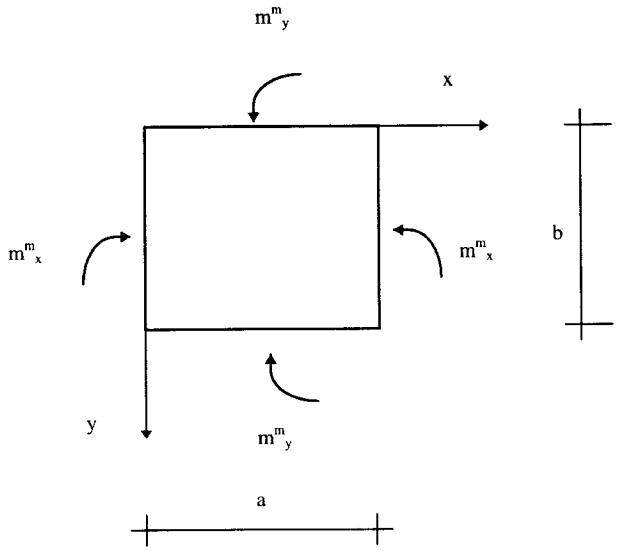

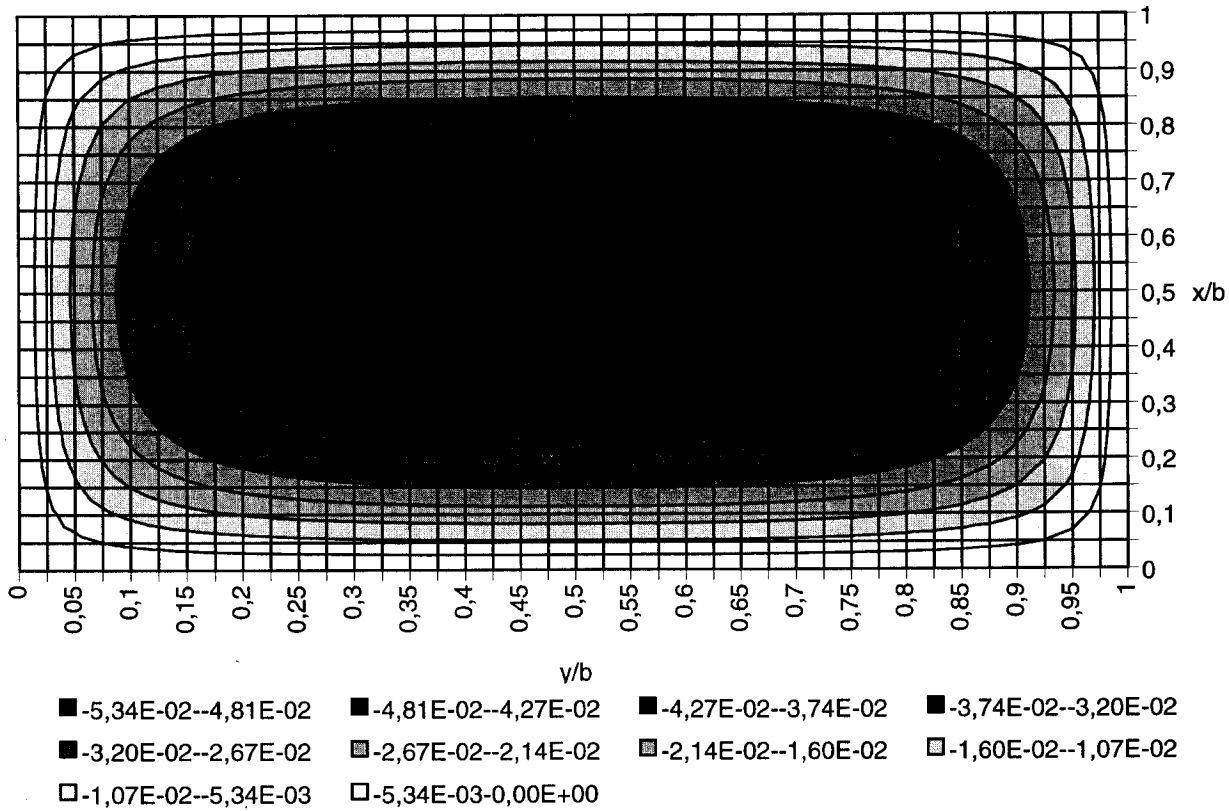

Figure 1 Calculated curves for case 1

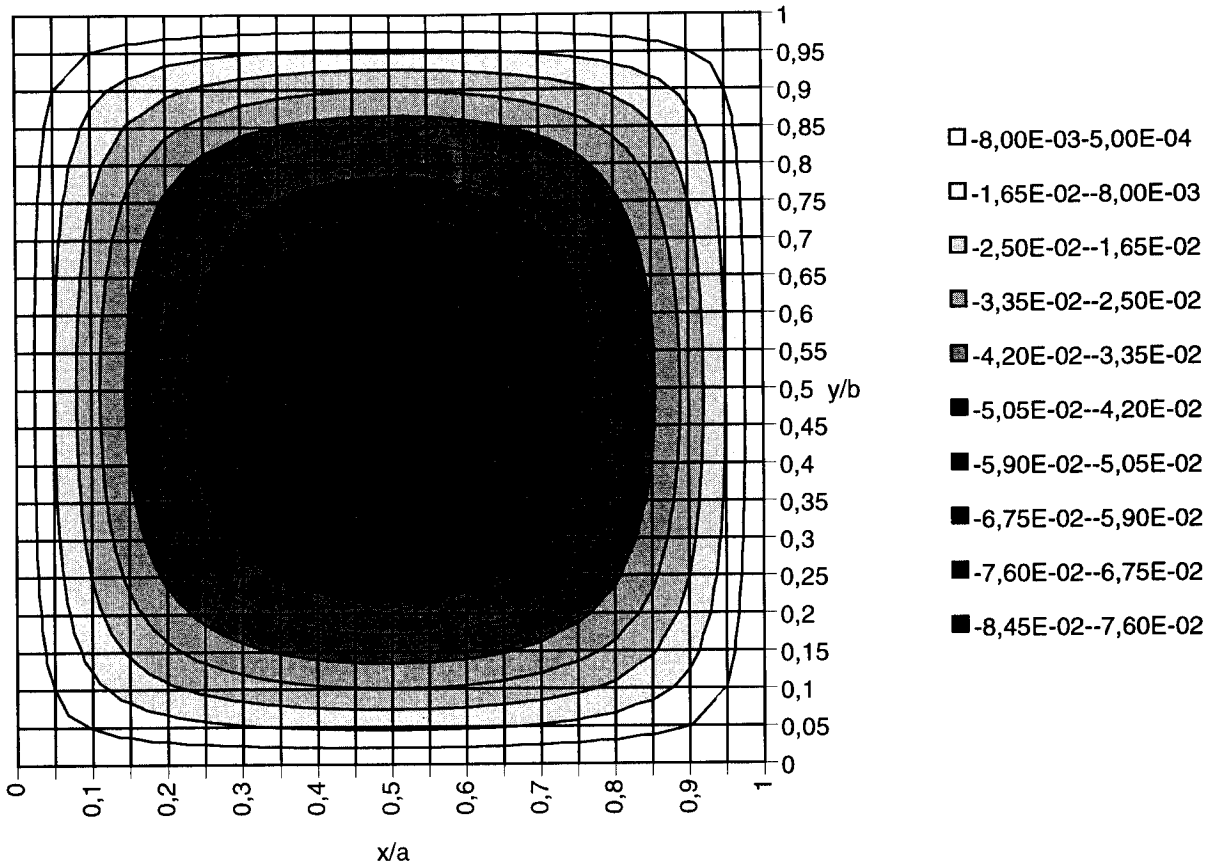

Figure 2 Calculated curves for case 2

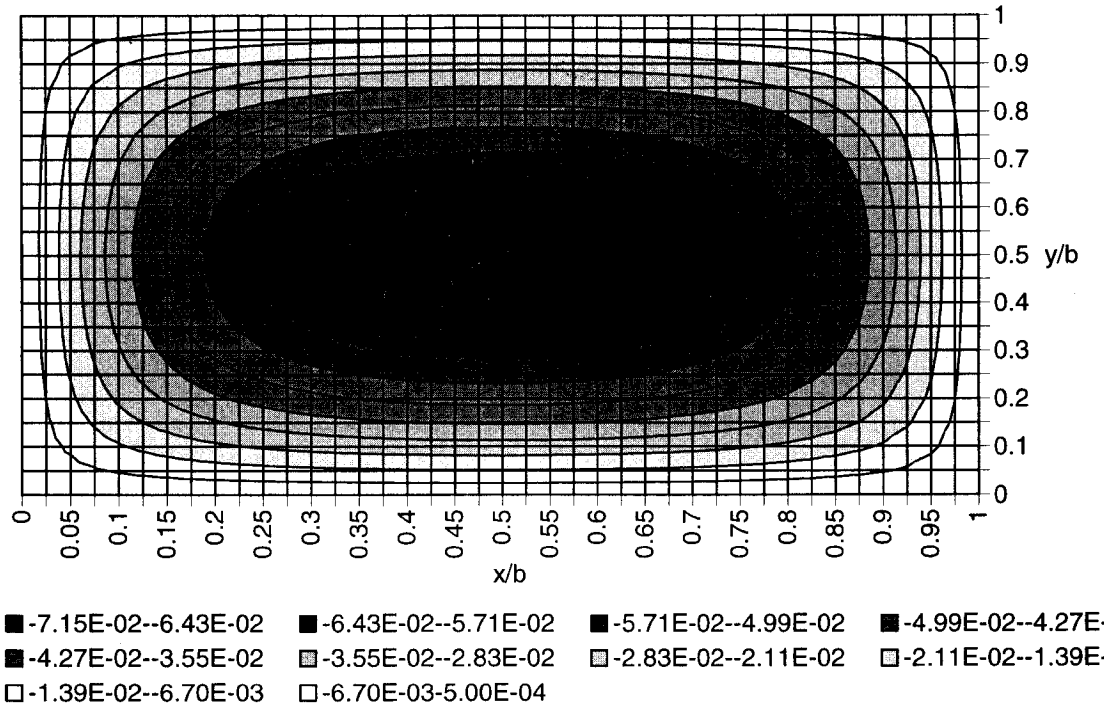

Figure 3 Calculated curves for case 3

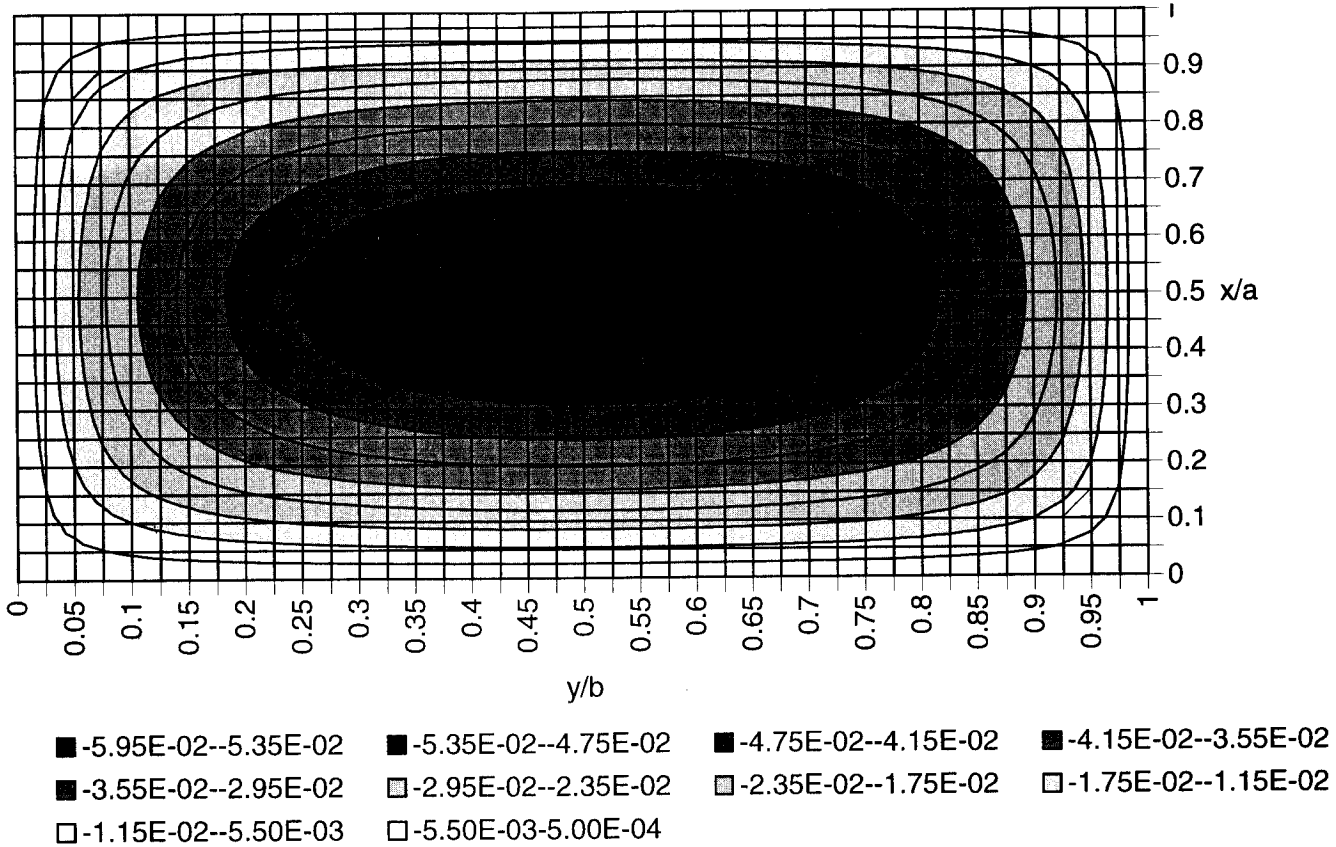

Figure 4 Calculated curves for Case 4

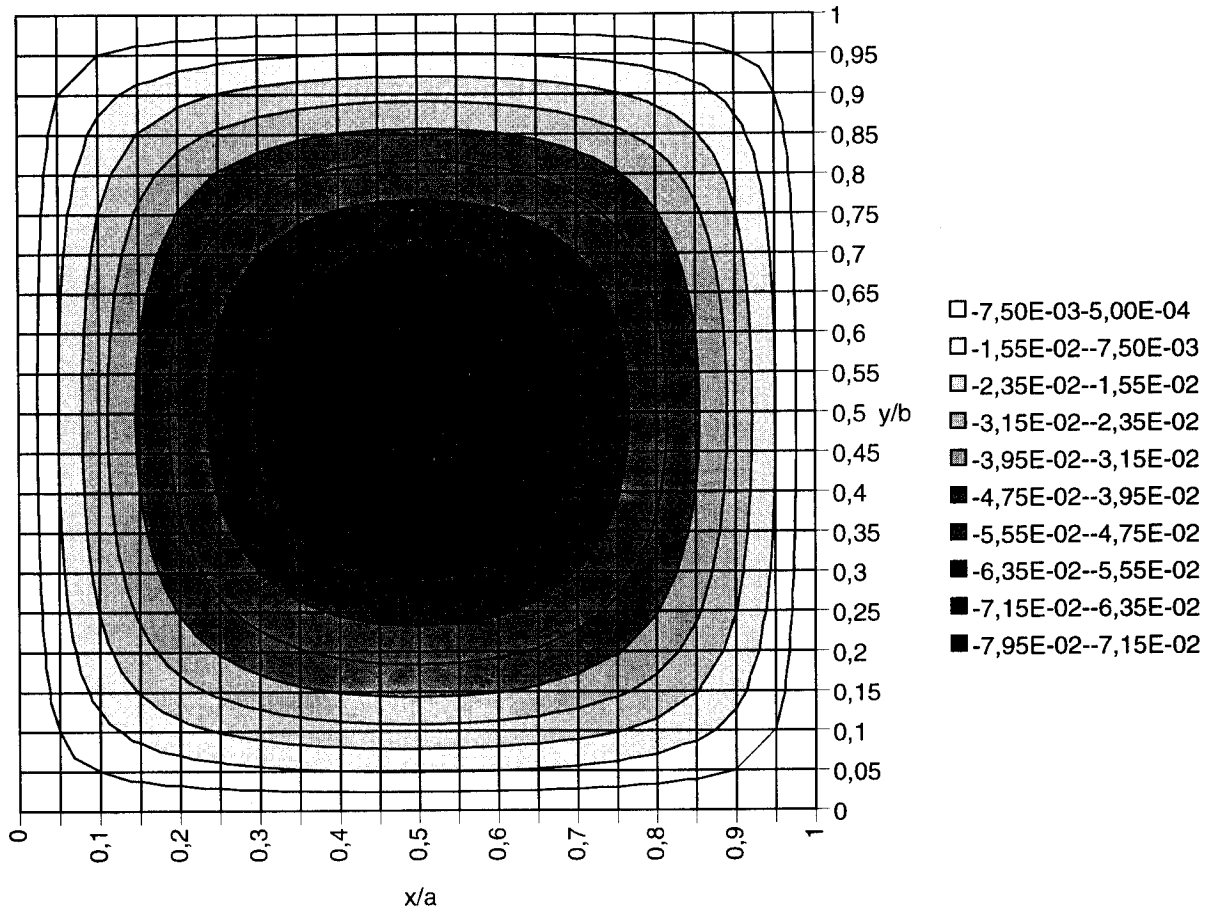

Figure 5 Calculated curves for Case 5

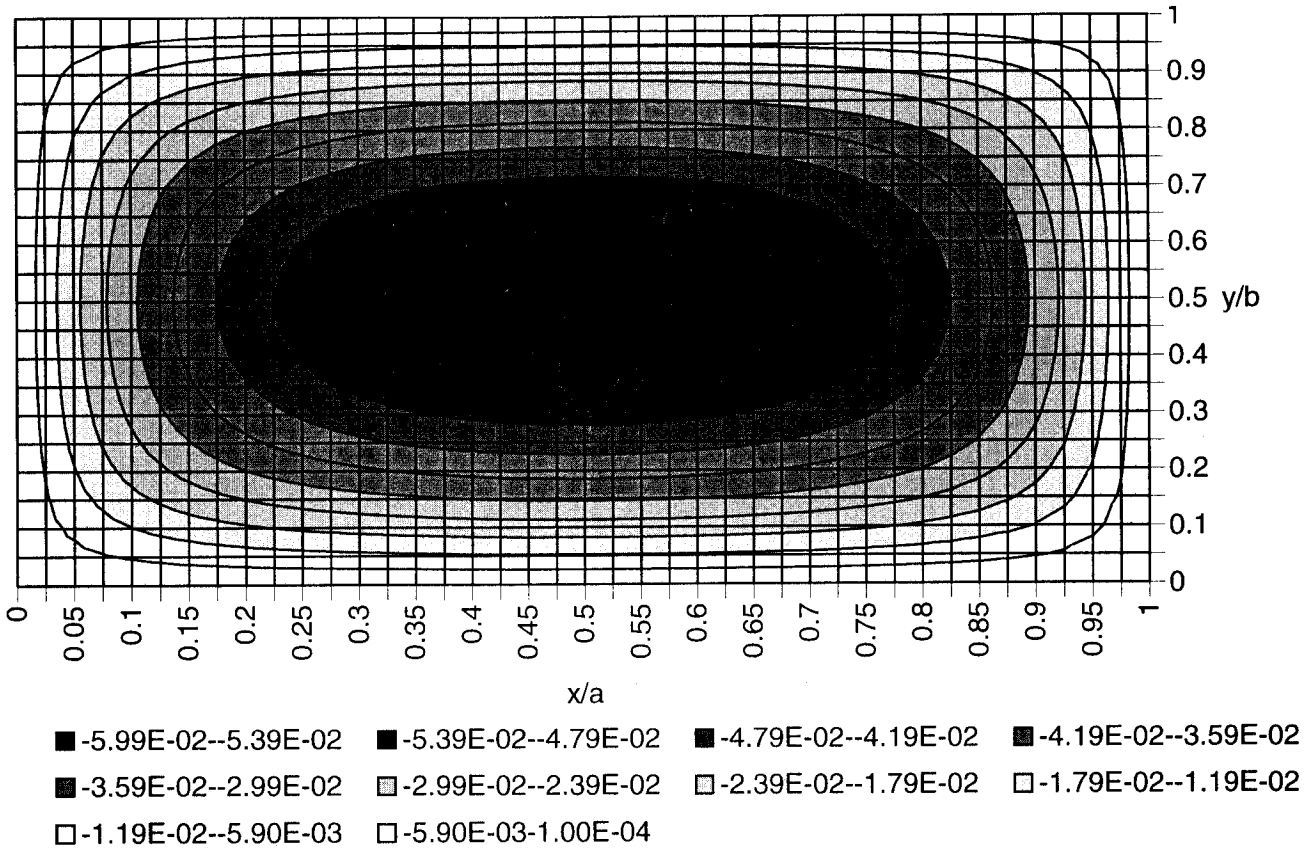

Figure 6 Calculated curves for Case 6

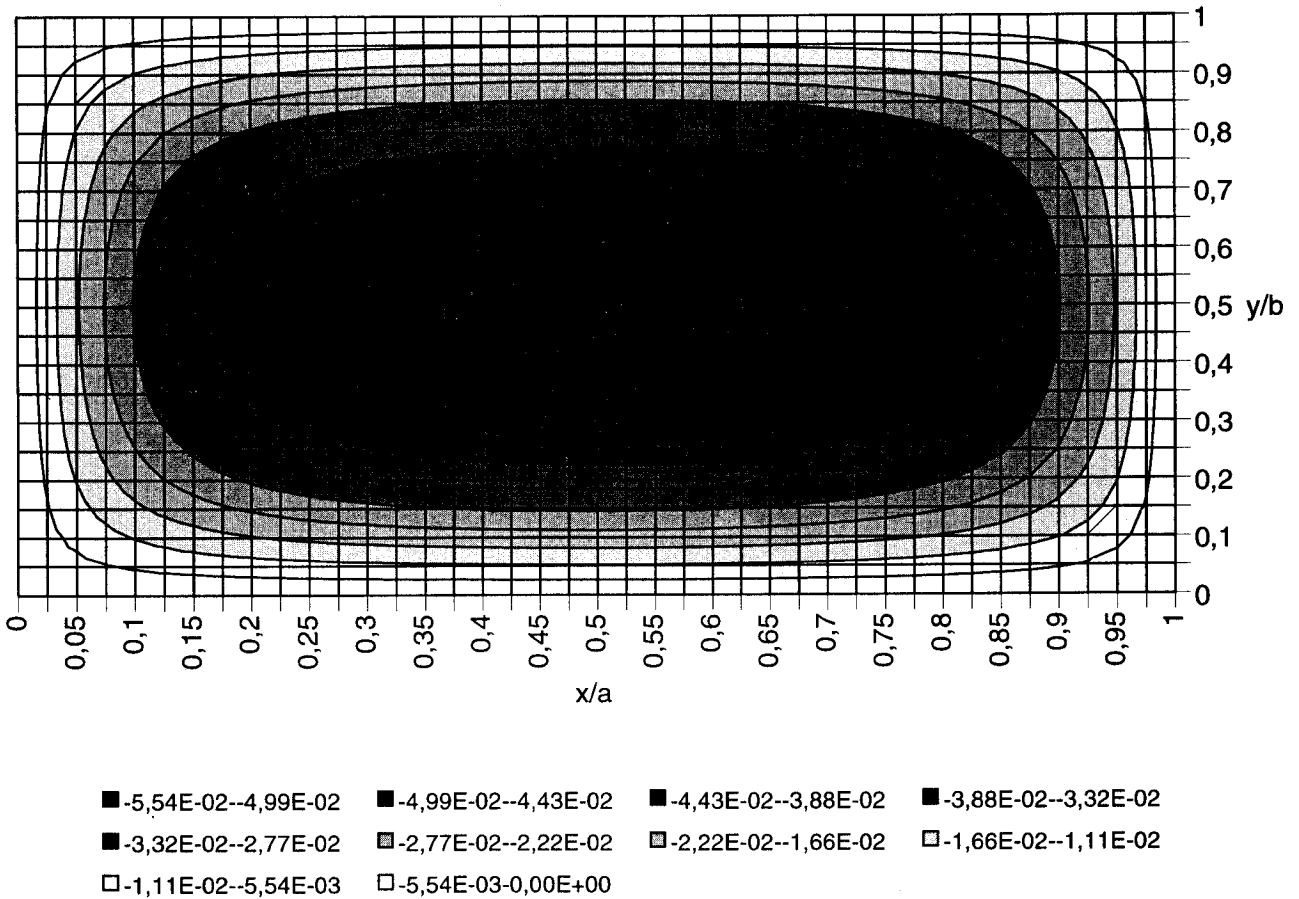

Figure 7 Calculate curves for Case 7

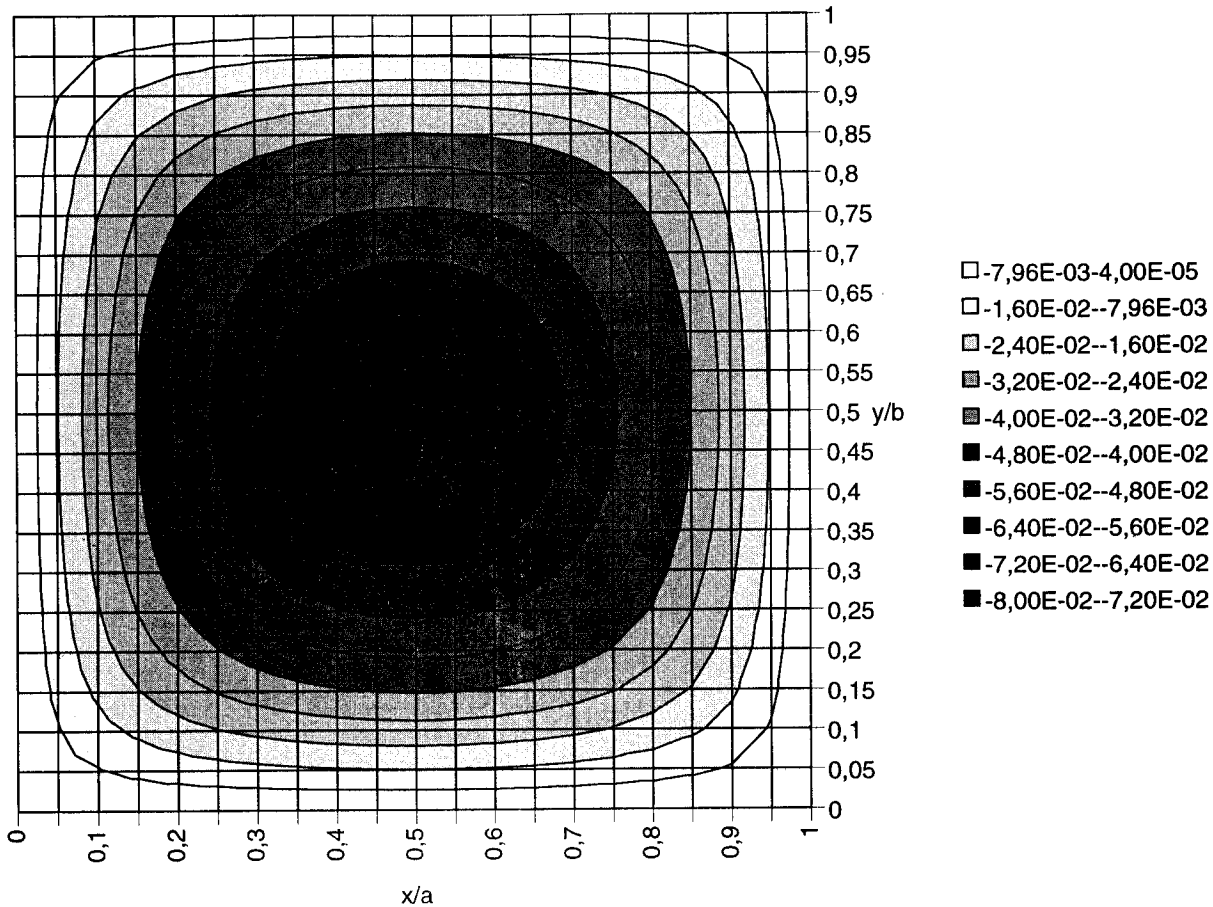

Figure 8 Calculated curves for Case 8

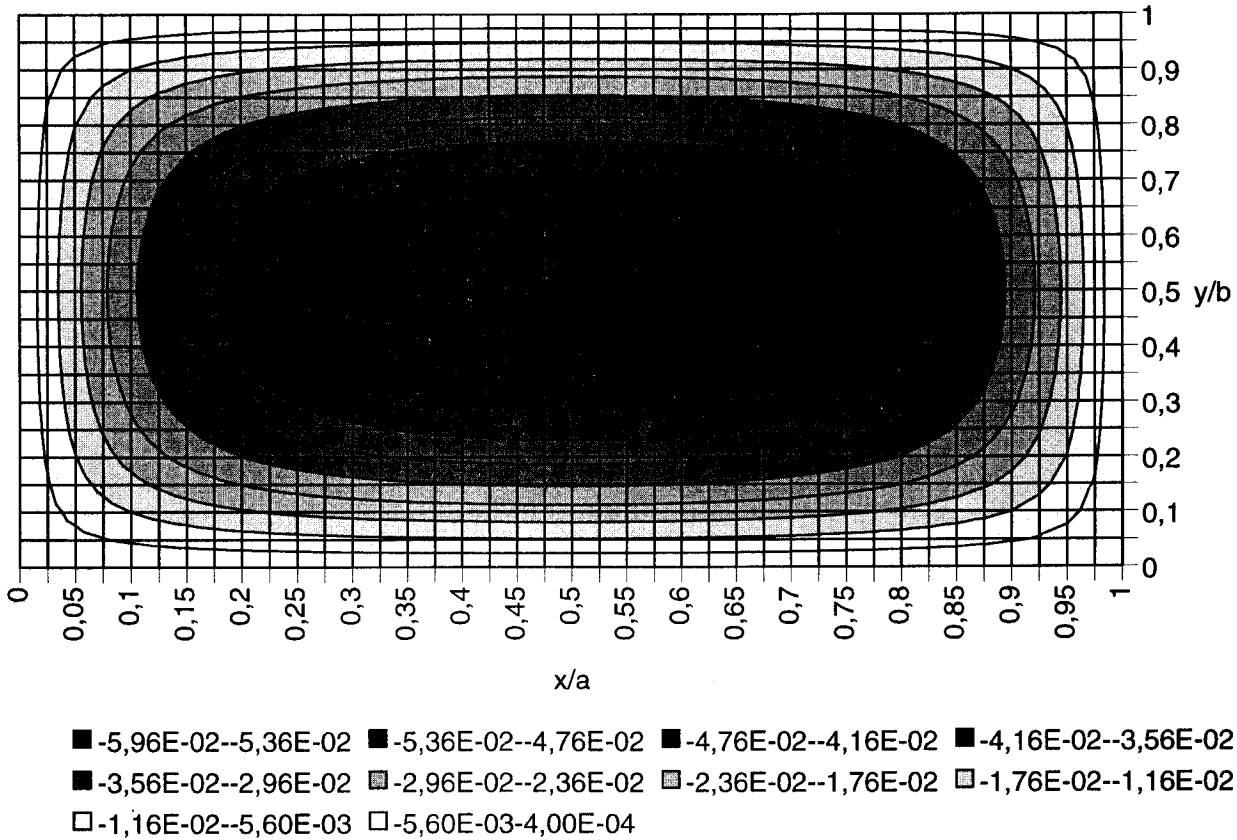

Figure 9 Calculated curves for Case 9

Distribution:

Department of Building Physics
Chalmers University of Technology
S-412 96 Göteborg, Sweden
P-98:4

ISBN 91-7197-704-X